

# **Simulation-based Investigation of Microwave Treatments for Printed Circuit Boards: Exemplified by Coating Cures**



Dissertation

**Trinh Dung Bui**



# **Simulation-based Investigation of Microwave Treatments for Printed Circuit Boards: Exemplified by Coating Cures**

## **Dissertation**

Zur Erlangung des akademischen Grades  
Doktor-Ingenieur  
(Dr.-Ing)

der Fakultät für Informatik und Elektrotechnik  
der Universität Rostock

vorgelegt von

**MSc. Trinh Dung Bui**  
geboren am 11.März 1981 in Hanoi Vietnam

aus Rostock

Rostock, März 2014

**Dekan**

Prof. Dr.-Ing. habil. Kühn

**Gutachtern**

Prof. Dr.-Ing. habil. Nowottnick

Prof. Dr.-Ing. Schacht

Prof. Dr.-Ing. Hohlfeld

Tag der Promotion: 28.10.2014

Universität Rostock

Fakultät für Informatik und Elektrotechnik

Institut für Gerätesysteme und Schaltungstechnik

# LIST OF CONTENTS

<b>List of Figures.....</b>	<b>v</b>
<b>List of Tables.....</b>	<b>ix</b>
<b>Danksagung .....</b>	<b>x</b>
<b>Kurzzusammenfassung.....</b>	<b>xi</b>
<b>Abstract .....</b>	<b>xiii</b>
<b>Chapter 1: Introduction.....</b>	<b>1</b>
<b>Chapter 2: Fundamentals and State of The Art.....</b>	<b>6</b>
<b>2.1 Electromagnetic Wave .....</b>	<b>6</b>
2.1.1 Maxwell´s Equations .....	7
2.1.2 Wave Equations and Plane Waves.....	8
<b>2.2 Microwave Heating Theory .....</b>	<b>15</b>
2.2.1 General of Microwave Heating.....	15
2.2.2 Dielectric Materials.....	17
<b>2.3 Coatings and their Curing Processes .....</b>	<b>22</b>
2.3.1 Types of Coatings .....	22
2.3.2 Curing Processes of the Coatings .....	23
2.3.3 Microwave Processing of Polymers.....	24
<b>2.4 Simulation .....</b>	<b>26</b>
2.4.1 The Choice of Suitable Numerical Method .....	26
2.4.2 The Choice of a Suitable Software Program and geometrical Problems .....	27
2.4.3 Finite Element Approximation of the Microwave Process.....	30
2.4.4 Estimation of Differences Between the Simulation Results and Accurate Results	34
<b>2.5 Experimental Support.....</b>	<b>36</b>
<b>Chapter 3: Interaction of PCB Structures with Microwave Radiation .....</b>	<b>38</b>
<b>3.1 Observing Standing Waves.....</b>	<b>38</b>
3.1.1 Model Definition of Microwave Oven .....	38
3.1.2 Observing Regular Heating.....	40
<b>3.2 Estimation and Discussion about Microwave Processes for PCBs .....</b>	<b>48</b>
3.2.1 Critique of the Investigated Results for PCBs with the Typical Substrate Material.....	48
3.2.2 The Influence of PCB´s Positions and Wire´s lengths.....	48
3.2.3 The Influence of Permittivities of PCB Substrates. ....	53
<b>3.3 Combination of wired PCBs and Coating Layers .....</b>	<b>56</b>
<b>3.4 Summary .....</b>	<b>57</b>

<b>Chapter 4: Optimizing Interactions of PCB Structures with the Microwave Radiation for Supporting Coating Cures.....</b>	<b>59</b>
<b>4.1 Heating Cavity Optimization.....</b>	<b>60</b>
4.1.1 Microwave Horn .....	60
4.1.2 Using Rectangular Waveguides as Heating Cavities .....	65
<b>4.2 Shielding/Protecting Sensitive Structures of Electronic Assemblies .....</b>	<b>83</b>
4.2.1 Ceramic shields .....	83
4.2.2 Conductive Shields .....	84
<b>4.3 Improving Microwave Processes of Coating Cures.....</b>	<b>90</b>
4.3.1 Based on Coating Materials .....	90
4.3.2 Based on Substrate Materials .....	92
<b>4.4 Summary .....</b>	<b>98</b>
<b>Chapter 5: Conclusion .....</b>	<b>100</b>
<b>Chapter 6: Outlook .....</b>	<b>104</b>
<b>Appendix A .....</b>	<b>106</b>
<b>Appendix B .....</b>	<b>110</b>
<b>Appendix C .....</b>	<b>113</b>
<b>Appendix D .....</b>	<b>114</b>
<b>References .....</b>	<b>116</b>
<b>Erklärung.....</b>	<b>125</b>

# LIST OF FIGURES

Figure 1.1: Process of building a model and the interplay between experiment, simulation and theory [10].....	4
Figure 2.1: Electromagnetic wave [12] .....	7
Figure 2.2: Plane wave reflection in arbitrary medium; normal incidence; where $E_i$ is the incident electric field (assume no loss of generality), $E_t$ is the transmitted electric field and $E_r$ is the reflected electric field [14] .....	12
Figure 2.3: The interaction of microwaves with different materials [15] .....	15
Figure 2.4: Application of a sinusoidal electric field for an ideal dielectric (top) and the out-of-phase displacement current which is induced (bottom) [20].....	17
Figure 2.5: Phase diagram for an ideal dielectric where energy is transmitted without loss (a); where there is a phase shift $\delta$ and the current acquires a component $I \times \sin \delta$ in-phase with the voltage and consequently there is a dissipation of energy (b); the illustration of the relationship between $\epsilon_r, \epsilon', \epsilon''$ .....	18
Figure 2.6: Penetration depth [16].....	19
Figure 2.7: Propagation of a plane wave in lossy medium [21].....	20
Figure 2.8: The process for solving the microwave heating problem operated by ANSYS ....	28
Figure 2.9: The process for solving the microwave heating problem operated by COMSOL	29
Figure 2.10: Boundary of medium 1 and medium 2 with normal vector $n$ [45, 46] .....	31
Figure 2.11: Particular laboratory microwave oven.....	37
Figure 3.1: The simulation model of half microwave oven and PCB load.....	39
Figure 3.2: Single wired PCBs with different wire's lengths .....	41
Figure 3.3: The overlay picture combining a real image and a thermal image of the single wired PCB taken by thermo-graphic camera of 200 mm long PCB after microwave heating.....	42
Figure 3.4: Simulation results of temperature distributions on quadratic PCBs.....	42
Figure 3.5: The substantial similarity of simulation result (left) and experimental result (right) of quadratically wired PCB after microwave heating.....	43
Figure 3.6: The diagram expresses the temperature of the point within hotspot which has highest temperature and the point in other area in 30 seconds microwave heating process .....	44
Figure 3.7: The temperature distribution of the quadratically wired PCB in some positions where the open corners are rotated .....	45
Figure 3.8: The simulation results of wired PCBs which all copper wire corners are open (left) and close (right) .....	45
Figure 3.9: The metallic structures on two sides of a real PCB .....	46
Figure 3.10: The real PCB simulation model built in 3D (left) and metallic structures on two sides (middle and right) .....	46
Figure 3.11: The simulation results and experimental result after microwave heating a real PCB.....	47

Figure 3.12: The influence of $E$ field to the temperature distribution.....	49
Figure 3.13: Relationship between wire's length and maximal induced $E$ field intensity on wired PCBs in position 1 and 2.....	50
Figure 3.14: The coupling of 30 mm, 65 mm copper wired PCBs and electric field in position 1 and 2.....	51
Figure 3.15: Diagram of maximal $E$ field strengths, induced by the wired PCBs in position 1 (blue) and by the wired PCBs in a position which is translated 20 mm horizontally (red) .....	53
Figure 3.16: Interaction of the wired PCBs with microwave radiation depends on the substrates' relative permittivities .....	53
Figure 3.17: Dependence of the conductor wavelength $\lambda_c$ and the relative permittivity on the base material $\varepsilon_{PCB}$ (blue plot with markers). The dashed curve represents an interpolation based on the shown equation .....	54
Figure 3.18: Simulation results of wired PCBs after microwave heating with variable frequencies while material properties are kept at the frequency of 2.45 GHz.....	55
Figure 3.19: Temperature distribution on the wired PCB without coating (left) and the PCB with the coating combined (right).....	56
Figure 3.20: The different temperature distribution on the PCB without coating and on the PCB with coating .....	57
Figure 4.1: The structure of the study .....	60
Figure 4.2: The microwave horns fed by rectangular waveguide .....	61
Figure 4.3: Cross section of waveguide cut in $E$ plane (left) and $H$ plane [58] .....	61
Figure 4.4: coordinate system used, center of the horn antenna opening. ....	62
Figure 4.5: The system, utilized the horn antenna to heat electronic assemblies.....	63
Figure 4.6: The polarization of $E$ field (inside the air box) of the horn antenna in stream line expression (left) and in arrow expression (right), the line in the center is the location where the electronic assemblies is set.....	63
Figure 4.7: The PCB is set along the polarization of microwave horn .....	64
Figure 4.8: Simulation result of heating the PCB sample ( $150 \times 30 \times 2.5 \text{ mm}^3$ ) in 50 s by microwave horn (with power of 200 W) in the case the PCB is set along the polarization .....	64
Figure 4.9: The PCB is set crossed the polarization of microwave horn .....	64
Figure 4.10: Simulation result of heating the PCB sample ( $150 \times 30 \times 2.5 \text{ mm}^3$ ) in 50 s by microwave horn (with power of 200 W) in the case PCB is set cross the polarization....	64
Figure 4.11: A rectangular waveguide [61].....	65
Figure 4.12: Cross section of a waveguide with the width $a$ and the height $b$ .....	66
Figure 4.13: The sketch of the system using the waveguide as the heating cavity .....	68
Figure 4.14: The polarization of electromagnetic waves (red arrows; left) and the slice view of the electric field distribution in a rectangular waveguide .....	69
Figure 4.15: The model of the rectangular waveguide ( $86.36 \times 43.18 \times 230 \text{ mm}^3$ ), which the slits locate at the small sides with surrounding air .....	69
Figure 4.16: The electric field loses from the inside of waveguide to the surrounding air.....	70
Figure 4.17: Display slices of electric field strengths cut the rectangular waveguides through the half of their heights .....	70



Figure 4.18: The chart shows electric field strengths of the calculated points of the case of no slit on the waveguide and slit-height= 0, 8, 12, 16, and 20 mm .....	71
Figure 4.19: The slits are removed to the big sides of the rectangular waveguide [59] .....	72
Figure 4.20: Display slices of electric field strength cut the rectangular waveguides through their half height in the case of slits in the big side .....	72
Figure 4.21: The comparison of $E$ field at calculated point in cases waveguide with slits at small sides (blue) and waveguide with slits at big sides (red) for slit-height= 0, 8, 12,16, 20 mm .....	73
Figure 4.22: The sketch of system using a multi-U form waveguide as a heating cavity.....	74
Figure 4.23: Electric fields in a U form waveguide and a multi-U form waveguide.....	75
Figure 4.24: Simulation result illustrates the interaction of the PCB structure with microwave radiation of a U-form waveguide. The $E$ field spreads out to the air following the copper wires .....	76
Figure 4.25: The polarization (red arrows) crosses the copper wire on PCB (left picture) and a close view describes the dominant dielectric heating in this case (right) .....	77
Figure 4.26: Simulations of PCBs with 2 copper wires (left), 4 copper wires (middle) and 6 copper wires which crossed the polarization show the homogeneous heat distribution...	77
Figure 4.27: The temperature distribution on PCB (left) with highest temperature 79°C and the temperature distribution on the coating with 1mm thickness and $\epsilon = 5.5-j$ (right), which is coated on the PCB. The highest temperature of the coating is about 88°C; simulation in 10 s .....	78
Figure 4.28: The copper wire on PCB is along with the polarization (left picture) and the close view shows the periodical heating in this case (right) .....	79
Figure 4.29: The temperature distribution on PCB (left) and coating (right); all four half eclipses are the overheated areas where temperature are over 140°C .....	79
Figure 4.30: The temperature distribution on multi-copper-lines PCBs, which the angle of the connecting line with the other ones changes from 0 to 360° .....	80
Figure 4.31: Temperature distribution on the simulated PCB where the dark red areas express the overheated areas (over 140°C) .....	81
Figure 4.32: The coupling of microwave radiation and copper wires on the original real PCB (left) and the coupling on the PCB, on which the wire in the center is removed (right) ..	82
Figure 4.33: The impact of polarization on the real PCB tests with half PCB .....	82
Figure 4.34: The temperature distribution of PCB without shield (left) and with ceramic shield (right) after microwave heating (simulation results).....	83
Figure 4.35: PCB sample with single wire on the top (left) and full copper shield at the bottom (right) .....	84
Figure 4.36: The simulation results and experimental results of the interaction between single wired PCBs in cases without shield (left) and with shield (right) with the microwave radiation .....	85
Figure 4.37: Simulation results exhibited the coupling of metallic structures of a real PCB and the microwave radiation when it is shielded (left) and unshielded (right).....	86
Figure 4.38: Temperature distribution on the coating which covers the shielded real PCB ....	87
Figure 4.39: The model of real PCB with local shields .....	88

Figure 4.40: Simulation result of heated PCB with local shields (left) and heated PCB without shield (right).....	88
Figure 4.41: The effect of real parts of coatings' permittivities on the temperature distribution on the coatings .....	91
Figure 4.42: The effect of imaginary parts of coatings' permittivities on the temperature distributions on coatings .....	92
Figure 4.43: Temperature distributions on the PCBs depending on the thermal conductivity	95
Figure 4.44: Relation between $\kappa$ and $\Delta T$ in the series tests of single wired samples.....	96
Figure 4.45: The temperature distribution of real PCB with FR-4 substrate (left), $\text{Al}_2\text{O}_3$ -ceramic substrate (middle) and AlN-ceramic substrate (right) after microwave heating .	97
Figure 4.46: The simulation results of the real PCBs with coatings covered on for the $\text{Al}_2\text{O}_3$ -ceramic and AlN-ceramic as substrates .....	97
Figure 4.47: The simulation result (left) and experimental result (right) of the tested sample	98
Figure B.1: Metallic structure designed by external program (left) and the real sample (right) .....	110
Figure B.2: The 2D metallic structure designed by external program can be embedded on the PCB substrate.....	111
Figure B.3: The simulation result of the sample above after 30 seconds microwave process with the power of 200 W .....	111
Figure B.4: The metallic structures on the top and at the bottom of PCB substrate including holes connecting them.....	112

# LIST OF TABLES

Table 2.1:	The loss factors of some Materials [13].....	19
Table 3.1:	Basic data of microwave cavity.....	39
Table 3.2:	Properties of materials used in the simulation.....	40
Table 3.3:	The E field intensities corresponding to the calculated temperature of the point in hotspot and the point in the other area.....	44
Table 4.1:	Frequency band and dimension of rectangular waveguide WR340 [62].....	68
Table 4.2:	The E-field strength of the calculated point (figure 4.17) and its loss energy for variable slit-heights.....	71
Table 4.3:	The E-field strength at calculated point and its loss energy for variable slit-heights in the case slits locate in the big sides of the waveguide.....	73
Table 4.4:	Relation between the distance from a shielded point in PCB to the shield and its $E$ field intensity.....	89

# DANKSAGUNG

Die vorliegende Dissertation entstand am Institut für Gerätesysteme und Schaltungstechnik der Universität Rostock.

Mein besonderer Dank gilt Herrn Professor Dr.-Ing. habil. Mathias Nowottnick für die wissenschaftliche Betreuung dieser Arbeit. Insbesondere möchte ich mich für die kreativen Freiräume, die stetige Unterstützung, als auch für die angenehme Zusammenarbeit herzlich bedanken.

Ich danke allen Kollegen des Instituts für Gerätesysteme und Schaltungstechnik für die Unterstützung bei der Durchführung dieser Arbeit. Besonderer Dank gilt Dr.-Ing. Felix Bremerkamp und Dipl.-Ing. Dirk Seehase, denen ich für Ihre Mithilfe bei Experimenten, Versuchsaufbauten und interessanten sowie fruchtbaren Diskussionen danken möchte.

Bedanken möchte ich mich auch bei den anderen vietnamesischen Studenten in Rostock für die schöne gemeinsame Zeit in Deutschland.

Abschließen möchte ich mich für den Zuspruch, Rückhalt und die Unterstützung meiner Familie bedanken. Insbesondere für den meiner Eltern, meines kleinen Bruders und meiner Frau Loan.

Rostock, März 2014

Trinh Dung Bui

# KURZZUSAMMENFASSUNG

Auf Grund der gesellschaftlichen Anforderungen nimmt der Einsatz elektronischer Geräte stetig zu. Die Entwicklung von Elektronik für den Hochtemperatur Einsatz ist die kritische Technologie des 21. Jahrhunderts [2]. Hochtemperatur-Elektronik ist meist rauen Umweltbedingungen ausgesetzt für die eine neue Klasse elektronischer Bauelemente und entsprechender Gehäuse benötigt wird, welche für den Einsatz bei höheren Temperaturen geeignet sind. Die Nutzungsmöglichkeit solcher Hochtemperatur Elektronik kann, durch den Wegfall komplexer Kühlsysteme, die Produktkosten senken und die Zuverlässigkeit erhöhen. Für diesen Fall werden häufig Schutzschichten aufgetragen welche die elektronischen Baugruppen vor Umwelteinflüssen schützen. Diese Beschichtungen müssen vollständig ausgehärtet werden um optimale Schutzeigenschaften auf den Baugruppen zu gewährleisten. Für eine temperaturgestützte Aushärtung werden hauptsächlich konvektive Erwärmungsverfahren eingesetzt. Jedoch gibt es für spezielle Anwendungen einige technische Herausforderungen, wie z.B. Schwierigkeiten beim Aushärten von dicken Beschichtungen auf Baugruppen der Leistungselektronik. Diese Art von Beschichtung muss, auf Grund der Höhe der metallischen Strukturen, eine größere Dicke besitzen. Die vollständige Aushärtung solcher Schichten mittels Infrarot und Konvektion gestaltet sich schwierig, da hierbei die Beschichtungen von außen nach innen aushärten.

Im Gegensatz zur herkömmlichen Erwärmung, wird durch eine Bestrahlung mit Mikrowellen das gesamte Material durchdrungen und gleichzeitig erwärmt. Somit kann durch die Aushärtung mittels Mikrowellenstrahlung Zeit und Energie eingespart werden, da eine dicke Schicht aus dem Volumen heraus erwärmt wird anstatt über die Oberfläche. Viele Untersuchungen haben gezeigt, dass, im Hinblick auf chemische und physikalische Parameter, eine mikrowellengestützte Aushärtung der Polymerstoffe effektiver ist als eine konvektive Erwärmung [7]. Das Thema der Mikrowellenbehandlung von elektronischen Baugruppen war bereits Gegenstand einiger Forschungsprojekte [5]. In diesen Projekten bestand die Gemeinsamkeit in der selektiven Erwärmung eines Materials aus dem Inneren heraus. Gleichzeitig gab es aber auch ähnliche Herausforderungen wie die Inhomogenität der Feldverteilung auf Grund von leitenden Strukturen und die Beschädigung von Bauteilen durch die hohe Feldstärke.

Da die Beschichtungsstoffe vor dem Aushärten auf elektronische Baugruppen appliziert werden, nehmen diese ebenfalls am Erwärmungsprozess teil. Hierbei besteht die Herausforderung die Baugruppe vor Schäden zu schützen und gleichzeitig eine vollständige Aushärtung der Beschichtung zu erreichen. In diesem Zusammenhang soll die Wechselwirkung von Mikrowellenstrahlung auf Leiterplatten Strukturen untersucht werden. Diese Arbeit soll einen Beitrag zum besseren Verständnis des Einflusses einer homogenen Mikrowellenerwärmung auf den Aushärteprozess leisten. Für die Analyse, Vorhersage und Optimierung dieser Untersuchungen werden numerische Simulationen verwendet. Um zuverlässige Simulationsergebnisse zu erhalten wurde ein geeignetes numerisches Verfahren gewählt. Die Mikrowellen Prozesse und ihr Einfluss auf verschiedene Leiterplatten Strukturen wurden untersucht. Anhand dieser Ergebnisse wurde das Prozessfenster gefunden, welches ein sicheres Aushärten der Beschichtung ohne Schäden auf der Leiterplatte erlaubt. Hierbei wurden die Parameter, welche die mikrowellengestützte Erwärmung von elektronischen Baugruppen beeinflussen, bestimmt. Basierend auf diesen Ergebnissen wurde eine Optimierung der Wechselwirkung zwischen Leiterplatten Strukturen mit der Mikrowellenstrahlung, zum Unterstützen der Aushärtung und zum Schutz der Baugruppe, durchgeführt. Ein experimenteller Aufbau dient zur Bewertung und Vergleichbarkeit der errechneten Simulationsergebnisse.

# ABSTRACT

The electronic devices are grown up rapidly due to the needs of people. Thereby the development of electronics which operate at high temperatures has been identified as the critical technology for 21<sup>st</sup> century [2]. The high temperature electronics are often applied in harsh environments, thus new classes of electronic components capable of operating at higher-than-normal temperature and associated packaging to support them is required. The ability of use such high temperature electronics can reduce the cost of the products and increase the reliability by removing complex cooling systems. In this case, coatings are often applied to protect electronic assemblies from environmental attacks. The coatings have to be fully cured in order to reach their optimum properties for protecting the electronic assemblies. The heat curing processes are preferred to realize and they are usually convectional heating. However, there are technical problems in some special cases e.g. the difficulty in the curing process caused by thick coatings of electronic assemblies used in power electronics. This kind of coating is required thicker-than-normal due to the thickness of the metallic structures of the electronic assemblies. Therefore with infrared heating and convection, it is difficult to achieve a full cure, because the coatings will be cured from the outside to the inside.

Unlike conventional heating, microwave irradiation penetrates and simultaneously heats the bulk of materials. The cure by the means of microwave irradiation saves time and energy because it is able to directly heat the thick layer through their volume instead of their outer surface. Many investigations proved that the microwave process is more efficient than convectional heating for supporting polymer cure in term of chemical kinetics and physical properties [7]. There have been some research projects concerning microwave treatment for electronic assemblies [5]. All these projects have a common approach that is the selective heating of materials from the inside. They also have the similar challenges such as the inhomogeneity of the field distribution due to the conductive structures and the components' damages because of the high field intensity.

Because the electronic assemblies have coatings applied on before curing, they participate in the heating process. In this case the challenge is the simultaneousness of successful coating cure and safekeeping of the electronic assemblies. Thus the investigation of how metallic structures of PCBs interact with microwave radiation is carried out. This work is realized in

order to support a homogeneous microwave heating of the curing process. For that reason, numerical simulation is utilized in order to assist the investigation in term of analysis, prediction and optimization. In this investigation, a suitable numerical method was chosen to produce reliable results. The microwave processes and their effect on different kind of PCB structures were analyzed. Afterwards the results were used for identifying the process window, which allows a safe coating cure without damage of the participating PCBs. Thereby the parameters which influenced on the microwave heating of the wired PCBs are determined. Based on the knowledge achieved, an optimization of interaction between PCB structures with microwave radiation in order to support coating cure and protect the electronic assemblies was carried out. To qualify the simulation results, experimental models were built. This evaluation can ensure the reliability of the approximate solutions.







# CHAPTER 1

## INTRODUCTION

Since the first appearance, electronic devices have been growing rapidly. Many electronic products are increasing years after years in mobile phones, automotive control units, car information control systems, laptops and computers.... [1]. Thereby the development of electronics that operate at high temperature has been identified as a critical technology for 21<sup>st</sup> century. In this area, avionics, automotives, and geographical electronic systems require components and packaging reliable to 200°C and beyond [2]. The high temperature electronics can be applied in harsh environments where the use of conventional electronics is inapplicable such as under the hood of automobile or in exposed areas of aircraft. In this case, it is necessary to have a new class of electronic components capable of operating at higher-than-normal temperature and the associated packaging to support them. The ability to use electronic systems at high temperature therefore can reduce the cost and enhance the reliability of products by removing complex cooling systems, cabling and interconnections required for remote replacement needed of the electronics [2].

Due to the progressing sophistication and the automation of industrial processes, the need of conditioned power is growing up rapidly nowadays [3]. In this case, power electronic converters presenting the conditioning are high reliable and efficient. Metallic structures of the electronic assemblies thereof have to be very thick, because of the high current density (can reach to thousands ampere). The coatings protected this kind of electronic assemblies requires to be thick either. This somehow creates the difficulty for the coating cure.

For the expectation of long lifetime and reliable products, the effective techniques to deal with electronic assemblies have been taken into account especially to protect the particular electronic assemblies mentioned above. In recent years, microwave heating has been applying in many areas such as: food industries, sintering, joining and chemical industry...etc [4]. Thereby the microwave heating is utilized to deal with the soldering of electronic assemblies or with the curing process of the coatings either. There have been at least three projects concerning “Microwave heating” of electronic assemblies recently [5]:

- **Micro-flow** (2003-2007) BMBF/PTKA: Deal with the soldering to joint components of electronic assemblies by the means of microwave irradiation.
- **Micro-flam** (2009-2012) AiF/IGF 16128BG: Utilize the microwave heating to deal with the residual stress-free curing of coating materials, thermosetting resins and flowable thermosets for the electrical insulation.
- **Nanowave** (2010-2014) BMBF/PTJ: Optimizing insulation coordination for high-performance electronics using nanoscaled-filled coating materials, sealing compounds and combinative curing by the innovative microwave technology.

All these three research projects have a common approach that is the selective heating of materials from the inside. And the facing challenges are also familiar:

- Inhomogeneous field distributions because of metallic components
- Risk of components' damages due to the high field strength

The microwave process performing selective heating can be applied in some special cases as:

- In soldering, the high temperature solder alloys with increasing melting soldering-temperature are difficult to process. However the component/solder joints can be selectively heated by the means of microwave irradiation, whereas the printed circuit board (PCB) remains colder and safe.
- As mentioned above, the power electronic need thickness copper wires, thus thicker insulating coatings required. These coatings are difficult to cure with infrared heating or convection, because they will be cured from the outside to the inside. With microwave heating, it is possible to cure the coatings from the inside and lead to the full cure.

## COATINGS AND COATING CURES BY THE MEANS OF MICROWAVE IRRADIATION

To protect the electronic assemblies from environmental attacks, coatings are used. They were originally developed for military, aerospace and marine applications but now are widely used in telecommunication, automotive, consumer, industrial and control applications to increase quality and reliability of products [6]. Coatings actually are solvent-free, curable resins which are applied on electronic assemblies to protect them from a variety of environmental, mechanical, electrical and chemical stresses including [6]:

- Moisture and humidity

- Dust and dirt
- Mechanical and thermal shock
- PC board processing solvents
- Excessive handling
- Fungus and mildew
- Corrosion
- Vibration
- Chemical fuels, hydraulic fluids
- Harsh environment applications

Coatings need to be cured to gain their optimum properties. Recently, there have been many researches concerning the curing process of polymeric materials by the means of microwave irradiation. Unlike conventional heating where thermal energy, produced by an external heat source, transfers from the outside of materials to the inside of materials through conduction, convection or radiation, microwave irradiation penetrates and simultaneously heats the bulk of materials. Hence the cure by the means of microwave irradiation saves time and energy, because it is able to directly heat the thick layer through their volume instead of their outer surface. It has been demonstrated that microwave irradiation could support and accelerate the polymerization in many publications so far [7].

The coatings normally have to be applied on electronic assemblies before curing process. Therefore the sensitive structures of electronic assemblies participate in the curing process.

### SIMULATION

The curing process by the means of microwave irradiation is considered as a necessary engineering-change for efficient and effective products. The engineering-change originates from an internal source in order to improve products' performance, eliminate defect and upgrade technology or enhancing their functionality [8]. A simulation model of this process could help in predicting and analyzing the results, and effects of different policies adopted, thereby assisting in an optimization of the whole process.

Simulation actually is an operation that imitates a real-world process or system overtime [9]. For simulating something, a model is required to develop. This model represents the behaviors of the real system. Meanwhile the simulation represents the operation of the real system overtime.

Simulation is used in many contexts, such as testing, training, education, video games...etc. In this research work, simulation is used for safety engineering, which assures that the engineered systems provide acceptable levels of safety.

Since digital computers appeared, there have been powerful tools to solve complicated problems in various fields. A mathematical model of an engineering problem can be built so that computers are possible to calculate with their benefit. From this model, simulations can be performed. Because of being based on approximate methods, simulation results should be evaluated by experimental results. The theoretical predictions, simulation results and experimental results need to be compared to each other to upgrade themselves as shown in figure 1.1 below.

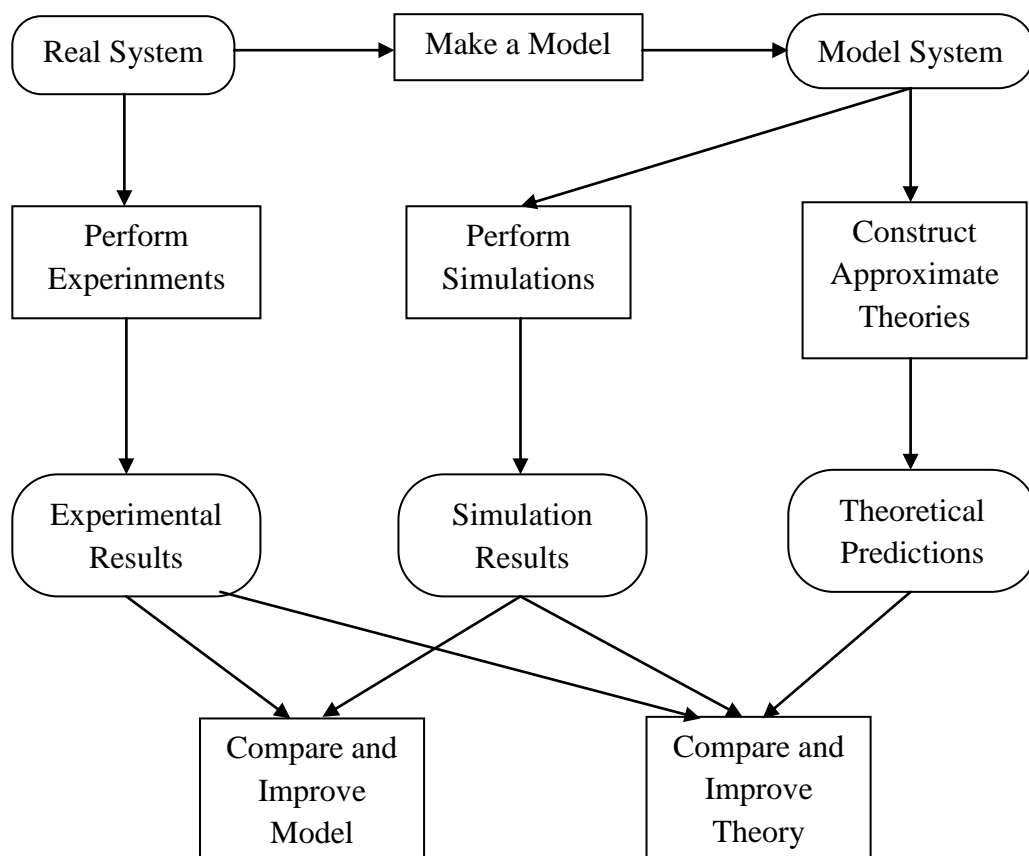


Figure 1.1: Process of building a model and the interplay between experiment, simulation and theory

[10]

## MOTIVATION AND OBJECTIVES

From the discussion above, microwave process is able to cure coatings effectively. Because the electronic assemblies participate in the curing process, the conductive structures can be damaged. Electronic assemblies normally include printed circuit boards, which are the main

core of them and components. A printed circuit board (PCB) is a board made from glass reinforced epoxy with copper tracks on the places of wires. The copper tracks link components together to form a circuit. Hence to understand how the PCB structures (copper tracks) react to microwave radiation is very important to develop the cure by the means of microwave irradiation. However the investigations lack in the study of the interaction of PCB structures and the microwave radiation. For safety engineering, simulation should be considered as the approach to this problem. The simulation can be assisted in the analysis, prediction and optimization of the problem. The question needs to be answer here that is it possible to check the ability of PCB designs for microwave treatment by the simulation in advance. Beyond that, finding out the process window, which allows a safe coating cure without damage of the participating PCBs is the main challenge. This leads to the objectives of the study, needed to fulfill:

- Finding out especially sensitive structures
- Describing influences of designs and interactions
- Simulating the maximum allowed field strength for a safe microwave treatment
- Finding methods to protect or shield sensitive structures.

All of those contents motivated us to work on “Simulation-based investigation of microwave treatment for printed circuit boards: exemplify by coating cures”.

## CHAPTER 2

# FUNDAMENTALS AND STATE OF THE ART

The use of microwave radiation in term of heating food was found unintentionally by Dr. Percy Spender in 1945 [11]. Nowadays the non-communication applications of microwave power have been spreading in many fields such as: medicine, chemistry, sintering, etc. There are many literatures about the microwave theory. This chapter will represent a very basic knowledge of the microwave theory concerning its heating mechanisms and electromagnetic wave. This basic knowledge is necessary to understand the physical problems in order to decide the choice of approximation method. In this chapter, an overview of the coatings and the existing techniques of curing process will be also exhibited. Thereby the response of polymeric materials to the microwave radiation will be revised in term of chemical kinetics and physical properties of microwave-cured polymers. A very important part in this chapter is the simulation. In this part, the popular existence of numerical methods will be compared to reach the most suitable approach for solving this problem. The approximation equations as well as the boundary conditions for solving microwave heating problem will be expressed either. The challenges, faced in the simulation and the solutions to release them will be taken into account. Finally, the view of the experimental system to evaluate the simulation results will also be exposed.

### 2.1 ELECTROMAGNETIC WAVE

The microwave heating utilizes energy of electromagnetic wave for the heating process. Normally in a microwave oven, the electromagnetic wave is transferred from a magnetron through a waveguide to the heating cavity. Hence this part will exhibit some knowledge about the electromagnetic wave. Basically, the electromagnetic wave includes two components: electric field and magnetic field as shown in figure 2.1.



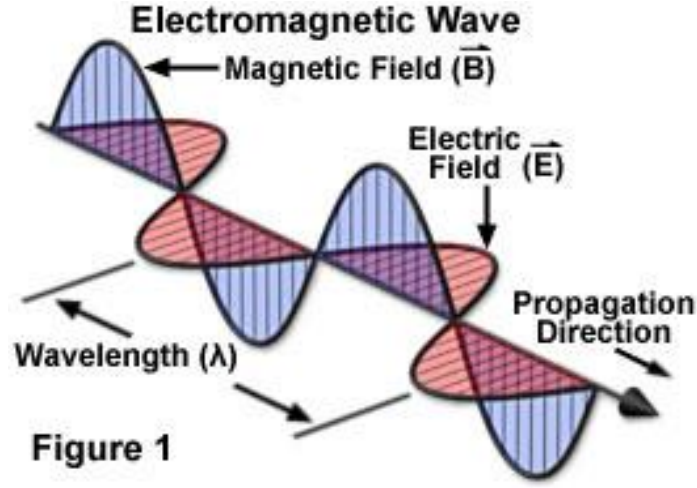


Figure 2.1: Electromagnetic wave [12]

### 2.1.1 MAXWELL'S EQUATIONS

The equations which govern the behavior of the electromagnetic wave are Maxwell's equations [13]:

$$\nabla \times \vec{E} = -\frac{\partial \vec{B}}{\partial t} \quad (2.1)$$

$$\nabla \times \vec{H} = \vec{J} + \frac{\partial \vec{D}}{\partial t} \quad (2.2)$$

$$\nabla \cdot \vec{D} = \rho \quad (2.3)$$

$$\nabla \cdot \vec{B} = 0 \quad (2.4)$$

From above, equation (2.1) is Faraday's law of induction, equation (2.2) expresses Ampere's law as amended by Maxwell to include the displacement current  $\partial \vec{D} / \partial t$ . Equation (2.3) and (2.4) are Gauss's law for electric and magnetic field.

Where  $\vec{E}$  is the electric field strength,  $\vec{H}$  is the magnetic field strength,  $\vec{B}$  is the magnetic induction, and  $\vec{D}$  is the electric flux density.  $\rho$  and  $\vec{J}$  are the free charge and the current density as a source of the electromagnetic field. In source-free region of space  $\rho$  and  $\vec{J}$  are zero and equation (2.3) and (2.4) become simpler as [14]:

$$\nabla \times \bar{H} = \frac{\partial \bar{D}}{\partial t} \quad (2.5)$$

$$\nabla \cdot \bar{D} = 0 \quad (2.6)$$

The relation between electric flux density and electric field is given by [14]:

$$\bar{D} = \epsilon_0 \epsilon_r \bar{E} \quad (2.7)$$

where  $\epsilon_0 = 8.85 \cdot 10^{-12}$  (F/m) is the permittivity of vacuum and  $\epsilon_r$  is the permittivity of the dielectric or medium.

In case of linear magnetic material, the magnetic induction and magnetic field relates as [14]:

$$\bar{B} = \mu_0 \mu_r \bar{H} \quad (2.8)$$

where  $\mu_0 = 4\pi \cdot 10^{-7}$  (Vs/Am) is the permeability of free space and  $\mu_r$  is the permeability of the magnetic media.

The relationship between current density and electric field strength following Ohm's law is given by [13]:

$$\bar{J} = \sigma \bar{E} \quad (2.9)$$

where  $\sigma$  is the electric conductivity of the material.

## 2.1.2 WAVE EQUATIONS AND PLANE WAVES

The space and time dependence of electric field and magnetic field give the wave equation and describe the wave nature of time-varying macroscopic electromagnetic field [13]. The wave equation solution for electromagnetic field is derived from Maxwell's equations in source-free and non-conducting media. In this case,  $J$  and  $\rho$  is zero.

### 2.1.2.1 THE HELMHOLTZ EQUATIONS

Assuming an  $e^{j\omega t}$  time dependence, equation (2.1) and (2.2) can be written as [14]:

$$\nabla \times \bar{E} = -j\omega \bar{B} \quad (2.10)$$

$$\nabla \times \bar{H} = j\omega \bar{D} + \bar{J} \quad (2.11)$$

Use equations (2.7) and (2.8) to replace  $\bar{B}$  and  $\bar{D}$  in (2.10) and (2.11) applying in source-free, linear, isotropic and homogeneous region equation (2.10) and (2.11) become:

$$\nabla \times \bar{E} = -j\omega\mu_0\mu_r\bar{H} \quad (2.12)$$

$$\nabla \times \bar{H} = j\omega\epsilon_0\epsilon_r\bar{E} \quad (2.13)$$

To find a solution for  $\bar{E}$ , taking curl of (2.12) and use (2.13) gives:

$$\nabla \times \nabla \times \bar{E} = \nabla(\nabla \cdot \bar{E}) - \nabla^2 \bar{E} = -j\omega\mu\nabla \times \bar{H} = \omega^2\mu\epsilon\bar{E} \quad (2.14)$$

where  $\mu = \mu_0\mu_r$  and  $\epsilon = \epsilon_0\epsilon_r$ .

In source-free, from equation (2.6) and (2.7),  $\nabla \cdot \bar{E} = 0$ , and now replace it into equation (2.14) and do the same for  $\bar{H}$ , the wave equations for  $\bar{E}$  and  $\bar{H}$  (also called Helmholtz equations) can be achieved [14]:

$$\nabla^2 \bar{E} + \omega^2\mu\epsilon\bar{E} = 0 \quad (2.15)$$

$$\nabla^2 \bar{H} + \omega^2\mu\epsilon\bar{H} = 0 \quad (2.16)$$

Propagation constant  $k$  (unit:1/m) which is also called as phase constant or wave number of the medium is defined as  $k = \omega\sqrt{\mu\epsilon}$ .

### 2.1.2.2 PLANE WAVE IN LOSSLESS MEDIUM

In lossless medium, the loss factor  $\epsilon''$  is zero, therefore  $\mu$ ,  $\epsilon$  and  $k$  are real number. The electric field can be considered with only a  $\hat{x}$  component and uniform (no variation) for the plane wave solution. Hence,  $\partial/\partial x = \partial/\partial y = 0$  and the wave equation (2.15) can be written as [14]:

$$\frac{\partial^2 E_x}{\partial z^2} + k^2 E_x = 0 \quad (2.17)$$

The solution for (2.17) is

$$E_x(z) = E^+ e^{-jkz} + E^- e^{jkz} \quad (2.18)$$

where  $E^+$  and  $E^-$  are arbitrary amplitude constants.

In time domain, for time harmonic case at frequency  $\omega$ , equation (2.18) can be expressed as [14]:

$$E_x(z, t) = E^+ \cos(\omega t - kz) + E^- \cos(\omega t + kz) \quad (2.19)$$

Assume that  $E^+$  and  $E^-$  are real constant. First term of (2.19) describes the wave travelling in  $+z$  direction and second term describes the wave travelling in negative  $z$  direction when the time increases. The travel of wave maintains a fixed point on the wave (means  $\omega t - kz = \text{constant}$ ). The notation  $E^+$  and  $E^-$  are the waves amplitudes.

The velocity of the wave at a fixed phase point on a travelling wave is called phase velocity and is given by [14]:

$$v_p = \frac{dz}{dt} = \frac{d}{dt} \left( \frac{\omega t - \text{constant}}{k} \right) = \frac{\omega}{k} = \frac{1}{\sqrt{\mu\epsilon}} \quad (2.20)$$

In free space:  $v_p = 1/\sqrt{\mu_0\epsilon_0} = c = 2.998 \cdot 10^8$  (m/s).

Applying equation (2.13) on equation (2.18) to find  $\bar{H}$  then  $H_x=H_z=0$  and

$$H_y = \frac{j}{\omega\mu} \frac{\partial E_x}{\partial z} = \frac{1}{\eta} (E^+ e^{-jkz} - E^- e^{jkz}) \quad (2.21)$$

where  $\eta = \omega\mu/k = \sqrt{\mu/\epsilon}$  is the intrinsic impedance. The wave impedance which describes the ratio of  $\bar{E}$  and  $\bar{H}$  field component of electromagnetic wave is equal to the intrinsic impedance of the medium for plane waves (in free space,  $\eta_0 = 377\Omega$ ).

### 2.1.2.3 PLANE WAVE IN A GENERAL LOSSY MEDIUM

Making some substitutions from equations (2.9) to (2.11) then taking curl to find the solution for the electric field then the wave equation is given by:

$$\nabla^2 \bar{E} + \omega^2 \mu \epsilon \left( 1 - j \frac{\sigma}{\omega \epsilon} \right) \bar{E} = 0 \quad (2.22)$$

Here a complex propagation constant is defined as [14]:

$$\gamma = \alpha + j\beta = j\omega\sqrt{\mu\epsilon} \sqrt{1 - j \frac{\sigma}{\omega\epsilon}} \quad (2.23)$$

where  $\alpha$  is the attenuation constant and  $\beta$  is the phase constant.

Assume again that the electric field has only  $\hat{x}$  component and uniform in  $x$  and  $y$  direction then (2.22) can be reduced to [14]:

$$E_x(z) = E^+ e^{-\gamma z} + E^- e^{\gamma z} = E^+ e^{-\alpha z} e^{-j\beta z} + E^- e^{\alpha z} e^{j\beta z} \quad (2.24)$$

In time domain:

$$E_x(z, t) = E^+ e^{-\alpha z} \cos(\omega t - \beta z) + E^- e^{\alpha z} \cos(\omega t + \beta z) \quad (2.25)$$

And phase velocity  $v_p = \omega/\beta$ .

The associated magnetic field can be calculated as [14]:

$$H_y = \frac{1}{\eta} (E^+ e^{-\gamma z} + E^- e^{\gamma z}) \quad (2.26)$$

where  $\eta = j\omega\mu/\gamma$  is the complex intrinsic impedance of conducting medium.

#### 2.1.2.4 PLANE WAVES IN GOOD CONDUCTOR

A good conductor (not perfect) is a special case of preceding analysis. In this case, the conductive current is much greater than the displacement current ( $\sigma \gg \omega\epsilon$ ). In case of a complex permittivity rather than conductivity, which means  $\epsilon'' \gg \epsilon'$ , the complex propagation can be approximated by ignoring the displacement current [14]:

$$\gamma = \alpha + j\beta \approx j\omega\sqrt{\mu\epsilon} \sqrt{\frac{\sigma}{j\omega\epsilon}} = (1 + j) \sqrt{\frac{\omega\mu\sigma}{2}} \quad (2.27)$$

The depth penetration here is defined as:

$$D_p = \frac{1}{\alpha} = \sqrt{\frac{2}{\omega\mu\sigma}} \quad (2.28)$$

#### 2.2.2.5 REFLECTION OF PLANE WAVES

For a plane electromagnetic wave, the wave propagates across different dielectric medium (for example from dielectric media 1 into dielectric media 2). So a part of the electromagnetic

wave will be transmitted into media 2 and the rest will be reflected into media 1 depended on the dielectric properties of the medium (figure 2.2).

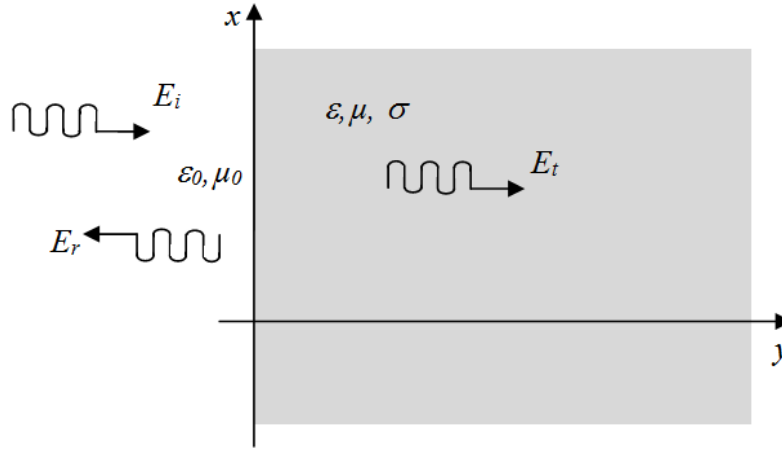


Figure 2.2: Plane wave reflection in arbitrary medium; normal incidence; where  $E_i$  is the incident electric field (assume no loss of generality),  $E_t$  is the transmitted electric field and  $E_r$  is the reflected electric field [14]

## POYNTING VECTOR

The Poynting vector is named after the inventor John Henry Poynting. It describes the directional flux density (unit:  $\text{W} \cdot \text{m}^{-2}$  - watt per square meter) of an electromagnetic field and is defined as:

$$\bar{S} = \bar{E} \times \bar{H} \quad (2.29)$$

Following [13], the complex Poynting vector for a time harmonic field and a plane electromagnetic wave is given by:

$$\bar{S}_e = \frac{1}{2} \bar{E}_e \times \bar{H}_e^* = \frac{1}{2} E_{xe} \bar{H}_{ye}^* e_z \quad (2.30)$$

where \* notices the conjugate complex value;  $E_x$  and  $E_y$  are the field components of electric and magnetic in direction  $x$  and  $y$ ;  $e_z$  is the unit vector of the positive  $z$ -direction of the propagation of the electromagnetic wave. The real part represents the time averaged power flow density and the imaginary part is the reactive component of flow density.

In case of wave reflection, the Poynting vector shows the power to be travelling in the negative  $z$ -direction for the reflected wave [14].

## PLANE WAVE REFLECTION AND TRANSMISSION IN GENERAL MEDIUM

The incident electric field and magnetic field as well as the reflected electric field and magnetic field following [14] can be written, for  $z < 0$  as:

$$\bar{E}_i = \hat{x}E_0e^{-jk_0z} \quad (2.31)$$

$$\bar{H}_i = \hat{y}\frac{1}{\eta_0}E_0e^{-jk_0z} \quad (2.32)$$

$$\bar{E}_r = \hat{x}\Gamma E_0e^{+jk_0z} \quad (2.33)$$

$$\bar{H}_r = -\hat{y}\frac{\Gamma}{\eta_0}E_0e^{+jk_0z} \quad (2.34)$$

where  $E_0$  is the arbitrary amplitude,  $\eta_0$  is the impedance of free space and  $\Gamma$  is the unknown reflection coefficient of the reflected electric field.

In (2.33) and (2.34), the sign in exponential terms has been chosen as positive, to represent wave travelling in negative  $-\hat{z}$  direction of propagation, as derived in (2.19). This is also consistent with the Poynting vector of the reflected wave as given:

$$\bar{S}_r = \bar{E}_r \times \bar{H}_r^* = \frac{-|\Gamma|^2|E_0|^2\hat{z}}{\eta_0} \quad (2.35)$$

The transmitted field for  $z > 0$  in the medium can be written as [14]:

$$\bar{E}_t = \hat{x}\Pi E_0e^{-\gamma z} \quad (2.36)$$

$$\bar{H}_t = \frac{\hat{y}\Pi E_0}{\eta}e^{-\gamma z} \quad (2.37)$$

where  $\Pi$  is the transmission coefficient of transmitted electric field,  $\eta$  is the complex intrinsic impedance of the lossy medium in region  $z > 0$  and  $\gamma$  is the propagation constant (see equation (2.23)).

Applying the boundary condition for  $E_x$  and  $H_y$  at  $z=0$  to find  $\Gamma$  and  $\Pi$ . At  $z=0$  the tangential field component still has to be continuous, therefore the following equation can be achieved:

$$1 + \Gamma = \Pi \quad (2.38)$$

$$\frac{1 - \Gamma}{\eta_0} = \frac{\Pi}{\eta} \quad (2.39)$$

Solve (2.43) and (2.44) then  $\Gamma$  and  $\Pi$  will be found as [14]:

$$\Gamma = \frac{\eta - \eta_0}{\eta + \eta_0} \quad (2.40)$$

$$\Pi = 1 + \Gamma = \frac{2\eta}{\eta + \eta_0} \quad (2.41)$$



## 2.2 MICROWAVE HEATING THEORY

Heating by the means of microwave irradiation results in a very efficiency. In term of energy, in a comparison with the convectional heating, the microwave heating promises a potential savings. In general, it consumes 10 – 100 times less energy and requires 20 -200 times less time [11].

### 2.2.1 GENERAL OF MICROWAVE HEATING

Microwave heating which uses electromagnetic waves in the frequency range 300 MHz (0.3 GHz) to 3000 MHz (30 GHz), corresponding to wavelengths of 1cm to 1m, that pass through dielectric materials and cause its molecules to oscillate and generate heat [11].

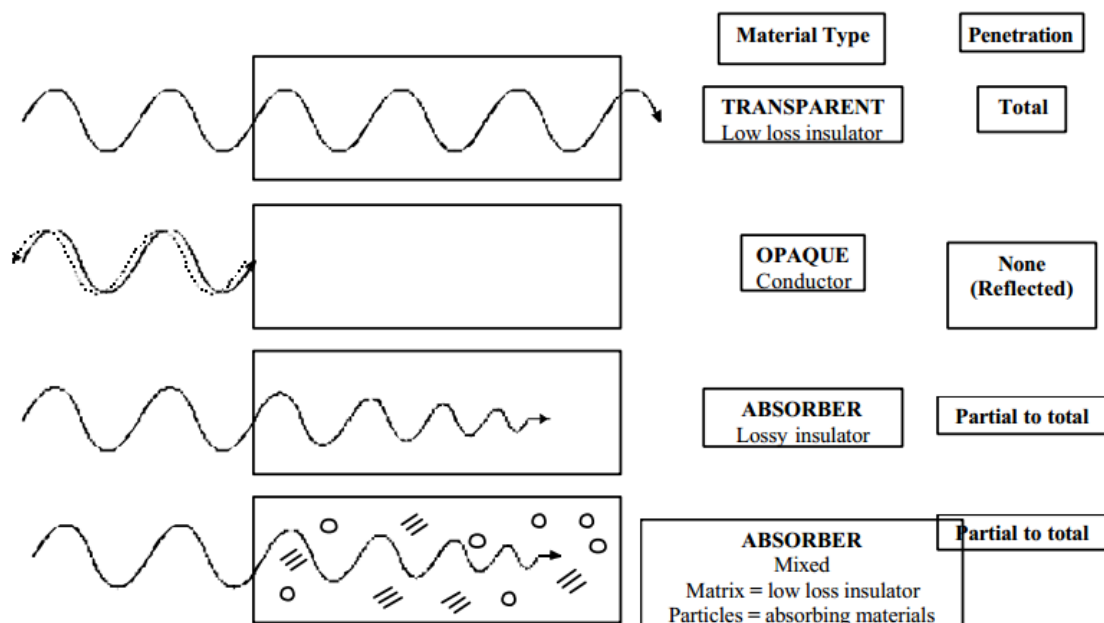


Figure 2.3: The interaction of microwaves with different materials [15]

Microwave heating can be divided into two types: pure microwave heating and hybrid microwave heating [16].

In pure microwave heating, the materials (heated objects) absorb the microwave energy and are heated up. The pure microwave heating is often applied to materials which can couple well to the microwave radiation (high tangent loss). Because there are many materials which have properties that are not able to directly couple to microwave frequency of 915 MHz and 2.45 GHz at room temperature.

In the hybrid microwave heating, both microwave and conventional heating are combined for the thermal treatment of poorly absorbing materials. The materials are treated until they reach a temperature where they are capable of absorbing microwave effectively [17].

The mechanisms that aid energy distribution process of microwave heating are dipole friction, current loss and ion jump relaxation [18, 19].

- **The dipole friction** or dipolar polarization is a mechanism of microwave heating in which the polar molecules of the heated objects interact with the electric field component. The molecular dipoles align in the applied electric field being exposed to microwave frequency. The dipole field follows the oscillations of the applied electric field and therefore the energy is lost in form of heat through molecular friction and dielectric loss. There will be no heating in high-frequency irradiation because the dipole does not have sufficient time to reorient or in low-frequency irradiation due to the too slow reorientation. The frequency of 2.45 GHz is the most popular used in commercial systems because this frequency is in between two extremes and gives the molecular dipole sufficient time to reorient in the field but not follow the alternating field precisely. When the molecular dipole aligns itself to the field, the field is already changing to next phase. This different phase causes an energy loss through molecular friction and collisions and makes dielectric heating increase.
- **Current loss** occurs when the loss is attributed to current leakage caused by the big different electrical resistivity of material (high) and the loss current (low). This mechanism often takes place at radio frequencies and can occur at high microwave frequencies.
- **Ion jump relaxation** or ionic conduction is a mechanism, in which under the impact of electric component of electromagnetic field the ions of the heated objects jump forth and back. And thus they collide with other molecules or atoms in the neighborhood. This collision causes oscillation or motion and creating heat consequently.

Those mechanisms above can be implemented with different materials. Nevertheless, there will be available frequency so that materials with permanent dipoles have high dielectric loss and materials polarized only by electronic or ionic distribution have low dielectric loss. Hence the materials with high dielectric loss can be heated rapidly and uniformly and the others almost remain at room temperature. And consequently the heating process by the means of microwave irradiation can lead to a reduced processing time and energy conservation [18].

## 2.2.2 DIELECTRIC MATERIALS

Materials which have dielectric properties, also called dielectric materials are electric isolators that can be polarized by an electric field. As the electric field is applied, the polarization of dielectrics appears from the finite displacement of charges [20]. Due to the dielectric polarization, an internal electric field is created which reduces overall field in the dielectric material itself. With dielectric materials which have weakly bonded molecules, the molecules will be polarized and try to reorient so that their symmetry axis aligns to the field [19]. This kind of molecular level is especially significant in the context of microwave dielectric heating.

### 2.2.2.1 COMPLEX PERMITTIVITY

Permittivity  $\varepsilon$  is a property of dielectric materials which describes the behavior of them in the high frequency microwaves. The relative permittivity is the permittivity of a material to that relative of free space [20]. The relative permittivity is given by:

$$\varepsilon_r = \varepsilon' - j\varepsilon'' \quad (2.42)$$

where  $\varepsilon'$  is the real part of the permittivity (the dielectric constant) and  $\varepsilon''$  is the loss factor which reflects the conductance of material.

The reorientation of the dipoles and the displacement of charges is equivalent to an electric current, known as Maxwell displacement current. The ideal dielectric materials will have no delay between the orientations of molecules and the variations of the alternating voltage. The displacement current will be  $90^\circ$  out-of-phase with the oscillating electric field (figure 2.4).

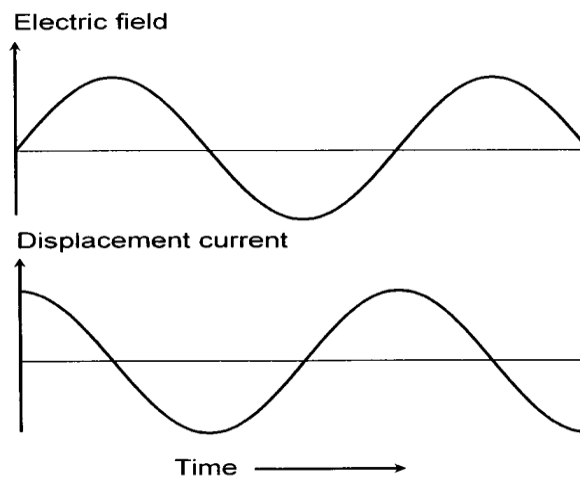


Figure 2.4: Application of a sinusoidal electric field for an ideal dielectric (top) and the out-of-phase displacement current which is induced (bottom) [20]

From the figure above, there is no component of the displacement current in-phase with the electric field. Therefore the product of  $E \times I = 0$  and no heating takes place. The rotation of the polar molecules will start to have a delay behind the electric field when the frequency of an electromagnetic radiation reaches to the microwave region. Hence this results in a phase shift  $\delta$  which current acquires a component  $I \times \sin \delta$  in phase with electric field (figure 2.5). Thus the resistive heating takes places in the medium and is described as dielectric loss which causes the energy to be absorbed from the electric field [20].

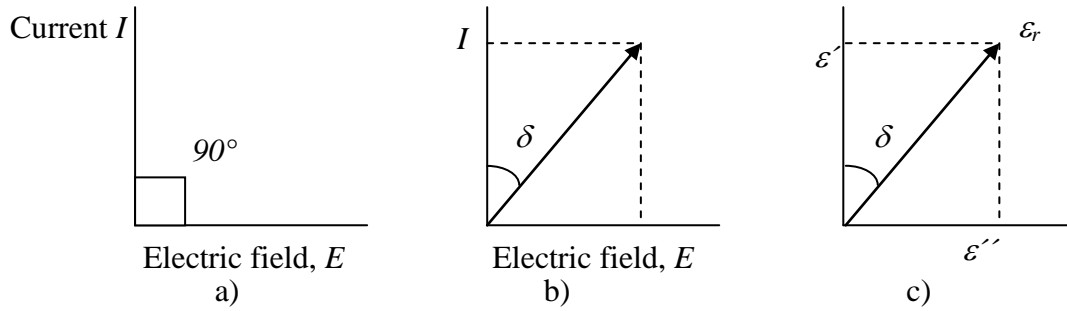


Figure 2.5: Phase diagram for an ideal dielectric where energy is transmitted without loss (a); where there is a phase shift  $\delta$  and the current acquires a component  $I \times \sin \delta$  in-phase with the voltage and consequently there is a dissipation of energy (b); the illustration of the relationship between  $\epsilon_r$ ,  $\epsilon'$ ,  $\epsilon''$

In figure 2.5 (c),  $\tan \delta = \epsilon' / \epsilon''$  is described as the energy dissipation factor or loss tangent [20].

### 2.2.2.2 LOSS FACTOR

In equation (2.42),  $\epsilon''$  is called the loss factor. The loss factor describes the absorption ability of a material to microwave radiation. If the absorption ability of a material is big then most of the incident energy will be absorbed after penetrating a few millimeters into the materials. Therefore the external part of the material will have only little effect. This can cause the unexpected non-uniform heating. Following [21], the loss factors in between the interval  $10^{-2} < \epsilon'' < 5$  are considered as good individuals for a microwave heating application.

Loss factors of some materials may be dependent on temperatures. Thus materials which have no response to microwave at low temperature should be pre-heated by other means and then can be applicable in microwave heating [7]. The positive coefficient of the loss factor may cause the thermal runaway. This will become seriously in the case when phase change causes the increase of loss factor suddenly. Table 2.1 lists some loss factor values of some common materials in variable frequencies.

Material	27.12 MHz	900 MHz	2450 MGz
Pork fat	51	17	2.7
Polyethylene	<0.1	<0.1	0.001
PVC	<0.1	<0.1	0.1
Salt water	900	29	19.6
Pure water	0.4	3.9	10.7

Table 2.1: Loss factors of some common materials [22]

### 2.2.2.3 PENETRATION DEPTH

Penetration depth is a value which is used to present the measure of how deep light or electromagnetic radiation can penetrate into a material. The penetration depth of the electric field or current density is defined as the distance as the field has to traverse so that its magnitude reduces to  $1/e$  of its surface value [23]. The magnitude reduces to  $1/e = 0.368$  that means the depth in the material at which the transferred power has been reduced to 37% of its original value [16].

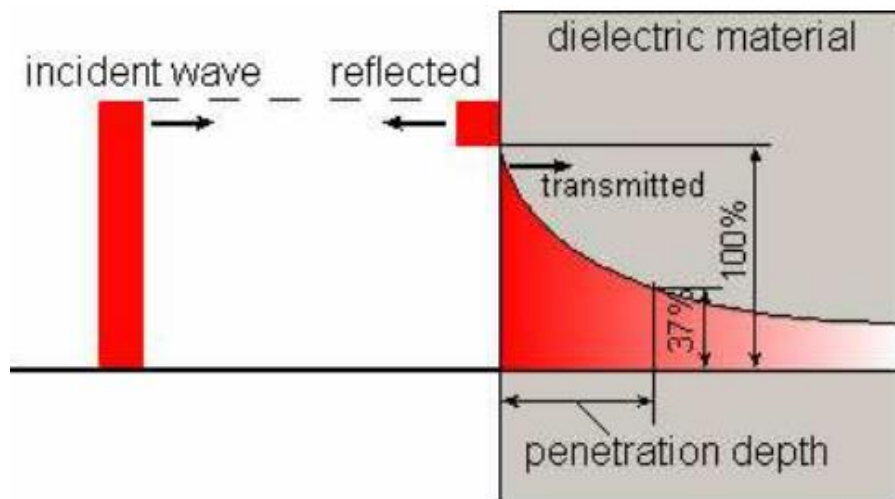


Figure 2.6: Penetration depth [16]

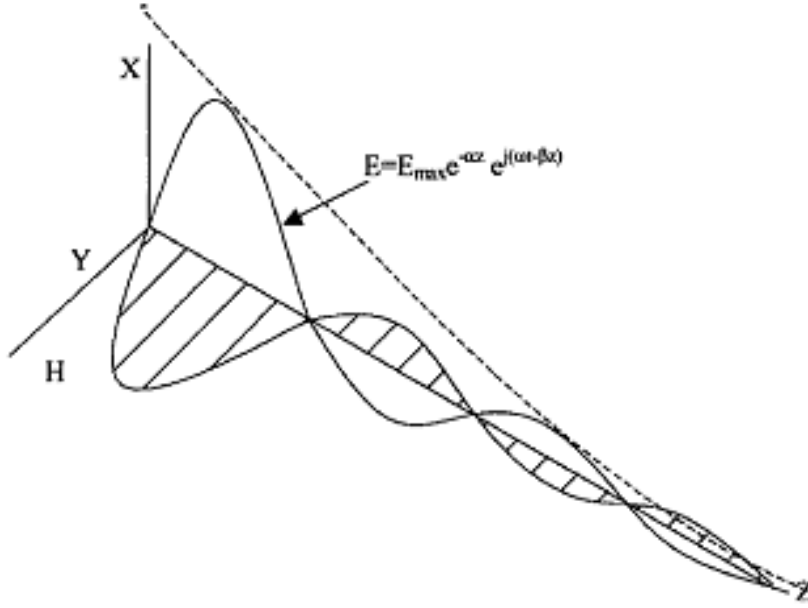


Figure 2.7: Propagation of a plane wave in lossy medium [21]

Following [12], the calculation of the penetration depth can be derived by Maxwell equation:

$$D_p = \frac{c}{2\pi f \sqrt{2\epsilon' \left( \sqrt{1 + \left( \frac{\epsilon''}{\epsilon'} \right)^2} - 1 \right)}} \quad (2.43)$$

The approximated equation can be achieved for the materials with low loss factor [21]:

$$D_p = \frac{c\sqrt{\epsilon'}}{2\pi f \epsilon''} \quad (2.44)$$

where  $D_p$  is the penetration depth of the wave (m),  $c$  is the speed of light (m/s) and  $f$  is the frequency of the electromagnetic wave.

From equation (2.44), the lower frequency is the bigger penetration depth is. However the more depth increases, the more electric field reduces which can result in no increase in heating.

#### 2.2.2.4 POWER DISSIPATION

The equation of the power dissipation is given by [18]:

$$P_d = \frac{1}{2} \omega \epsilon_0 \epsilon'' |E|^2 \quad (2.45)$$

where  $P_d$  is the power dissipation density (watt per cubic meter)  $\omega$  is the angular frequency,  $\epsilon_0$  is the permittivity of the free space,  $\epsilon''$  is the loss factor and  $E$  is the electric field intensity (Volt per meter).

From equation (2.4), there are some features that can be concluded as follow [4, 16]:

- The power density dissipated in work load is a proportional to the frequency where other parameters are constant. That means the volume of work load in an oven may be reduced as the frequency rises, resulting in a compact oven.
- The power density is proportional to the loss factor.
- For the constant power dissipation density, the electric field intensity reduces as the frequency rises.
- Generally but not always,  $\epsilon''$  rises with frequency due to the effects of the angular frequency and volumes of dielectric materials.
- The electric field is the field within dielectric. The electric field just outside the dielectric at least equal to  $E$ . The voltage breakdown is possible limitation due to the high value voltage of the external electric field.
- In practice,  $\epsilon'$  varies not only with frequencies but also with temperature, moisture and physical state (solid or liquid) and composition. It is important to consider  $\epsilon'$  and  $\epsilon''$  during the process.

## 2.3 COATINGS AND THEIR CURING PROCESSES

As mentioned in the previous chapter, coatings are useful in term of protecting electronic assemblies from environmental attacks. When an electronic assembly must undergo harsh environments, then added protection is necessary. Most of circuit board assembly houses coat a layer of transparent conformal coating rather than potting, which is a process of filling a complete electronic assembly with a solid or gelatinous compound for resistance shock and vibration, and for exclusion of moisture and corrosive agents [24]. This part will represent an overview about coatings and their curing processes.

### 2.3.1 TYPES OF COATINGS

The types of coatings are classified by the cured chemistry of the coatings [6]. They are:

- **Type AR- Acrylic (Acrylic Resin):** These are the coatings which are easy to apply and easy to remove and repair due to their thermoplastic lacquer base. Their moisture resistances are similar to urethane and silicone but they show poor resistance to petroleum solvents and alcohol. Dielectric withstand is greater than 1500 volts and temperature range is from -59°C to 132°C [25].
- **Type ER- Epoxy (Epoxy Resin):** This type is extremely good for solvent and moisture resistance and very difficult to repair or remove. Epoxy resins are usually available as two part compounds that start curing upon mixing but single part coatings are available to be cured thermally or by UV exposure. Due to the excellent solvent resistance, epoxy coatings are virtually impossible to strip.
- **Type SR- Silicone (Silicone Resin):** It is easy to apply and but difficult to remove. Because of its flexibility, this type of coating can resist well against thermal shock. The dielectric withstand is generally lower than for other coatings (1100 volts/mil) but due to the flexibility, it is possible to build a thicker silicone coating than the thickness build of acrylic and urethane. The operating temperature range is from -55°C to 200°C [26].
- **Type UR- Polyurethane or Urethane (Polyurethane Resin or Urethane Resin):** These are hard and durable coatings, therefore they are very good in abrasion and solvent resistance. The significant shrinkage during the curing process and extremely hard film can stress the electric components [25]. This type of coatings are difficult to apply on PCBs and almost impossible to remove. The UR coatings can be soldered through for rework, but usually result in a brownish residue which affects the



appearance of the assembly [26]. The operating temperature range is the same as type AR.

- **Type XY- Paraxylylene:** This type has a good dielectric property, low thermal expansion good abrasion resistance and outstanding chemical resistance and has been used to protect PCBs from harsh environment [25]. The XY coatings have consistent thickness with true conformance to the board assembly contour and being pinhole and bubble-free either. The disadvantages are high cost, poor exhibition in reparability, sensitivity to contaminant and the need for vacuum application technique.

### 2.3.2 CURING PROCESSES OF THE COATINGS

Coatings can be applied on electronic assemblies by brushing, spraying and dipping before the curing process. There is something to notice here that a curing and a drying are distinctly different in the coating process. The drying is where the coating is fit to be handled after the application of coatings and the curing is where the optimum properties of the coating are reached for the full performance of protection [25].

As the knowledge from [27, 28] there are three stages of the coating that can be taken into account. They are:

- **Tack free:** This is where the coating is dry enough to handle carefully.
- **Fully dried:** This is where the coating and the PCB can be handled normally but the coating is not fully cured.
- **Fully cured:** The coating has reached its optimum properties.

The state, required for coating might be achieved at room temperature by air drying. To achieve the desired results, accelerated heat or moisture must be applied, or the application of UV light may be necessary alternatively.

The curing process implies that the optimum properties of the coatings are met for example electrical and mechanical characteristics and thereby the coatings do not impede the operation of the PCBs. There are some curing techniques (accelerated method) which are used to dry and cure the coatings quicker [27, 28]. They are:

- **Heat curing:** using heat to rise up the temperature curing, therefore dry out the carrier of the coating resin and speed up the film forming process. Film forming process is where the majority of coating solvent or liquid has been removed and stable dry films have been formed on PCBs. Because most of the coatings benefit from the raised

temperature curing, thus this method is often utilized. Time of the heat curing is about minutes, for instance the time for the solvent based acrylic coating from 20°C to reach 80° is 10 minutes, the total time for this curing process is 20 minutes including cooling process [27].

- **Moisture curing:** This is the application of moisture creates a chain of reaction in many conformal coatings such as polyurethanes which effectively cure the coating. Moisture cure coating need to be handled carefully in process and storage to avoid premature curing before application, because this method is one wave process and if a coating exposed to moisture then it is difficult to reserve the process [28].
- **UV curing:** UV curing is normally used for curing UV coatings which have response to the specific wavelengths of the UV light applied [27].
- **Chemical reaction:** For some products, it is able to obtain curing by mixing two separated parts of material which chemical reacts to create a cure product, when combined correctly [28].
- **Combination cure:** Some coatings have a dual cure process. For instance, now many UV cure products have a primary cure mechanism of UV light but secondary cure mechanism of moistures [28].

### 2.3.3 MICROWAVE PROCESSING OF POLYMERS

There are many technical challenges of heating polymers associated with conventional processing due to their low thermal conductivity. Hence there are many researching works concerning microwave processing for polymers [7].

#### 2.3.3.1 MATERIAL BEHAVIOR

The material behavior (here means the dielectric properties of polymeric resins) undergoing cure has been investigated at microwave frequencies [29] and lower frequencies [30, 31]. In this case, the change of net-work structure of the polymers results in the change of dielectric properties, which directly corresponds with the changes in viscosity of the resins. Initially, the resins couple well with the microwaves. However, when crosslinking proceeds and viscosity increases, the dielectric loss will decrease because changes in the resin viscosity will affect the ability of dipoles to orient in the electric field [32]. The knowledge of these changes in dielectric properties can be utilized to optimize the cure cycle of in microwave processing. Last but not least, the ability of microwave processing of polymers is up to the dipole

structure, microwave frequencies, temperatures and additives or fillers which are included with the polymers [7].

### 2.3.3.2 POLYMER PROCESSING

Since the early experimental investigations of microwave curing of composites, there were so many attempts to get the knowledge of the microwave effect on the chemical kinetics and physical properties of microwave-cured polymers. Nevertheless, there are controversial and conflicting results of the existing researches of microwave effect on thermosetting resins.

Many commonly scientific reports have exposed that microwave effect could accelerate the cure kinetics of thermosetting resins. Following [33], an early literature on the microwave processing of polymers, the required cure time of polymers reduced strongly in microwave processing. All the investigations in cure kinetics of epoxy resin systems according to [34], [35] and [36], proved that the reaction rates were enhanced and the time to gelation and vitrification were reduced due to microwave heating. In [34], the author has demonstrated that molecular structures and curing agents affected the magnitude of the acceleration in the microwave heating. A conclusion of the investigation of the author in [35] was that the molecular structures of some microwave-cured polymers are different in comparison with the conventionally cured ones. Contrarily, the works of [37] and [38] have shown that there was no change in the cure kinetics as well as a retardation of cure kinetic when cured by microwave. In their recent study, the crosslinking of several different polymeric materials have been investigated by using an in-situ monitoring method and the result was that the accelerated cured kinetics was unfounded [37]. The confliction of different laboratories' works lead to the need of more study in this area.

About the physical properties, follow [39], the tensile strength of microwave samples below 80% degree of cure was significantly lower than thermally cured samples. And as the extent of cure raised up, the tensile strength of microwave samples improved. At 100% degree of cure, the mechanical strength of microwave-cured samples has beaten the thermally cured ones. Moreover, the modulus elasticity was a little bit higher in microwave-cured samples. The hint given by the author of [39] was that the reduced strength at lower degree of cure was a result of less molecular entanglement of the polymer network due to the alignment in the electric field. Still according to this author, the molecular arrangement in the electric field could cause the higher modulus because the alignment might produce higher packing with lower free volume resulting in a higher modulus. The results of this investigation were similar

as the results of the study in [40]. In that research, the author proved both tensile strength and modulus increased for microwave-cured samples. However, following the author of [36], there was no significant change in the elastic properties of epoxy resins cured by microwave heating.

## 2.4 SIMULATION

Simulation is a very important tool in this work. The roll of the simulation here is a presentation of the safe-engineering through predictions, analyses and optimizations for the whole process. Once the facing problems here are consistent with the microwave heating which includes electromagnetic wave and heat transfer problems, the suitable numerical method need to be determined.

### 2.4.1 THE CHOICE OF SUITABLE NUMERICAL METHOD

Since the digital computers appeared, mathematical modeling has been becoming easier by their help. Solutions are able to achieve for simple problems accurately. However, most of the interest engineering problems are elaborate. Hence the refinement that analyzed during the design process will decide how good the results are. This leads to a requirement that how to choose and use the numerical methods to obtain the best approximate solution for a real engineering problem.

In the field of numerical simulation, there are some numerical methods that can be taken into account. Three most popular approximation numerical methods that can be considered are: finite element method (FEM), finite difference method (FDM) and boundary element method (BEM). All these three methods by linear, stationary problems (or equivalent tasks the by other problems) are based on the equation system of the form  $Ax = b$  [41]. BEM actually is the method, which basic is integral equation to solve the engineering problems concerning only state functions at boundaries [41]. Therefore the considering approximation methods are down to two numerical methods, FEM and FDM.

FEM is a numerical method for finding the approximation solution of a differential or an integral equation. This method is possible to use for many engineering fields and physical problems, where the governing differential equations are available [42]. And FDM is an approximation method for solving partial differential equation [43]. Basically FDM uses finite difference equations to approximate derivatives. To have a clear point of these two methods, a comparison between these both is given as:

- The good characteristic of FDM is that it is easy to implement [41, 43].
- The good characteristic of FEM is that it can quite easily handle complicated geometries and boundaries [44, 45]. Meanwhile FDM is restricted in its basic form to handle rectangular shapes and their alterations [41].
- FDM could be considered as a special case of FEM approach [46]. For example, if the problem is discretized by a rectangular mesh with each rectangular divided by two triangles then the first order FEM will be identical to the FDM for Poisson's equation.
- The quality of the FEM approach is often higher than the corresponding FDM approximation [41]. Nevertheless, it should be noticed that is extremely problem-dependent and there are still some particularly contrary examples.
- Generally, the FEM is the choice of all type of analyses in structure mechanic whereas the FDM tend to be used in a computational fluid dynamic (CFD) [41].

With the comparison above, due to more dominated features, the suitable numerical method which is able to solve the problem is the FEM.

## 2.4.2 THE CHOICE OF A SUITABLE SOFTWARE PROGRAM AND GEOMETRICAL PROBLEMS

Recently in the market, there are two most popular software programs based FEM: ANSYS and COMSOL Multiphysics. Those both can handle the microwave heating problem in 3D geometry. ANSYS is a powerful software program which has been developing for a long time. Meanwhile COMSOL Multiphysics is latterly wide-known due to its friendly user-interface and power in solving physical fields and their couple problems.

### 2.4.2.1 THE CHOICE OF A SUITABLE FEM-BASED SOFTWARE

To have a right decision of which is the suitable choice, the processes to solve the microwave heating by using those programs are exhibited for the discussion as shown in figure 2.8 and figure 2.9:

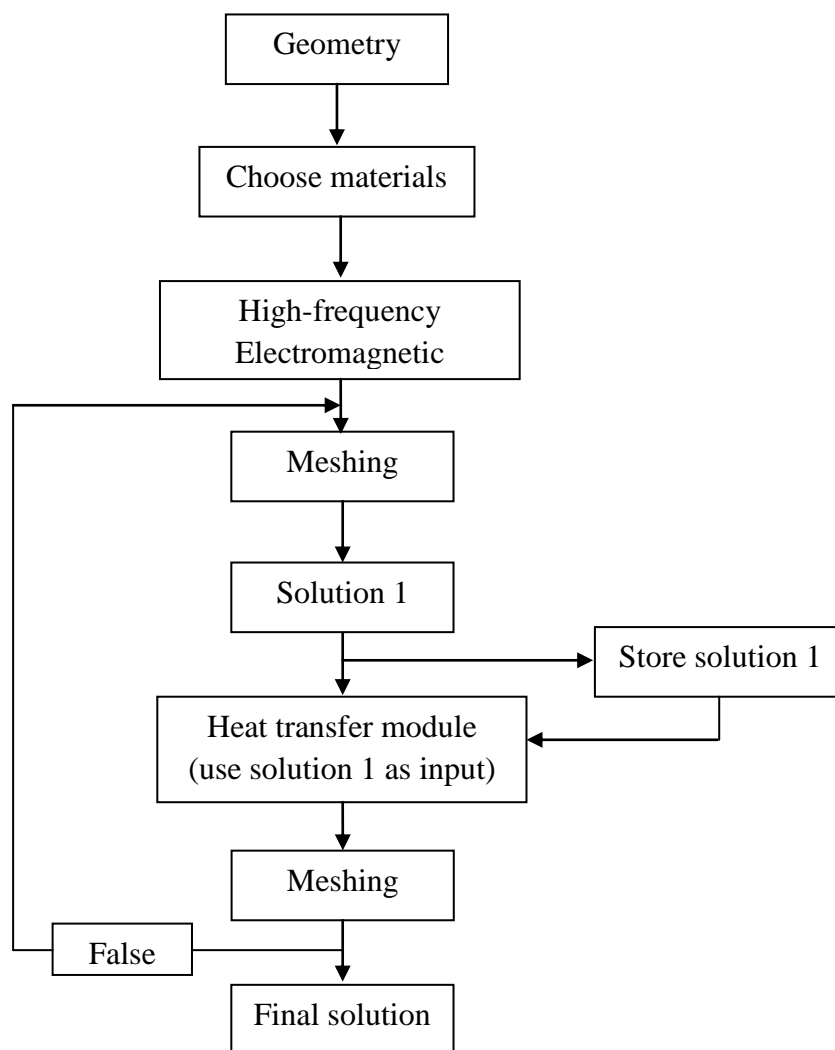


Figure 2.8: The process for solving the microwave heating problem operated by ANSYS

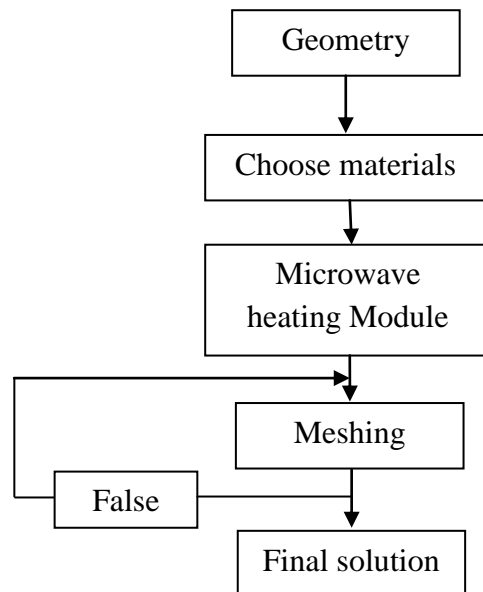


Figure 2.9: The process for solving the microwave heating problem operated by COMSOL

As seen in figure 2.8, the process for solving the microwave heating done by ANSYS is the normal way to solve couple problems and it is quite complicated. For the microwave heating, the users need to couple two fields, high-frequency electromagnetic and heat transfer module. The high-frequency electromagnetic module will be computed first. Afterwards the calculated result will be saved in storage and used as the input of the heat transfer module to get the final solution. Notice here that each module needs a meshing separately because the modules concerning to differently separated fields, and the correspondingly optimal element types for solving different fields may be not alike. Whereas with COMSOL, the software developers have supported the particular microwave heating module, which already combined the frequency electromagnetic module and the heat transfer module. Additionally, the meshing only needs to be done once and the software will select the optimally associated element types automatically. That really makes the simulation work become easier especially for the new users. Both these software programs are able to solve this problem with reliable approximation. The choice of software program here is dependent on the users. ANSYS interests the professional users because they can interfere more to the simulation process. Meanwhile COMSOL is attractive to the others due to their friendly interface and easy implementation. This is the reason why somehow ANSYS is more popular in the professional environment and COMSOL tends to appear more in the university environment.

With the scope of this study, COMSOL Multiphysics is the suitable choice for the simulation of the microwave treatment for PCBs.

### 2.4.2.2 GEOMETRICALLY FACING PROBLEMS

Once when the tool is determined, the problem of 3D simulation that one has to face in this case is the great range of dimensions between geometric objects. First challenge is the aberration of dimensions between the geometry of the heating cavity (in about hundred mm) and the geometry of PCBs (thickness is about 1.5 to 2.5 mm). The most trouble comes from the thin thickness of the copper structures on PCBs (about  $\mu\text{m}$ ). The different dimensions can cause a rush of mesh density, a high cost of CPU time and memory storage but a coarse mesh density can lead to unreliable solutions. To avoid the rush of mesh density and insure the reliable solutions are the challenge for the simulation works and this individual investigation either. With 3D geometries, the idea to have acceptable solutions is that neglecting the thickness of the metallic structures on PCBs. There are two ways to do it with COMSOL:

- Importing external geometric files of PCB designs from ECAD's extension, and then assigning the metallic structures to metal shells. Now the software will consider the metallic structures as metal layers without thickness. This way requires ECAD software tools to design the PCBs and export the ECAD extensions. The disadvantage here is sometimes failures could be occurred and users may get trouble to control the scale of the imported files [45].
- Using the geometry design tool of COMSOL to draw 3D objects but design the copper structures in 2D on working planes and then assigning them as perfect conductor layers.

The second way is prefer to use in this study, because a suitable ECAD software is not anytime possible and although the metallic structures on real PCBs are quit complicated but this does not mean it is impossible to design with COMSOL. Since the desired final result is the temperature distribution on PCB then the mesh for the air which does not influence much on the temperature can be set roughly. However, the high mesh density should be created for the PCB substrate and the copper layer. These setting can insure an acceptable result and less computing time.

### 2.4.3 FINITE ELEMENT APPROXIMATION OF THE MICROWAVE PROCESS

The microwave heating problem is a couple of problems including high-frequency electromagnetic module and heat transfer module. Therefore the outputs needed to find are electric field  $E$  and temperature  $T$ .



Recall the Maxwell's equations and assume for time harmonic dependence:

$$\bar{E}(x, y, z, t) = \bar{E}(x, y, z)e^{j\omega t} \quad (2.46)$$

$$\bar{H}(x, y, z, t) = \bar{H}(x, y, z)e^{j\omega t} \quad (2.47)$$

Then the Helmholtz's curl-curl equations can be written as [46]:

$$\nabla \times \frac{1}{\mu} \nabla \times \bar{E} - (\omega^2 \epsilon - j\sigma\omega)\bar{E} = 0 \quad (2.48)$$

$$\nabla \times \nabla \times \bar{H} - \mu(\omega^2 \epsilon - j\sigma\omega)\bar{H} = 0 \quad (2.49)$$

The boundary conditions:

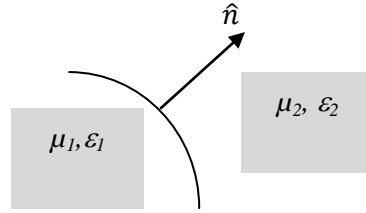


Figure 2.10: Boundary of medium 1 and medium 2 with normal vector  $\hat{n}$  [45, 46]

At the boundary:

$$\hat{n} \cdot (\bar{B}_2 - \bar{B}_1) = 0 \quad (2.50)$$

$$\hat{n} \cdot (\bar{D}_2 - \bar{D}_1) = \rho_s \quad (2.51)$$

$$\hat{n} \times (\bar{E}_2 - \bar{E}_1) = 0 \quad (2.52)$$

$$\hat{n} \times (\bar{H}_2 - \bar{H}_1) = J_s \quad (2.53)$$

where  $\rho_s$  and  $J_s$  are the charge and the current density at the boundary  $S_I$ .

A *Perfect Electric Conductor* condition happens when medium has a very high electric conductivity ( $\sigma \rightarrow \infty$ ) then [45]:

$$\hat{n} \times \bar{E}_2 = 0 \quad (2.54)$$

Robin boundary condition (also called *Impedance Boundary* condition in electromagnetism) is applied for the metallic walls of the heating cavity [45]:

$$\hat{n} \times \left( \frac{1}{\mu} \nabla \times \bar{E} \right) + \gamma \hat{n} \times (\hat{n} \times \bar{E}) = \bar{Q} \quad (2.55)$$

When  $\gamma=0$  and source  $\bar{Q}=0$  then (2.55) becomes:

$$\hat{n} \times \bar{H} = 0 \quad (2.56)$$

This is the condition when the boundaries are *Perfect Magnetic Conductors* [45]. This condition can be applied to the symmetric plane (in the case of symmetric geometry, the geometry can be reduced by a half. Hence the computation can be lighter).

Now the finite element analysis will be operated to find the electric field  $E$ . The equation (2.48) set in region  $\Omega$  (volume), the equation (2.54) set in boundary  $S_1$  and the equation (2.55) set in boundary  $S_2$  will be the basic equations of the analysis.

Multiplying by a continuous differentiable vector field  $\bar{F}$  then the integral form of (2.48) can be written as:

$$\int_{\Omega} \bar{F} \cdot \left( \nabla \times \frac{1}{\mu} \nabla \times \bar{E} \right) dV - \int_{\Omega} (\omega^2 \epsilon - j\sigma\omega) \bar{F} \cdot \bar{E} dV = 0 \quad (2.57)$$

Considering the first term of the right handside of the equation (2.57), applying the scalar triple product of the vector identity [47]  $A \cdot (B \times C) = B \cdot (C \times A) = C \cdot (A \times B)$  for the equation within the integral symbol then it will become:

$$\bar{F} \cdot \left( \nabla \times \frac{1}{\mu} \nabla \times \bar{E} \right) = \nabla \cdot \left( \frac{1}{\mu} \nabla \times \bar{E} \times \bar{F} \right) \quad (2.58)$$

Using the vector identity  $A \times B = -B \times A$  [47] twice then it gives:

$$\nabla \cdot \left( \frac{1}{\mu} \nabla \times \bar{E} \times \bar{F} \right) = \nabla \cdot \left( \bar{F} \times \frac{1}{\mu} \nabla \times \bar{E} \right) \quad (2.59)$$

Using the divergence of vector identities [47]  $\nabla \cdot (A \times B) = B \cdot (\nabla \times A) - A \cdot (\nabla \times B)$  then it gives:

$$\nabla \cdot \left( \bar{F} \times \frac{1}{\mu} \nabla \times \bar{E} \right) = \frac{1}{\mu} (\nabla \times \bar{F}) \cdot (\nabla \times \bar{E}) - \bar{F} \cdot \left( \nabla \times \frac{1}{\mu} \nabla \times \bar{E} \right) \quad (2.60)$$

Considering the second term of the left handside of the equation above and applying the divergence theorem ( can be seen in appendix D) and using the equation (2.55) to replace in, the integral equation (2.58) can be rewritten:

$$\int_{\Omega} \left\{ \frac{1}{\mu} (\nabla \times \bar{F}) \cdot (\nabla \cdot \bar{E}) - (\omega^2 \epsilon - j\sigma\omega) \bar{F} \cdot \bar{E} \right\} dV + \int_{S_2} \bar{F} \cdot (\bar{Q} - \gamma \hat{n} \times \hat{n} \times \bar{E}) dS = 0 \quad (2.61)$$

Now doing the approximation that the electric field is the total sum of the electric field of each element [48]:

$$\bar{E}(\bar{r}) \approx \sum_j^n E_j \bar{N}_j(\bar{r}) \quad (2.62)$$

where  $\bar{N}_j(\bar{r})$  is the edge element.

Using Garlekin's method [48, 49, 50] then the equation (2.61) can be expressed as:

$$\int_{\Omega} \left\{ \frac{1}{\mu} (\nabla \times \bar{N}_i) \cdot (\nabla \cdot E_j \bar{N}_j) - (\omega^2 \epsilon - j\sigma\omega) \bar{N}_i \cdot E_j \bar{N}_j \right\} dV + \int_{S_2} \bar{N}_i \cdot (\bar{Q} - \gamma \hat{n} \times \hat{n} \times E_j \bar{N}_j) dS = 0 \quad (2.63)$$

Implementing some changes then (2.63) can be rewritten [46]:

$$\int_{\Omega} \left\{ \frac{1}{\mu} (\nabla \times \bar{N}_i) \cdot (\nabla \cdot \bar{N}_j) - (\omega^2 \epsilon - j\sigma\omega) \bar{N}_i \cdot \bar{N}_j \right\} dV + \int_{S_2} (\gamma \hat{n} \times \bar{N}_i) \cdot (\hat{n} \times \bar{N}_j) dS E_j = - \int_{S_2} \bar{N}_i \bar{Q} dS \quad (2.64)$$

Comparing equation (2.59) with the basic equation of finite element method in the form  $Ax=b$  then:

$$A_{ij} = \int_{\Omega} \left\{ \frac{1}{\mu} (\nabla \times \bar{N}_i) \cdot (\nabla \cdot \bar{N}_j) - (\omega^2 \epsilon - j\sigma\omega) \bar{N}_i \cdot \bar{N}_j \right\} dV + \int_{S_2} (\gamma \hat{n} \times \bar{N}_i) \cdot (\hat{n} \times \bar{N}_j) dS$$

$$b_i = - \int_{S_2} \bar{N}_i \bar{Q} dS \quad x_j = E_j;$$

The temperature  $T$  is calculated by the equation of heat transfer [45, 51]:

$$\rho C_p \frac{\partial T}{\partial t} = \kappa \nabla^2 T + P \quad (2.65)$$

where  $T$  is the temperature in Kelvin,  $t$  is the time in second,  $P$  is the power loss in Joule,  $\rho$  is the density in  $\text{kg/m}^3$  and  $\kappa$  is the thermal conductivity in  $\text{W/(m}\cdot\text{K)}$ .

When  $t=0$  then  $T$  is equal to the ambient temperature.

#### 2.4.4 ESTIMATION OF DIFFERENCES BETWEEN THE SIMULATION RESULTS AND ACCURATE RESULTS

As the FEM is applied to a mathematical model, computed solutions contain differences due to the approximation. The differences here are defined as disagreements between the solutions computed by FEM and the accuracy of the mathematical model's results. This part will discuss about what kind of difference can be met and how to estimate them.

##### 2.4.4.1 DIFFERENCE CLASSIFICATION

Differences are unavoidable in an approximation in comparisons with the exact solutions, and can be expensive and even disastrous. Therefore the final results should be checked as in many ways as possible, because a single result is untrustworthy. The differences which appear in the simulation processes are classified as:

- **Modelling difference:** This is the difference caused by the inhomogeneity between a physical system and its mathematical model, because the mathematical model is normally simplified from the real model needed to analyze. The analysis does not cause differences but the simplification may cause differences. To simplify real models, geometric irregularities, mirror non-uniformity of material properties or small holes...etc...may be ignored, at least in the initial analysis. The simplification of loads and the idealization of boundary conditions are involved as well. The problems here are often prefer to be operated in 2D rather than 3D, linear rather than nonlinear or as time dependent rather than dynamic and so on. In general, the modelling difference indicates to a reasonable and considered approach made by deliberately rather than mistakes, and to the uncertainty of the real loads and boundary conditions [44].
- **User difference:** This implies to the differences caused by the users after the analysis of the problem has finished and the mathematical model has created. This kind of difference could be the reasons of the wrong selection of the general element type or poor element sizes and shapes selection and the mistakes in data input. This difference always should be checked when the computed results are still not available to understand after the other differences can be ignored.

- **Bug:** Bugs caused by the software itself. A bug may interrupt the execution, perhaps in the preprocessing phase. A bug will become more dangerous when it allows the execution to continue but lead to an inaccurate result which is serious but not great enough to realize immediately [52].
- **Discretization difference:** This refers to the difference which appears when the mathematical model is expressed by a finite element model. The number of degree of freedom is infinite in the mathematical model but finite in a finite element model [41]. A FEM solution can be affected by the parameters such as the number of used elements, the nature of shaped functions, integral rules used with isoperimetric elements and other formulation detail of particular elements.
- **Rounding difference:** This is the difference caused by the lost information due to truncations or rounding of numbers to fit a finite computer word's length. This kind of difference can be met in elements and structure matrices before a solution of the algorithm is applied [41, 44].
- **Manipulation difference:** This kind of difference is introduced as equations processed, for instance the truncated or rounded results of multiplication. Hence the manipulation difference can be accrued in some dynamic and nonlinear problems, because each step is built on the previous step and the calculation sequence is repeated [44].

#### 2.4.4.2 DIFFERENCE ESTIMATION

Techniques to estimate differences for analyzed problems have been developed in terms of technological aspects. Thereby optimizing the finite element analysis according to the behavior of the given problems could be taken into account. The size and placement of the element strongly affect the accuracy of the computed solution. The accuracy can be achieved by reducing element size or in other words, increasing the number of nodal points. This obviously costs more computing time and memory storages. The efficient also can be obtained by the placement of the element, which means creating a high mesh density for the regions with large gradient and a coarser mesh for the idle regions.

Using mathematics of a difference analysis can help a FEM program to determine which regions need to refine and generate a mesh corresponding to the problem automatically. The difference is calculated in each element and compared with a predefined limit. There are two distinct stages of the adaptive solution process: difference analysis and mesh refinement [44]:

- **Difference analysis:** In the case difference indications of each element is allowable and each element value is relative to other elements in the mesh, the absolute value of the difference can be calculated for the difference estimation. As the difference estimation is obtained, there are several ways to go to the next stage, e.g. improving the mesh.
- **Mesh refinement:** There are two basic approaches of mesh refinement. They are p-refinement and h-refinement [44, 51]. Actually p-refinement implies to the increase of the order of the polynomial approximation within an element. There are some advantages when combine p-refinement with a hierarchical formulation. It is more efficient, convergent, and faster and appeals to the purist by the virtue of its mathematic elegance [44]. However, in general incorporating, p-refinement means restructuring if the existing finite element code is not rewriting. Meanwhile h-refinement is a reduction of subdivision sizes and more universal accepted. There are two choices of h-refinement when adopting h-refinement: element subdivision or mesh regeneration [45]. By the element subdivision, all elements which surpass the allowable difference level are subdivided into smaller elements. It is more effective when using four-node elements but in other cases, it is very difficult to obtain the desired density distribution [45]. Otherwise constraints that allow only one level of subdivision at a time need to be introduced. The mesh regeneration means remeshing completely. This method can be done in regions of high differences only or over entire domain. The advantage of regeneration of entire mesh is that if the calculated difference is below the allowable difference, the mesh can be coarsened [45]. Thereby if every element has the same predefined level of difference approximately, a generation of optimal mesh is available. The disadvantage of mesh regeneration is that if it is applied in the case of abundant information provided by a difference estimation procedure, then a high degree of spatial flexibility is required [45].

## 2.5 EXPERIMENTAL SUPPORT

As mentioned above, the simulation results should be checked as in many ways as possible. Therefore the experiments are built to validate the computed solutions. The triangle of experimental result, simulation result and theory has the relationship that helps each other to improve by comparison to each other. When experimental result compares to simulation result, model that describes the real system can be improved and when theoretical prediction compares to simulation result, the theory can be improved.

To obtain the experimental results of microwave-processed electronic assemblies as well as the conformal coatings, two phases need to be realized: microwave heating and measurement. The laboratory microwave oven is a particular built that can adjust the power supported from 100 W to 1000 W (figure 2.11). This flexibility adjustment can help to choose the sufficient power for the microwave process which is not only enough to heat up the electronic assemblies but also bring no harm to them.



Figure 2.11: Particular laboratory microwave oven

After the microwave process, heated sample will be taken out and exposed beneath a thermographic camera (figure 2.12.a). Pictures which show the temperature distribution of samples will be taken. The post processing of the results will be shown in digital computer (figure 2.12.b).

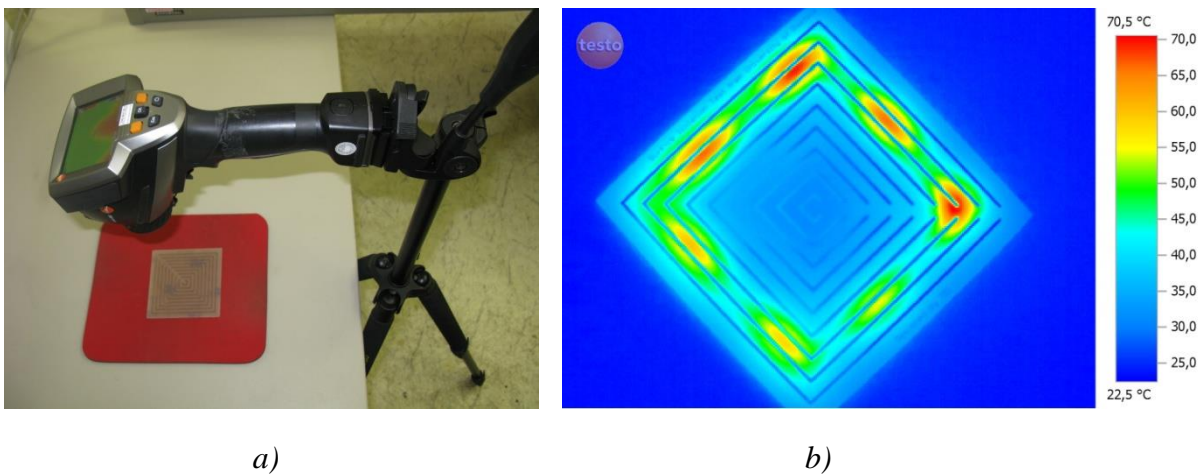


Figure 2.12: Taking thermo-graphic picture (a) and the post processing of result (b)

## CHAPTER 3

# INTERACTION OF PCB STRUCTURES WITH MICROWAVE RADIATION

Coatings can be applied on electronic assemblies by spraying or brushing. As the coatings are dried enough for manipulation, they are needed to be cured for reaching their optimum properties in order to protect electronic assemblies. Therefore the behavior of metallic structures in the microwave process weightily affect to the coating cure. This chapter will represent the investigation of microwave process for PCBs. The simulations are carried out in 3D. The investigations are realized itentionally from single wired PCBs to the complicatedly structured PCBs. The simulation results will be analyzed for predicting and improving the next models. Additionally, the factors which may affect the behavior of PCB structures are considered as well. The mesh refinement mechnism and experimental evaluation are realized to qualify the simulation results. This qualification can ensure repliable simulation results. This chapter rather shows the situations and analyses about which will occur in the microwave process for PCB structures than gives the solution for supporting coating cure.

### 3.1 OBSERVING STANDING WAVES

The first part of this chapter totally represents the observation. Here the interaction between wired PCBs and microwave radiation will be observed. To have the observation, models are built for simulations and experiments similarly. The 3D model of a microwave oven in simulation has the same structure as the laboratory microwave oven as well as the loads. The “standing waves” mentioned above means that the responses of investigated PCB structures to the microwave radiation are alike standing waves which propagate on them.

#### 3.1.1 MODEL DEFINITION OF MICROWAVE OVEN

For the study, a metallic microwave cavity with an antenna injection as well as electronic assemblies (here is metal-structured PCB) are modeled. Parameters such as: metallic structures, material properties and microwave frequencies are changed to specify the most impactful adjustment.



The model includes a rectangular waveguide in connection with a cylindered metallic antenna leading electromagnetic wave to the conductive cavity and PCB load is laid on an underlay (figure 3.1). Symmetry is utilized for saving memory and computing time due to the symmetric geometry. So the geometry is only a half of the microwave oven.

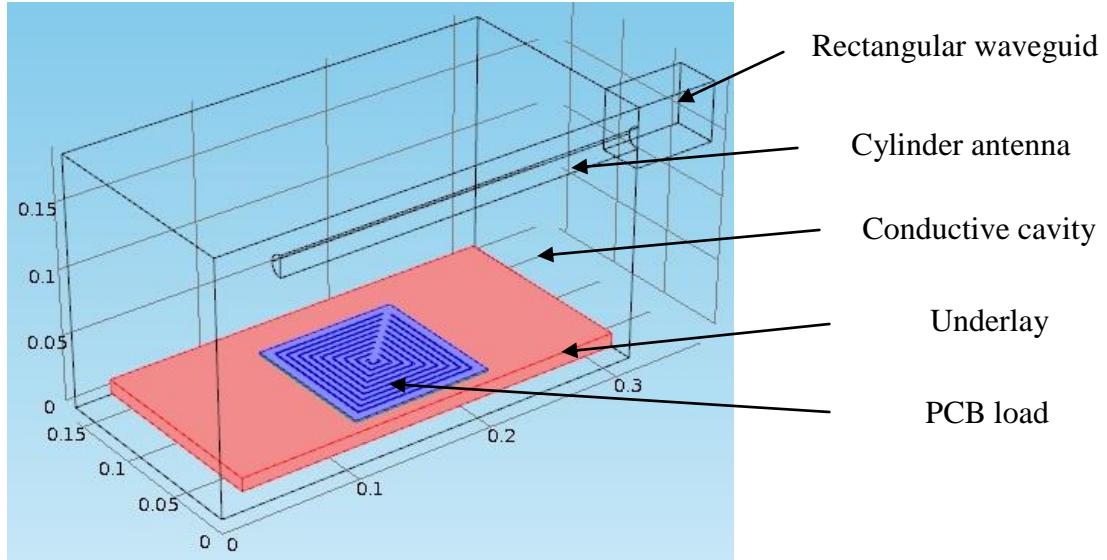


Figure 3.1: The simulation model of half microwave oven and PCB load

The basic data of the microwave cavity are exhibited in the following table:

Dimensions	Power	Time of testing	Frequency
315×310×190 mm <sup>3</sup>	200 W	30 seconds	2.45 GHz

Table 3.1: Basic data of microwave cavity

To reduce the resistive metal losses, *Impedance Boundary* condition is applied for all metallic walls of the cooking chamber. The *Impedance Boundary* condition is a boundary condition that is applied at the boundaries where the electromagnetic field penetrates only a short distance outside the boundaries. The *Perfect Magnetic Conductor* ( $n \times H = 0$ ) is applied for the symmetric boundaries [45]. They are on a plane which cuts vertically through the oven, waveguide, the antenna and the underlay.

The material properties used in the simulations are given in the following table:

Material	Properties	Value
Air	$\sigma$	0[S/m]
	$\mu$	1
	$\epsilon'$	1
Underlay	$\sigma$	0[S/m]
	$\mu$	1
	$\epsilon'$	2.55
Copper	$\sigma$	5.998e7[S/m]
	$\mu$	1
	$\epsilon'$	1
PCB	$\sigma$	0.004[S/m]
	$\mu$	1
	$\epsilon'$	4.5

Table 3.2: Properties of materials used in the simulation [53]

### 3.1.2 OBSERVING REGULAR HEATING

To get the knowledge of how PCB structures react with the microwave radiation, models of the microwave processes for single wired PCBs are built. Because it is not possible to simulate all conceivable conductive structures, thus it is necessary to simulate from PCBs with single wire to PCBs with more complex and typical structures. For the models, typical FR-4 is used as the substrate material, the thickness of PCBs is 1.5 mm and the thickness of copper wires is 0.02 mm.

#### 3.1.2.1 MICROWAVE PROCESSES FOR SINGLE WIRED PCBs

The investigation starts from the single wired PCBs with variable lengths. The meaning of this study is the first step to understand the coupling of copper wires and the microwave radiation. The first sample is a PCB which the copper wire's length is 50mm. Then the other ones are developed by increasing wire's length to 100 mm, 150 mm and 200 mm to observe the coupling of copper wires and the microwave radiation following increased wire's lengths (as see in figure 3.2). All the copper wires here are located at the lower edges on one side of

the PCBs. Figure 3.2 shows the temperature distributions on the single wired PCBs as the final simulation results. The color range from blue to red expresses a temperature scale from lowest temperature to highest temperature.  $T_{\min}$  here is  $25^{\circ}\text{C}$  as the initial temperature (ambient temperature as well).  $T_{\max}$  changes from  $26^{\circ}\text{C}$  to  $28^{\circ}\text{C}$  on each PCB corresponding to its wire's length. As in the figure 3.2, there are some significant heated areas (red and bright color) on the PCBs along the wires, which are called hotspots. The 50 mm long PCB has only two hotspots but the number of hotspots will increase when the wire's length enhances.

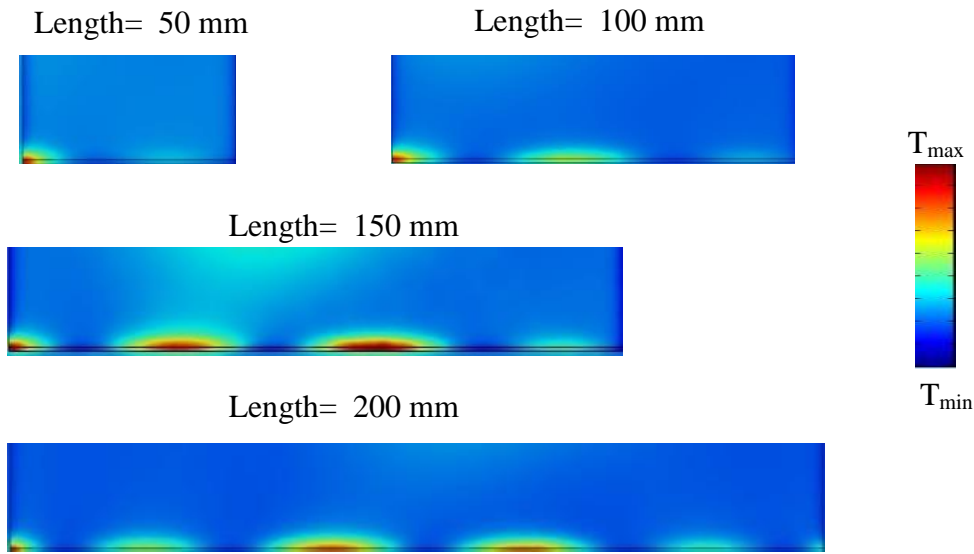


Figure 3.2: Single wired PCBs with different wire's lengths

A 200 mm long wired PCB sample is also created for the experimental test. The experiment is carried out for checking the accuracy of the simulation result. After heating in 30 seconds, the sample is taken out and photographed by the thermo-graphic camera to exhibit the temperature distribution. Figure 3.3 illustrates the overlay picture combining a real image and a thermal post processing image of the single wired PCB captured by the thermo-graphic camera. The PCB's length is 200 mm and it represents the corresponding temperature distribution as shown in the simulation result with 200 mm long PCB.

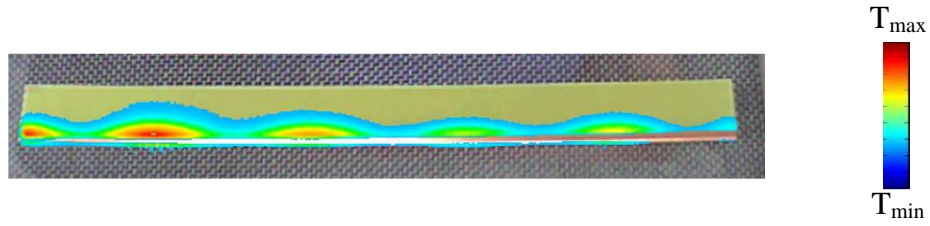


Figure 3.3: The overlay picture combining a real image and a thermal image of the single wired PCB taken by thermo-graphic camera of 200 mm long PCB after microwave heating

### 3.1.2.2 MICROWAVE PROCESSES FOR PCBs WITH QUADRATICALLY SHAPED WIRES LIKE FRAMES

As in the previous section, hotspots spread along copper wires of the PCB. The longer a copper wire is, the bigger number of hotspots is. So what will happen when the copper wire changes its direction suddenly for example turn  $90^\circ$ ? Therefore, for this investigation PCBs structures will be built more complicatedly. Quadratically shaped PCBs are selected which dimensions are  $(100 \times 100 \times 1.5 \text{ mm}^3)$  and the copper wires can be added following the edges of the PCBs to form a quadratic shapes. First of all, with these models the investigation starts from the unwired PCB. After that, one wire, three wires and nine wires are added. Thus the influences of copper structures on the temperature distribution can be understood step by step (figure 3.4 and figure 3.5).

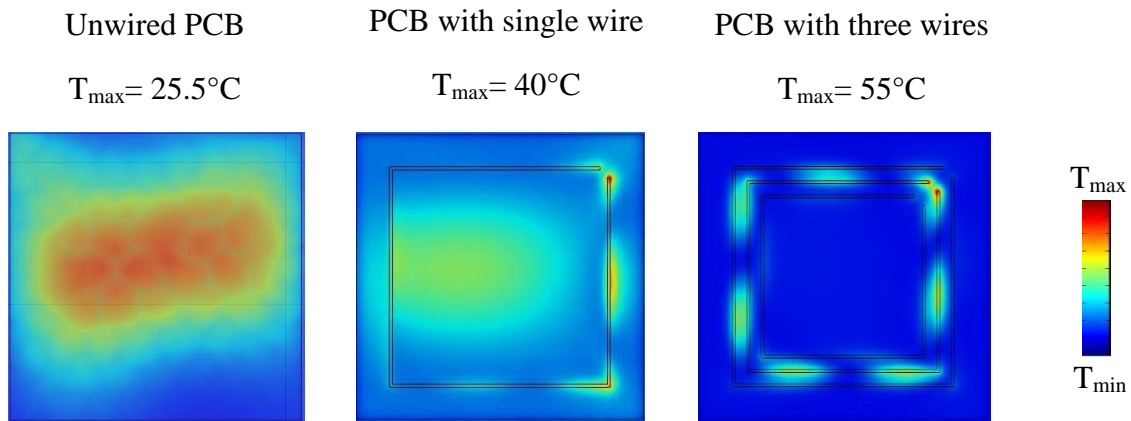


Figure 3.4: Simulation results of temperature distributions on quadratic PCBs

As seen in figure 3.4, the unwired PCB (only FR-4 substrate) is heated uniformly. The temperature distribution is homogenous and spreads from center to the outer side. The different temperature of minimal and maximal temperature is very small (about 0.5 K). As the copper wires are added, the copper structures disturb the homogeneity of the temperature distribution on the substrate. In the case of only one wire on the PCB, the disturbance is not

clear. There are not so many hotspots that appear and there is still an area with a homogeneous temperature distribution in the center. If the copper structure includes three wires, the effect of the metallic structure is clearer. There is no uniform heating anymore. The areas with high temperature disperse in many small hotspots locating along the wires. The simulations are carried on with more complicated copper structure. The wires are added full on the surface of the PCB which distance between each wire is 4 mm. The temperature distribution has the same look as the one on the PCB with three wires but the maximal temperature rises up. This is also evaluated by the experiment. The overlay picture of the experimental PCB shows the familiar hotspots as well as the temperature in comparison with the simulation result (figure 3.5).

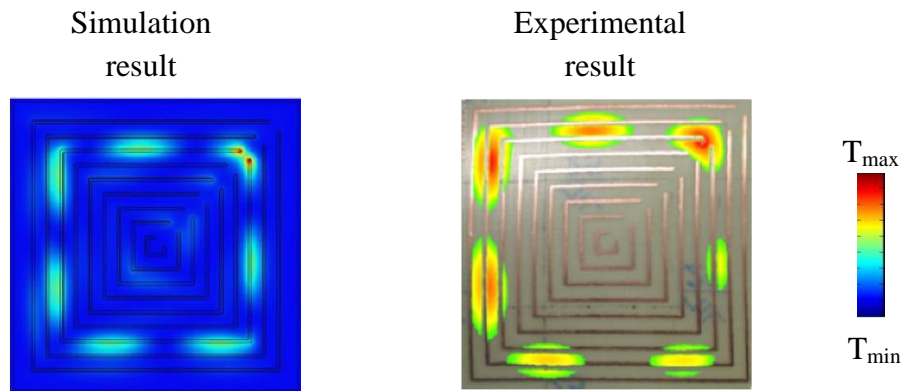


Figure 3.5: The substantial similarity of simulation result (left) and experimental result (right) of quadratically wired PCB after microwave heating

The initial temperature for the simulation is 25°C (the room temperature). After 30 seconds of heating, the highest temperature reaches 70°C. This is also the highest temperature of the experimental result. The hotspots caused a big different temperature between separated areas in the PCB. The following diagram (figure 3.6) expresses the temperature respecting to time of a point within the hotspot which has the highest temperature and another point which is not inside the hotspot areas.

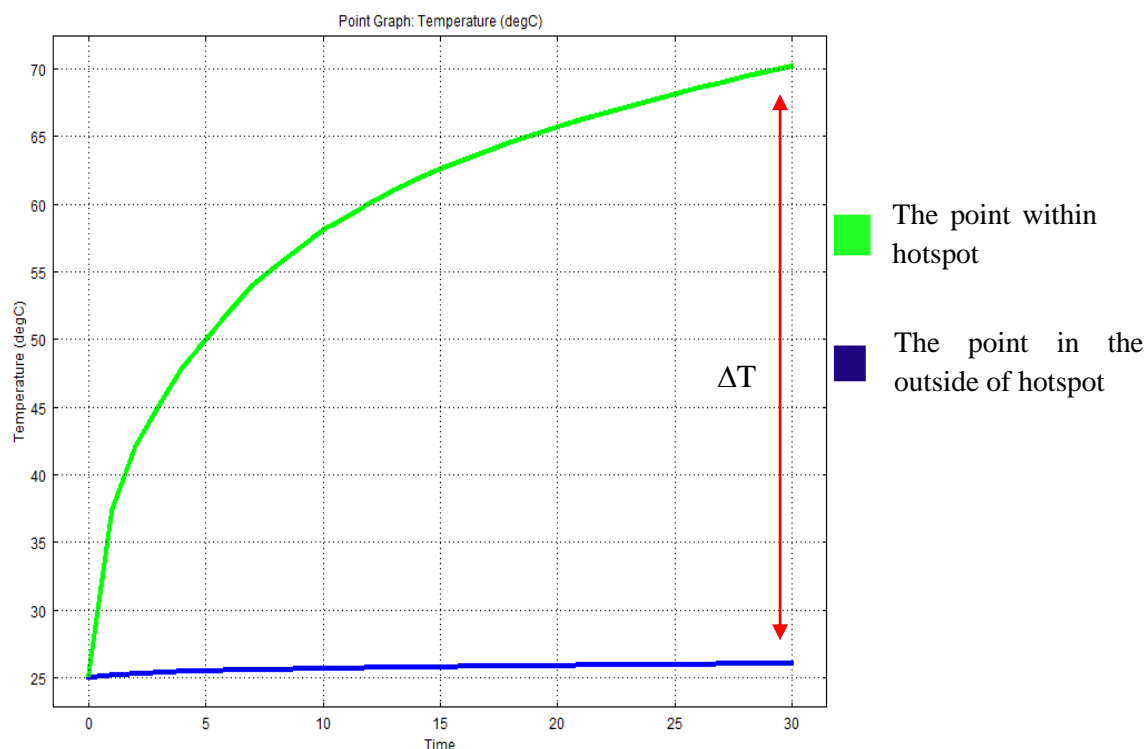


Figure 3.6: The diagram expresses the temperature of the point within hotspot which has highest temperature and the point in other area in 30 seconds microwave heating process

The corresponding electric field intensities of these two points above are independent on time. They are direct proportion with the temperature of these two points. These field intensities describe the ability of being heated up by the microwave irradiation as well. Table 3.3 below shows that the electric field intensity of the point within hotspot is much bigger than of the one in the other area.

Time (second)	<i>E</i> field intensity of point within hotspot (V/m)	<i>E</i> field intensity of point in other area (V/m)
0 to 30	204.710	21.575

Table 3.3: The *E* field intensities corresponding to the calculated temperature of the point within hotspot and the point in the other area

In those tests above, the copper structures have an open corner, the hotspots distribute along the wires starting from the open corner of the structures. The question here is how this open corner influences on the heating. Hence to understand more about this kind of structures, other simulations need to be carried out with different direction of the open corner.

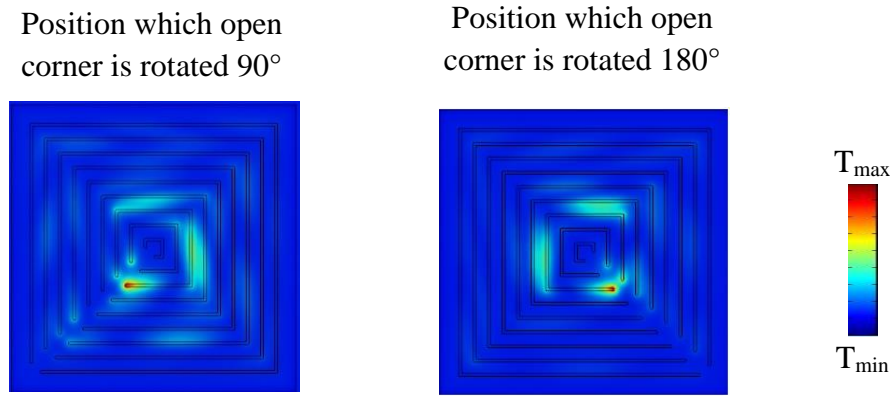


Figure 3.7: The temperature distribution of the quadratically wired PCB in some positions where the open corners are rotated

So if the open corner's direction changes from the original position, the temperature distribution is changed as well. However the heating still starts from the open corner.

The open corner can affect the distribution on the PCBs. This is definitely very important for the heating of this kind of structures. Therefore improving copper structures concerning the open corner is the next step. The copper structures on the PCB models are modified as all corners are open and all corners are close.

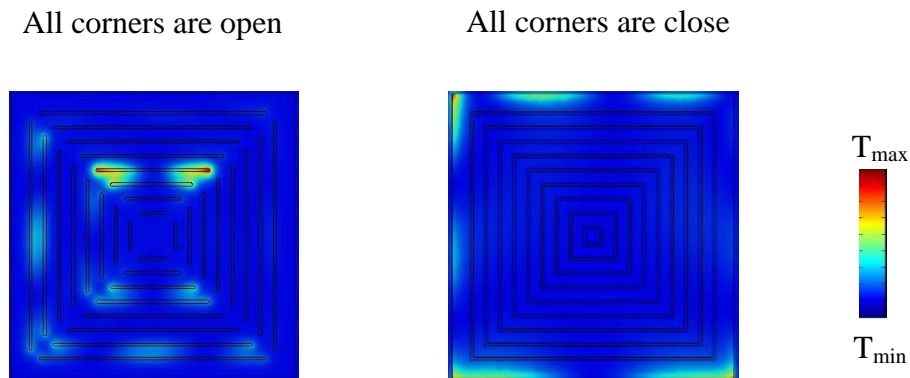


Figure 3.8: The simulation results of wired PCBs which all copper wire corners are open (left) and close (right)

As all corners are open, the conductive structure becomes a set of many short copper lines. Thus the interaction between copper structure and microwave radiation tends to occur in separated lines. In the case all corners are closed, the structure reflects all the microwave radiation. So within the structure, there is no heating within the structure but hotspots spread in the outer side.

### 3.1.1.3 MICROWAVE PROCESS FOR A REAL PCB EXAMPLE

Since the previous models are special for the investigation purpose and no products in reality, a real PCB used in reality should be considered. Following figures illustrated a two sides-metalized PCB and the simulation model built. The complicated structure of each side is connected together by the tiny conductive holes.

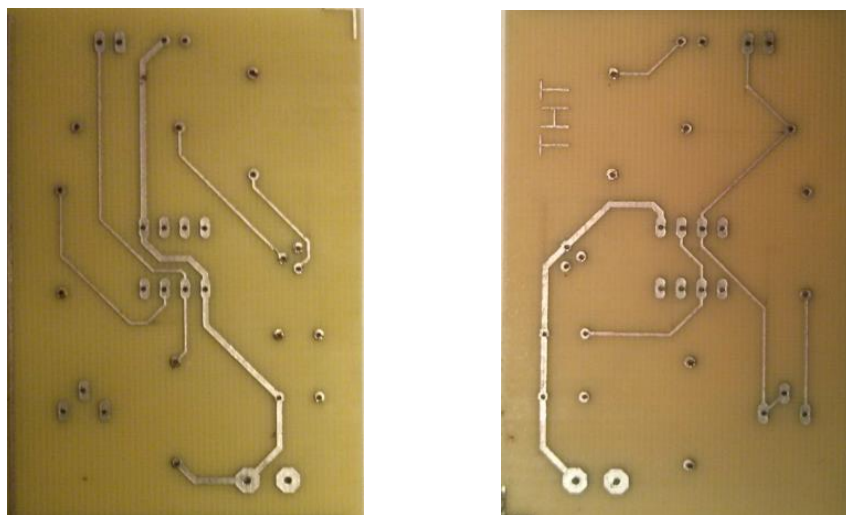


Figure 3.9: The metallic structures on two sides of a real PCB

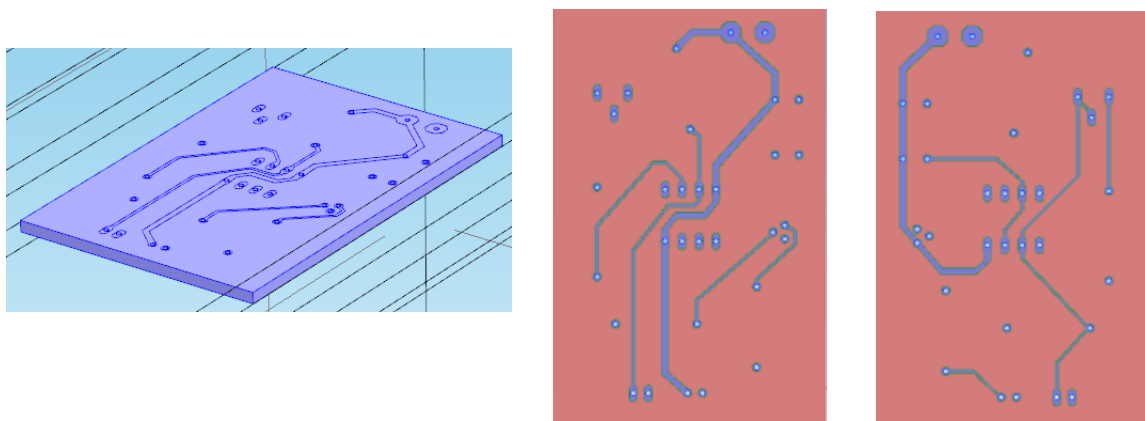


Figure 3.10: The real PCB simulation model built in 3D (left) and metallic structures on two sides (middle and right)

After building model, the simulation of the microwave process is run for 30 seconds. The side of PCB, which contacts to the air is called the top and the other side which contacts to the underlay is called the bottom in this simulation. Figure 3.11 illustrates the experimental result and the simulation results of temperature distribution on the top and bottom of the real PCB.



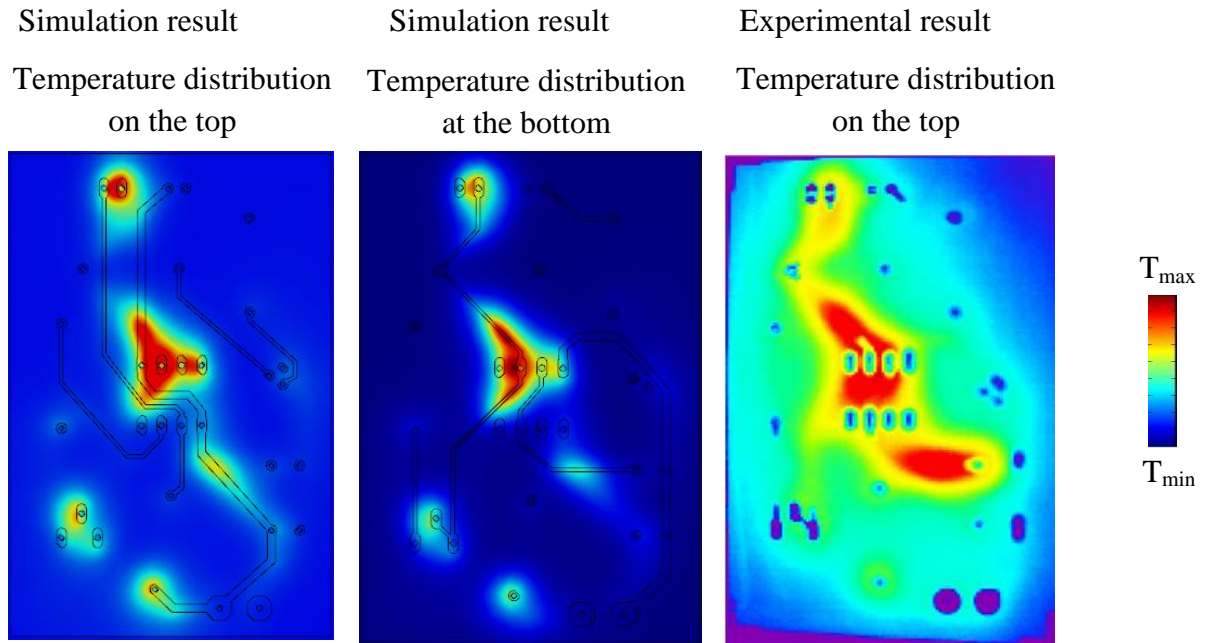


Figure 3.11: The simulation results and experimental result after microwave heating a real PCB

The simulation result and experimental result are basically similar in term of temperature distribution especially the hotspot in the center. The experimental result, taken by the thermographic camera shows the highest temperature around  $80^{\circ}\text{C}$ , distributed on the top side of the PCB. The highest temperature of the simulation result (on the top side) is lower than the one in experiment  $3^{\circ}\text{C}$ . The bottom side of the PCB is in contact with the underlay, thus this is the reason of temperature cooling down due to the heat transfer from bottom side to the underlay. Therefore the highest temperature of the bottom side is about  $15^{\circ}\text{C}$  smaller than the one on the top.

## 3.2 ESTIMATION AND DISCUSSION ABOUT MICROWAVE PROCESSES FOR PCBs

The previous section exhibited the results from the interaction between wired PCBs with the microwave radiation. In this section, the critique of the previous investigations will be given. Furthermore parameters which affect the temperature distribution on PCBs in microwave processes are considered either.

### 3.2.1 CRITIQUE OF THE INVESTIGATED RESULTS FOR PCBs WITH THE TYPICAL SUBSTRATE MATERIAL

The typical substrate material of PCBs is normally FR-4. Observing the illustrations of PCB tests, it would be happened that the distances between the hotspots are constants and the maximum amount to circa 40 mm. This observation can be interpreted as a formation of standing waves along the wires on PCBs. This causes a locally constant current and heating process based on the Joule effect like the antenna effect. The distance between the hotspots is a result from the reduced wavelength  $\lambda_c$  of the propagating waves on the PCBs.

From the tests with quadratic PCBs structures, the open corners display a very important role that influences on the temperature distributions. The heating of the enclosed copper wires due to microwave irradiation failed to appear. This indicates a total reflection of the incident microwaves.

Unlike the single wired PCBs and quadratically shaped PCBs which were created for the investigating purposes, the real PCB was created for the using purpose and had complicated metallic structures. Therefore it was not easy to learn its temperature distribution in the microwave process. This microwave heating result forecasted a difficult study concerning the goal of uniform heating.

### 3.2.2 THE INFLUENCE OF PCB ´S POSITIONS AND WIRE ´S LENGTHS

In microwave heating processes, the electric field distribution definitely influence on the temperature distribution of the heated objects. Since the  $E$  field strength is not constant and has a range from minimal to maximal intensity, then the position of PCBs in microwave oven will determine how the temperature distribution is and the maximal temperature of the heated objects is. To prove this opinion, some tests of the substrate material (FR-4) in different positions are realized. The simulation results, displayed in figure 3.12 will describe how the temperature distribution and highest temperature of the heated objects depend on the electric field.

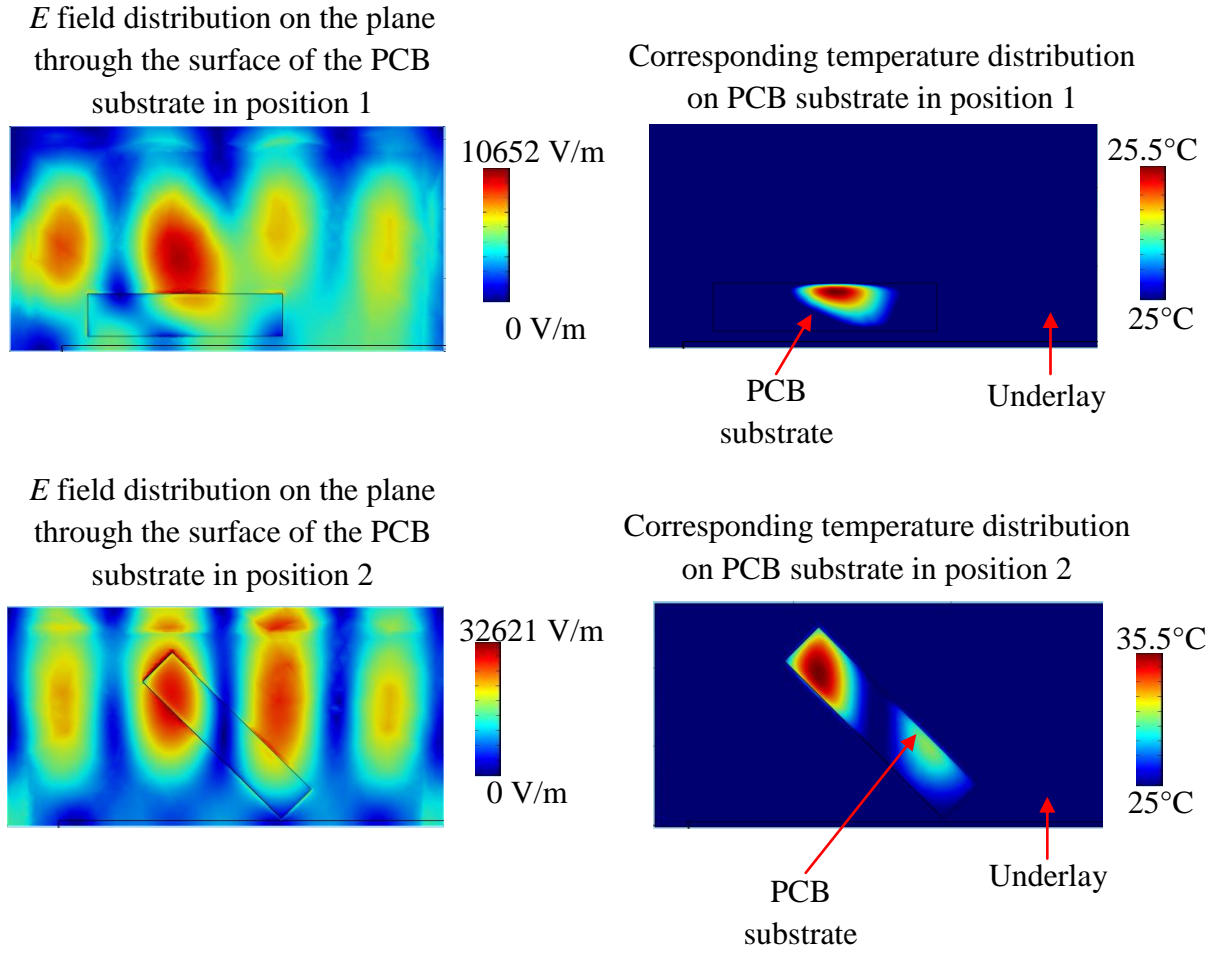


Figure 3.12: The influence of  $E$  field to the temperature distribution

As shown in the figure above, if the PCB substrate is laid in position 1, which is not the area of the highest value of  $E$  field intensity and contacts with only one significant  $E$  field strength (not the strongest area), then there will be only one area, which has a significant temperature distribution. The temperature increases in this position slowly ( $0.5^{\circ}\text{C}$  after 30 seconds). In position 2, the PCB substrate is in contact with two areas which have significant  $E$  field strengths. Hence on the PCB there are two meaningful temperature distributions. Furthermore, one of these areas has the effect of the highest  $E$  field strength, thus in this position the PCB is heated up faster than in position 1 ( $10.5^{\circ}\text{C}$  after 30 seconds).

Another point seen from figure 3.12 is that the coupling of substrate material and microwave radiation interfere the  $E$  field distribution, which in the contact with the substrate. The power dissipation density of the substrate in position 1, calculated by the software is  $P_{d1} = 0.28 \text{ W}$ . In position 2, it is greater,  $P_{d2} = 3.65 \text{ W}$ . Therefore when the substrate is in the contact with an

area which has stronger  $E$  field intensity, then the coupling will cause more significant heating.

Another interesting study now is the investigation of the effect of copper wire's lengths on wired PCBs in the microwave treatment. For that purpose, series of tests are carried out with varied wire's lengths from 0 to 130 mm. The charts in figure 3.13 illustrate the effect of the wire's length on the  $E$  field strength of the PCBs, induced by the copper wires. This effect can directly interfere in the microwave heating of PCBs in position 1 and 2.

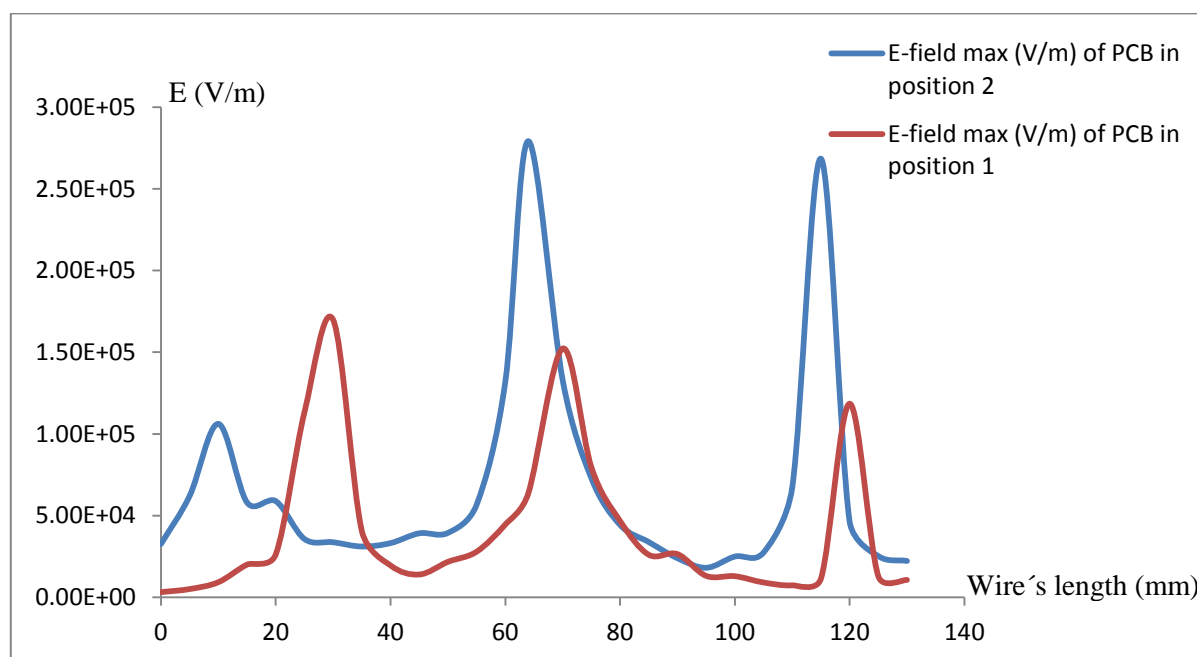


Figure 3.13: Relationship between wire's length and maximal induced  $E$  field intensity on wired PCBs in position 1 and 2

The chart describes the relation between the copper wire's length and the highest induced  $E$  field intensity of the PCBs. From the illustrations, there are some critical points, which expose a very big amount of  $E$  field strength. That means the PCBs with these wire's length will be very sensitive in the microwave heating. For PCBs in position 1, the noticed wire's lengths should be around 30 mm, 70 mm and 120 mm. For PCBs in position 2, the wire's lengths of around 10 mm, 65 mm and 115 mm would be the critical lengths. It is clear that the critical wire's lengths are variable. They depend on the starting point of the wire. If the position is changed then the critical wire's length will be different. Figure 3.13 is an example, which exhibits the reason why there are critical points for the PCBs with 30 mm and 65 mm long wires in position 1 and 2.

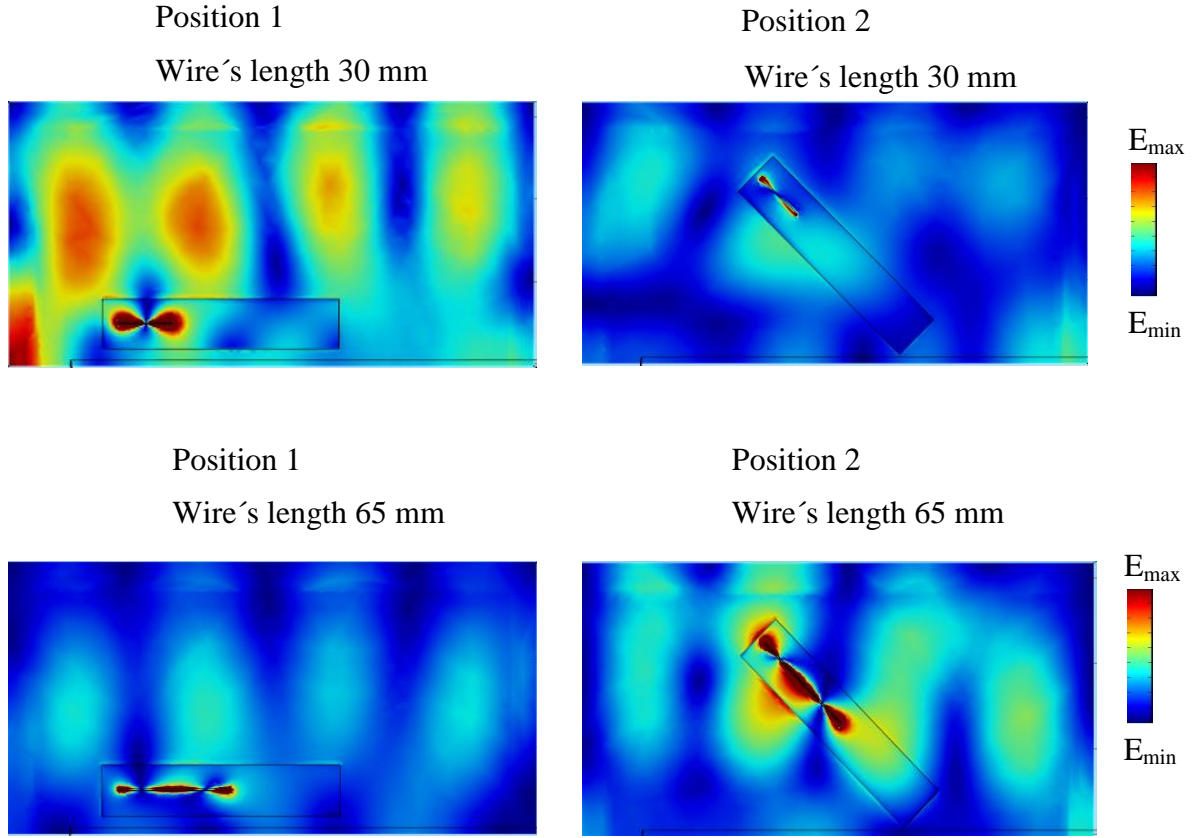


Figure 3.14: The coupling of 30 mm, 65 mm copper wired PCBs and electric field in position 1 and 2

The illustrations revealed there were some critical wires' lengths. As seen in figure 3.14, the electric field distributes in four big main areas, let call them nodes of the field. Each node has the strongest distribution in the center. The 30 mm wire's length in position 1 couplings with two nodes of the electric field, therefore the induced electric field caused by this wire's length, in this position, is very strong. Unlike that, the same wire's length in position 2, although the starting point of the wire is in the center of the node (strongest  $E$  field area) but does not couple with 2 nodes, the induced  $E$  field strength is low. For the 65 mm wire's length, in both position 1 and 2, the copper wires couple with the nodes. However, the difference is that in position 1, the starting point of wire is located in the low energy of the node and located in the highest energy of the node in position 2. Thus they result in high temperatures of the hotspots in both cases and the temperatures of the PCBs are higher in position 2 than in position 1.

The explanation may be that the copper wire coupled with the incident electromagnetic wave and acts like a transmission line in this case [54, 55, and 56]. The approximate frequency limit of the transmission line is given by [55, 56]:

$$f_l \approx \frac{21.3GHz \cdot mm}{(l + 2h)\sqrt{\varepsilon_r + 1}} \quad (3.1)$$

where  $l$  is the length of the copper line,  $h$  and  $\varepsilon_r$  is the thickness and the relative permittivity of the PCB.

In these simulations,  $h$  and  $\varepsilon_r$  are constant ( $h = 1.5$  mm and  $\varepsilon_r = 4.5$ ), therefore  $f_l$  depends on the length of copper wire. For a variable  $f_l$ , there may be values of  $l$  which create a resonance between the induced electromagnetic field on the wire and external electromagnetic field.

From the opinion above, for each position, there will be different critical wire's lengths. If a position here is considered in two factors location and direction of the copper wires, then positions 1 and 2 have different locations and different directions of copper wires. So let name the positions by their two factors, for instant, position 1 is  $D_1L_1$  (direction 1 and location 1) and position 2 is  $D_2L_2$  (direction 2 and location 2). The question here is whether the critical wire's lengths for example of  $D_1L_1$  (30 mm, 70 mm and 12 mm) are still the same in  $D_1L_2$  (same direction  $D_1$  but different location). So to get the knowledge of this point, other series of simulations are carried out for wired PCBs which are translated 20 mm horizontally from the original position 1 (from  $D_1L_1$  to  $D_1L_2$ ).

In this series tests, the location of the wired PCBs is translated 20 mm closer to the waveguide from location 1. Therefore the coupling of the microwave radiation and wires is different. The critical points of the wavelengths are also changed a bit. The first critical wire's length is still 30 mm, the second one is around 60 mm and the third one is around 115 mm but in this third critical point of wavelength the increase of induced  $E$  field strength is small (figure 3.15).

From the discussion above, it could be conclude that the critical wire's length depends on the location and direction of the copper wires in microwave oven.

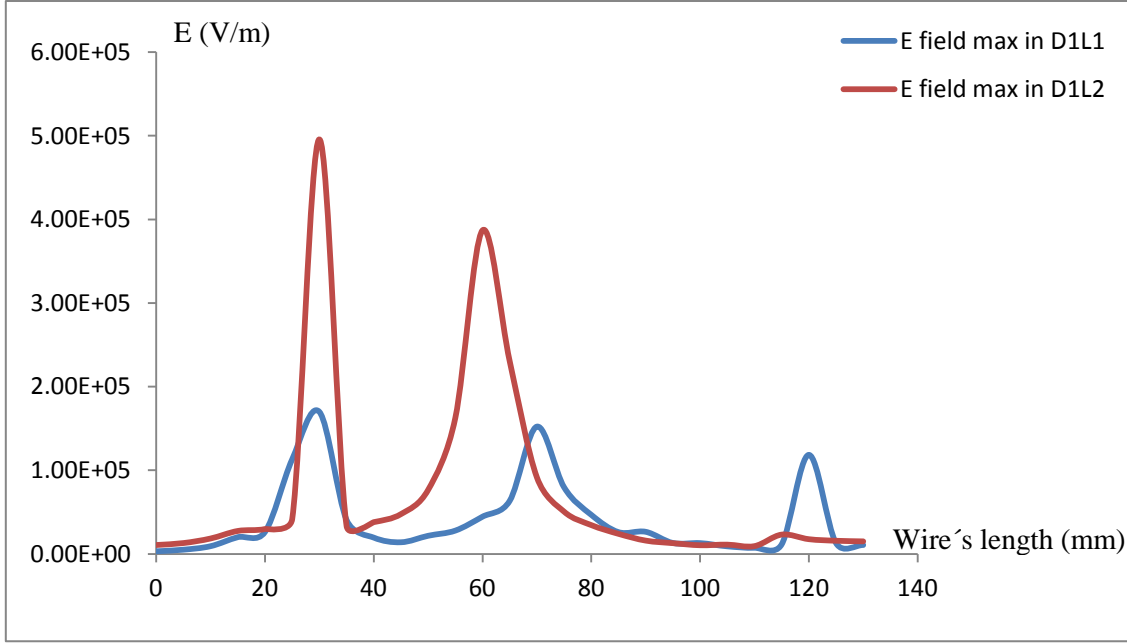


Figure 3.15: Diagram of maximal  $E$  field strengths, induced by the wired PCBs in position 1 (blue) and by the wired PCBs in a position which is translated 20 mm horizontally (red)

### 3.2.3 THE INFLUENCE OF PERMITTIVITIES OF PCB SUBSTRATES.

The next parameter, taken in to account is the relative permittivity of the PCB substrate (usually as FR-4). In these series tests, all parameters are kept constant but the relative permittivity of the substrate. At this point, the temperature distribution on the PCBs will be dependent on the relative permittivity  $\epsilon_{PCB}'$  of the substrate material. That means the conductive wavelength  $\lambda_c$  is a directive function of  $\epsilon_{PCB}'$ . In this case, the distance between hotspots decreases while  $\epsilon_{PCB}'$  increases as exhibited by figure 3.16 below.

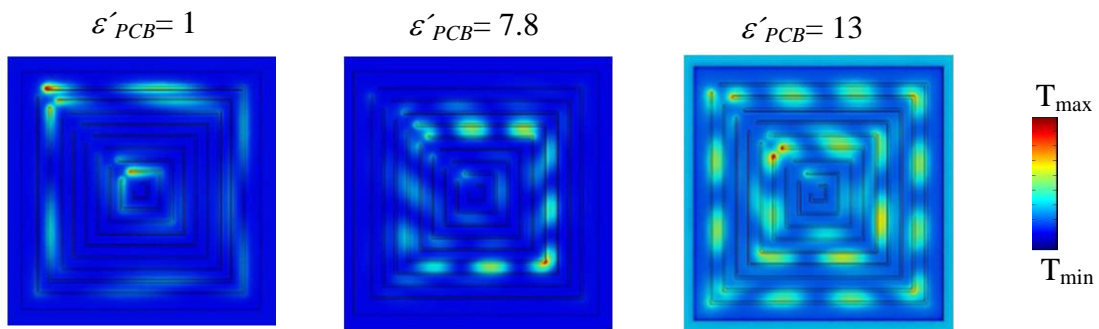


Figure 3.16: Interaction of the wired PCBs with microwave radiation depends on the substrates' relative permittivities

The wavelength of the free space is given by:

$$\lambda_0 = \frac{c}{f} \quad (3.2)$$

The conductive wavelength  $\lambda_c$ , which is double of the maximal distance between hotspots  $\lambda_c = 2d$ , is expressed as [57]:

$$\lambda_c = \frac{c}{f\sqrt{\epsilon_r}} = \frac{\lambda_0}{\sqrt{\epsilon_r}} \quad (3.3)$$

In this equation, the relative permittivity  $\epsilon_r$  is given by a sum of the permittivities of the participating materials  $\epsilon'_{PCB}$ ,  $\epsilon'_{AIR}$  and their corresponding weighting factors  $w_{PCB}$  and  $w_{AIR}$ . For the substrate material  $\epsilon_r \sim \epsilon'$  (loss tangent is almost 0), therefore from this point, the equation (3.2) can be written as:

$$\lambda_c = \frac{\lambda_0}{\sqrt{w_{PCB}\epsilon'_{PCB} + w_{AIR}\epsilon'_{PCB}}} \quad (3.4)$$

Based on equation (3.4), an interpolated equation is built, which displays the dependence of the conductive wavelength  $\lambda_c$  on the substrate's relative permittivity  $\epsilon'_{PCB}$ . This equation is described in a diagram shown in following figure 3.17. The diagram is established by series simulation results of testing PCBs with variable permittivities of the substrates.

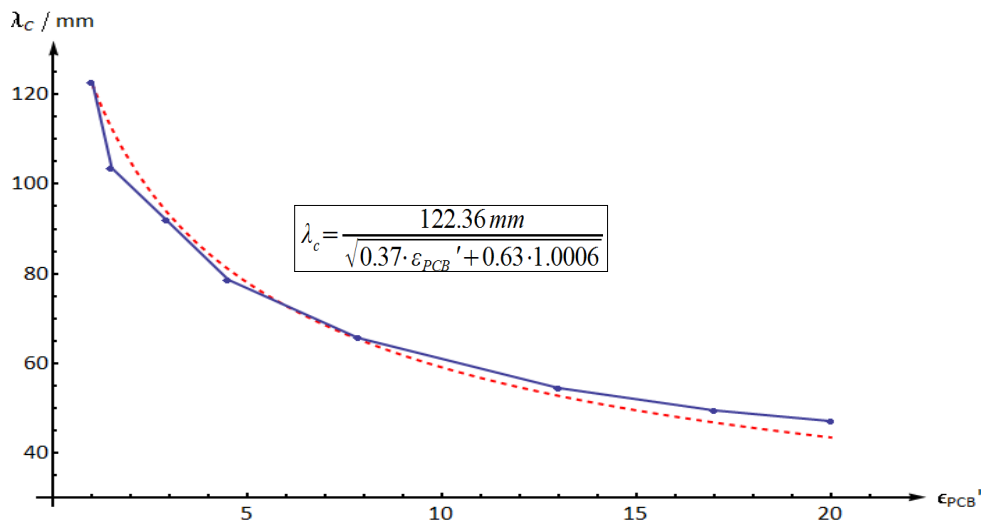


Figure 3.17: Dependence of the conductor wavelength  $\lambda_c$  and the relative permittivity on the base material  $\epsilon'_{PCB}$  (blue plot with markers). The dashed curve represents an interpolation based on the shown equation



The function  $\lambda_c(\epsilon_{PCB})$  identifies the influence of the substrate material's permittivity  $\epsilon_{PCB}$  and the surrounding air ( $\epsilon_{AIR} = 1.0006$ ) on the velocity of microwave propagation along the copper wires. It is affected by the weighting factors with  $w_{PCB} = 37\%$  for the substrate and  $w_{AIR} = 63\%$  for the air. The weighting factor of air is surpassed the one of substrate because the air is more in the surrounding of the copper wire, meanwhile the substrate is only in contact with the bottom of the wire. Therewith the temperature distribution can be attributed to real parts of relative permittivities of the participant dielectric materials.

### 3.2.4 THE INFLUENCE OF MICROWAVE FREQUENCIES

Since the frequency of the laboratory microwave oven is fixed at 2.45 GHz, the microwave frequency is adjusted only in the simulations. The study is realized to understand how the microwave frequency influences on the temperature distributions on the wired PCBs in the microwave process. In fact, materials have different permittivities at different microwave frequencies. However in these tests, the properties of the materials are kept at the frequency of 2.45 GHz. Figure 3.18 exhibits the effect of the microwave frequency on the temperature distribution of PCBs.

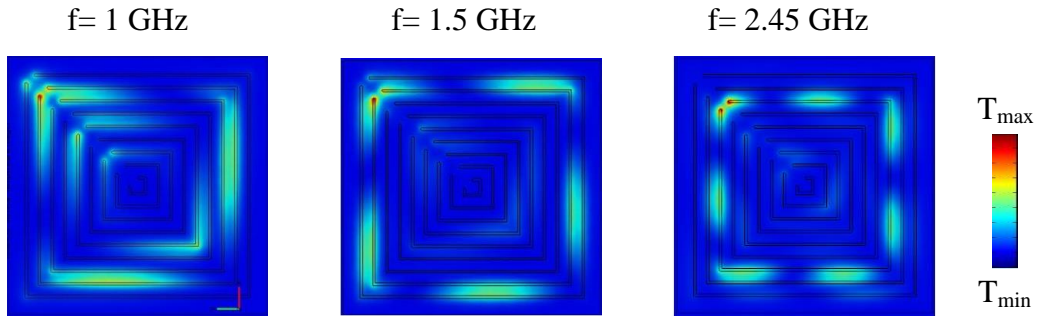


Figure 3.18: Simulation results of wired PCBs after microwave heating with variable frequencies while material properties are kept at the frequency of 2.45 GHz

It is not difficult to recognize from figure 3.18 that the distances between hotspots are smaller when the frequency value is bigger. That means  $\lambda_c$  decreases while microwave frequency increases.

The investigation of changing frequency has just proved the theory by the simulation images. The equation (3.1) exhibits that the wavelength in the free space decreases when the frequency increases and this indeed involves to the decrease of the conductive wavelength  $\lambda_c$ . The reduction of  $\lambda_c$  means that the distance between hotspots decreases and more hotspots appear.

### 3.3 COMBINATION OF WIRED PCBs AND COATING LAYERS

The interaction of wired PCBs with the microwave radiation is revealed. The expectation here is the uniform heating of the coating layer by the means of microwave irradiation. The mechanism of the heated coatings by the microwave oven is dielectric heating. The pure dielectric heating process of the coatings can support the curing process. In this case, the coatings are coated on the wired PCBs, and this combination can lead to a coating cure including the antenna effects caused by the microwave heating of the PCB structures. Figure 3.19 will illustrate the simulation result of a wired PCB with a coating on it.

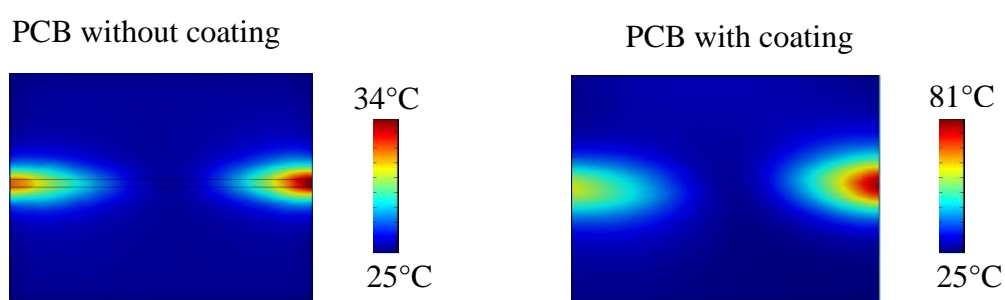


Figure 3.19: Temperature distribution on the wired PCB without coating (left) and the PCB with the coating combined (right)

As in the illustration above, the pure dielectric heating of the coating is disturbed by the antenna effect. The dielectric heating is not dominant to support the curing process. As the knowledge gained, the situation would be explained as:

- The coatings due to its material property can absorb the electromagnetic wave, the loss energy of the electromagnetic wave turn into energy which uses to heat up the coatings.
- The hotspots appear from heating wired PCBs means that the electric field strengths in the hotspots are stronger than the other areas. Therefore the coatings can absorb more energy from the hotspots than other areas and that make the temperature of the coatings around the hotspots increase rapidly.
- From the interpolated equation and figure 3.16, the conductive wavelength depends on the PCB substrates and the surrounding air. In this case, the air is replaced by the coatings with bigger relative permittivities. Thus, the conductive wavelength will be discounted and the temperature distribution will be different (figure 3.20).

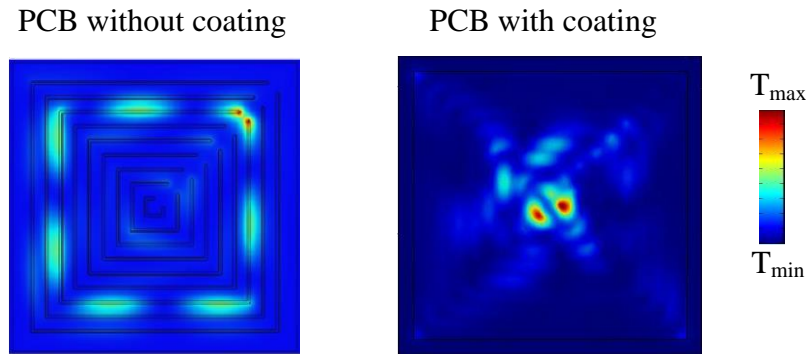


Figure 3.20: The different temperature distribution on the PCB without coating and on the PCB with coating

### 3.4 SUMMARY

This chapter has just exhibited the investigation about the interaction between wired PCBs with the microwave radiation in the microwave heating process. Numerical simulations were utilized to express the results from the coupling of the wired PCBs and the microwave radiation. The experimental results have evaluated the simulation results in some tests which the experiments are possible. The matching of simulation results and experimental results in the comparisons above (as seen in figure 3.2, figure 3.3, figure 3.5 and figure 3.11) leads to the ability of using simulation for the microwave process of the electronic assemblies in advance. There are some conclusions of this investigation as following:

- The PCB structures have significant effect on the microwave heating of the coating cure. The coupling of the copper wires and the electromagnetic field can lead to a weighting heating of the PCBs.
- The temperature rise of the wired PCBs by the means of microwave irradiation is based on the formation of standing wave and lead to a periodically temperature distribution. This applied to the straight wires and quadratically shaped wires.
- Close wires that close to each other can suppress this heating effect. In this case, the wired structure affects like a homogenously conductive area which reflects the microwave radiation. However, the dielectric heating of coating will fail to appear.
- It is difficult to analyze the coupling of the real PCBs and the microwave radiation due to their complicated metallic structures.
- The position of PCB in the microwave oven and the starting point of the wire influence on the temperature range distributing on the PCBs. For each position there will be critical points of the wire's lengths with which the wave in PCBs and

microwave in the cavity will be resonant. Thus the temperatures in these hotspots are extremely high.

- The temperature distribution on the wired PCBs depends on permittivities of attending materials and the microwave frequency. This is another indication of the formation of standing waves due to the microwave irradiation. Additionally, the numerical analysis confirmed a functional relationship concerning wave propagation on the wired PCBs.

The knowledge above indicates the opportunities to optimize the microwave process in order to support the uniform heating of the curing process.

## CHAPTER 4

# OPTIMIZING INTERACTIONS OF PCB STRUCTURES WITH THE MICROWAVE RADIATION FOR SUPPORTING COATING CURES

From the knowledge obtained, when no optimization is operated in order to reduce the periodical heating caused by the PCB structures, there will be no chance for a homogeneous heating of coatings by the means of microwave irradiation at frequency 2.45 GHz. The distance of hotspots undergoing high microwave frequency can be shorter and may lead to a uniform heating. Nevertheless, this investigation is restricted in the microwave radiation at the fixed frequency of 2.45 GHz. Therefore the optimization is based on the analyzed effects of the microwave radiation on PCB structures. The first factor is the position and direction of the copper structures. An oriented electric field distribution may be utilized. Due to a known field distribution, the antenna effect can be reduced in microwave process by locating the electronic assemblies in a place with less effectiveness of antenna effect. Because of the reflective electromagnetic wave in the heating cavity, the distribution of electromagnetic field is irregular and it leads to a difficulty to control. So it is hard to implement by the microwave oven. There is also another way to optimize the distribution of electromagnetic field. The incident electromagnetic wave can be interfered right before it couple with conductive structures by using accessories such as shields. Another factor should be considered is the material properties. The heating process can be affected by changing material properties. Therefore in this chapter, the microwave process for electronic assemblies in the mean “Optimization” will be investigated in three cases:

- **Heating cavity optimization:** make the field distribution as homogeneous as possible and minimize the field distorted by electronic assemblies.
- **Shielding/Protecting sensitive structures of the electronic assemblies:** shielding by metallic faces and absorption by dielectric layers.
- **Improving the microwave process of the coating cure:** to minimize the needed microwave energy by changing material properties.

Figure 4.1 illustrates the analysis of the work so far.

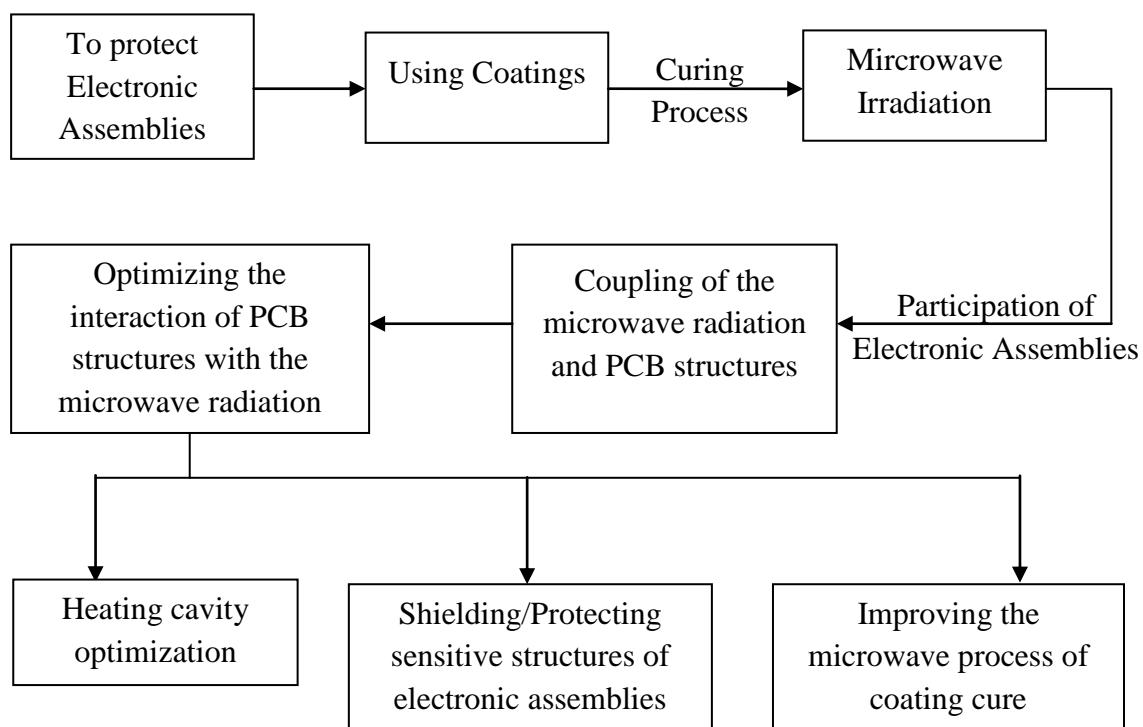


Figure 4.1: The structure of the study

## 4.1 HEATING CAVITY OPTIMIZATION.

The irregular field distribution of microwave oven is caused by the strong reflection of microwave from metallic walls of the cavity. To avoid the reflection, the investigation of a microwave horn and rectangular waveguide as a heating cavity is now taken into account. They both have known electromagnetic field distributions which can be utilized to optimize the interaction between wired PCBs with the microwave radiation.

### 4.1.1 MICROWAVE HORN

Microwave horn or horn antenna is an antenna that consists of a waveguide shaped like a horn to propagate radio wave. Horn antennas provide a high gain, low standing wave ratio VSWR (with waveguide feed), relative wide bandwidth and easy to make [13].

Horn antennas are taken into account because the microwave radiation will be transfer directly to the sample without reflective wall. In this part, horn antennas fed by rectangular waveguides are considered. They are pyramidal horn, *E*-plane horn, *H*-plane horn. The most

popular horn antenna in those three is the pyramidal horn antenna, which horn is flared in both planes [13, 58].

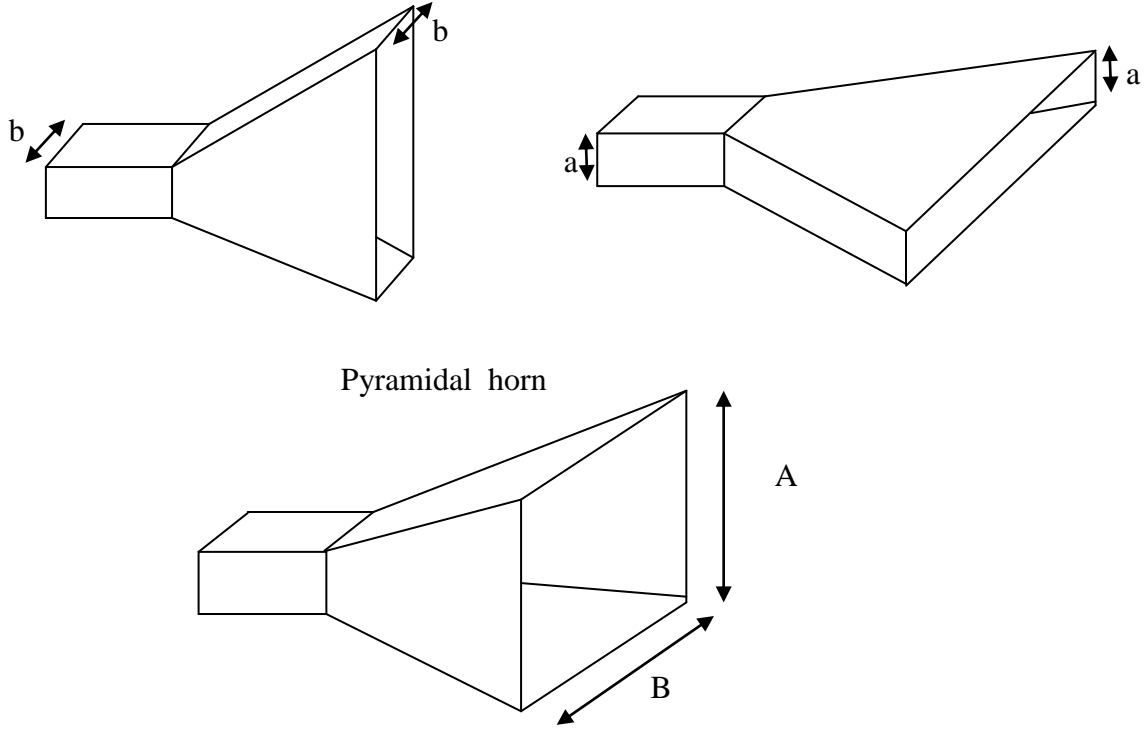


Figure 4.2: The microwave horns fed by rectangular waveguide

#### 4.1.1.1 BASIC EQUATIONS

The radiation pattern of horn antenna depends on  $A$  and  $B$  (the dimension of the horn at opening) and  $R$  (the length of the horn), along with  $a$  and  $b$  (dimension of the waveguide). These parameters are optimized and shown in the following figure.

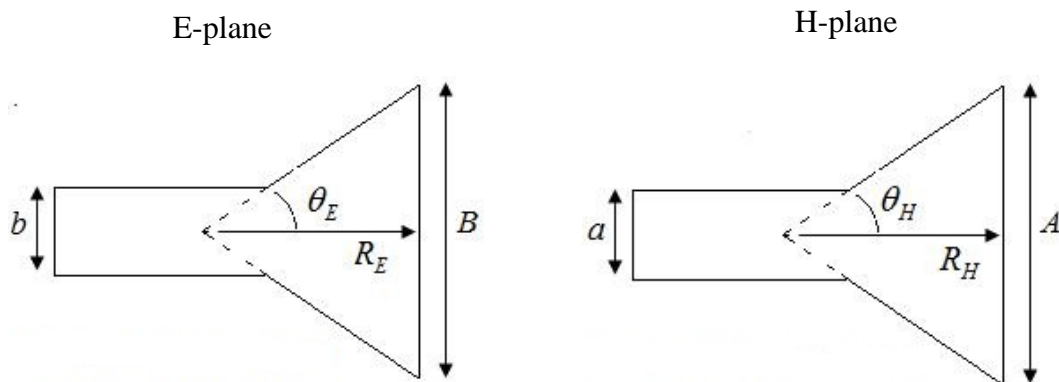


Figure 4.3: Cross section of waveguide cut in  $E$  plane (left) and  $H$  plane [58]

The flare angles  $\theta_H$  and  $\theta_E$  depend on the height, width and length of the horn antenna. Since the given coordinate system with the base in the center of the opening of the horn and the  $x$ ,  $y$  directions along with  $A$  and  $B$  then the radiation will be maximum in  $z$ -direction.

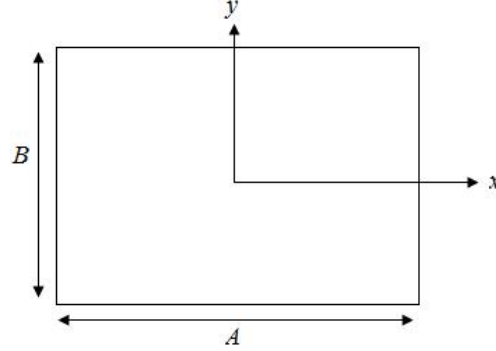


Figure 4.4: coordinate system used, center of the horn antenna opening.

Following [13, 58], the  $E$  field across the opening of the horn antenna can be approximated by:

$$E_A = \hat{y}E_0 \cos\left(\frac{\pi x}{A}\right) e^{-j\frac{k}{2}\left(\frac{x^2}{R_H} + \frac{y^2}{R_E}\right)} \quad (4.1)$$

And the  $E$  field in the far field will be polarized and the magnitude will be given by:

$$|E| = \frac{k}{4\pi r}(1 + \cos \theta) \int_{-B/2}^{B/2} \int_{-A/2}^{A/2} E_A(x, y) e^{jk(x \sin \theta \cos \phi + y \sin \theta \sin \phi)} dx dy \quad (4.2)$$

#### 4.1.1.2 SIMULATION RESULTS

The idea here is to use the microwave horn as a heater in a system as shown in figure 4.5 [59]. The electronic assemblies will run underneath the horn antenna, on a conveyor and be heated up. There is no cavity at all.



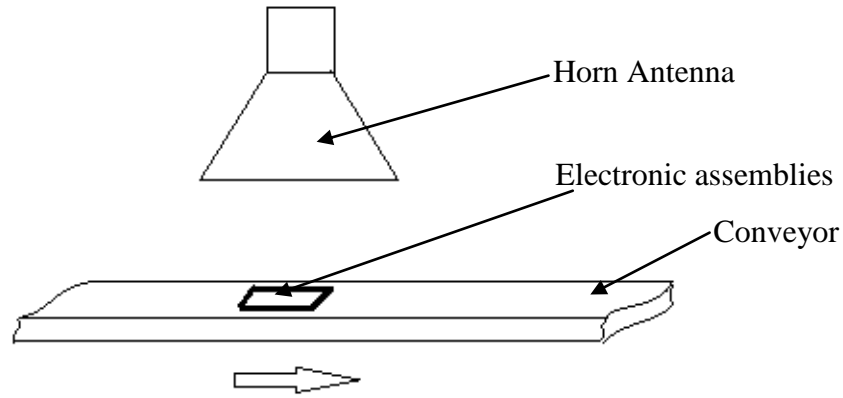


Figure 4.5: The system, utilized the horn antenna to heat electronic assemblies

In simulation, a part of air surrounding PCBs is also simulated but assigned to a box on continuous boundaries condition (figure 4.6).

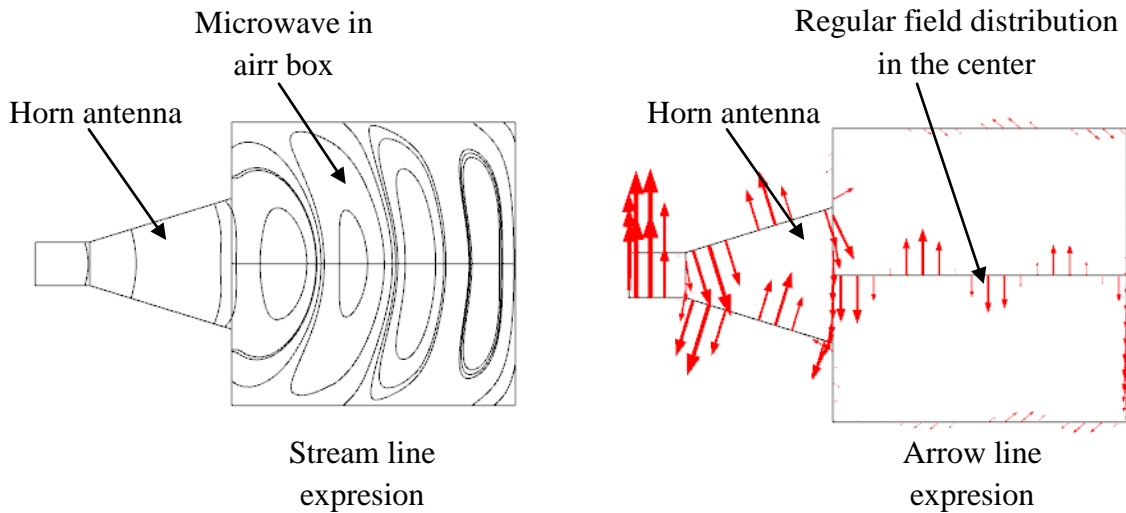


Figure 4.6: The polarization of  $E$  field (inside the air box) of the horn antenna in stream line expression (left) and in arrow expression (right), the line in the center is the location where the electronic assemblies is set

As seen in figure 4.6, the electromagnetic field spreads wider in the air (stream line expression). In the center, the field distributes regularly, and is strong near the microwave horn and fades out in the far distance. So the oriented polarization in the center of the horn antenna can be utilized in heating wired PCBs.

Simulations will be realized in three dimensions. PCBs will be set in the direction of being along (figure 4.7) or being cross (figure 4.9) the microwave polarization through the center of the horn. This setting will show the effect of the polarization on the temperature distribution (figure 4.8 and figure 4.10).

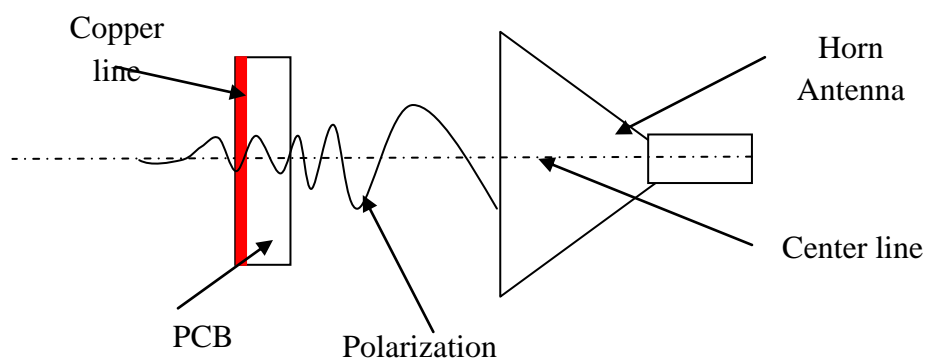


Figure 4.7: The PCB is set along the polarization of microwave horn

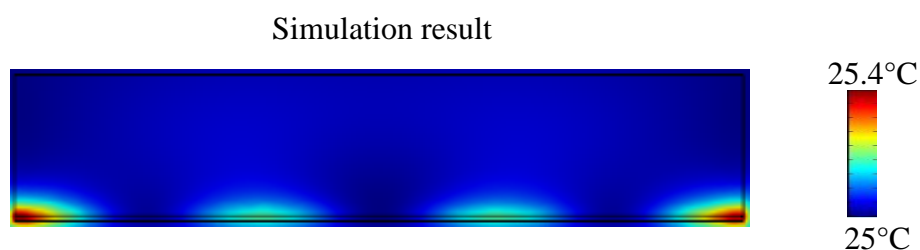


Figure 4.8: Simulation result of heating the PCB sample ( $150 \times 30 \times 2.5 \text{ mm}^3$ ) in 50 s by microwave horn (with power of 200 W) in the case the PCB is set along the polarization

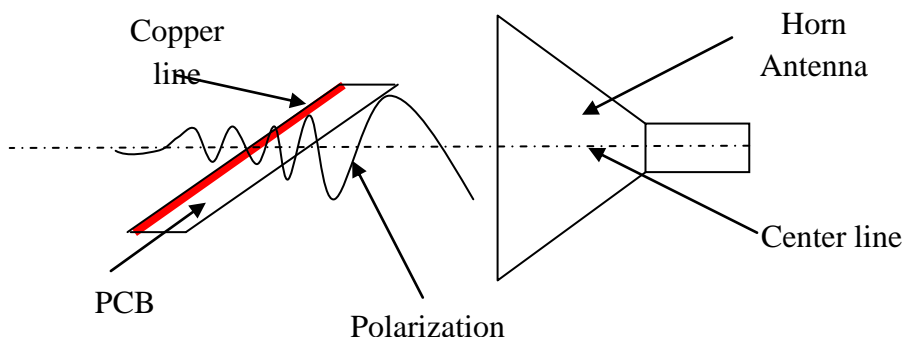


Figure 4.9: The PCB is set crossed the polarization of microwave horn

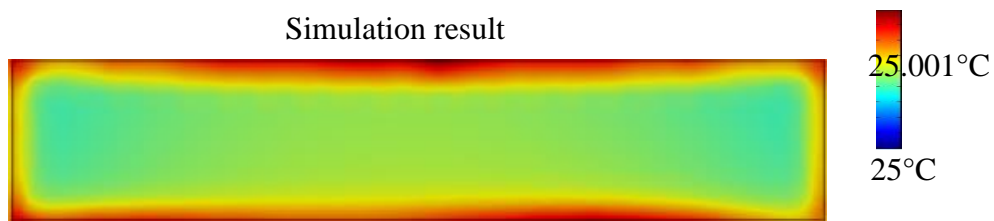


Figure 4.10: Simulation result of heating the PCB sample ( $150 \times 30 \times 2.5 \text{ mm}^3$ ) in 50 s by microwave horn (with power of 200 W) in the case PCB is set cross the polarization

As seen in figure 4.8 and 4.10, the temperature distributions on PCBs can be intervened by positing the PCBs. This cannot be realized by using microwave oven due to the reflection of microwave radiation from metallic walls. However there is lack of effectiveness in heating up the samples. When the copper wire is set along the polarization, there are hotspots but the temperature increases only a bit ( $0.4^{\circ}\text{C}$ ). In the case the copper wire is set crossed the polarization, the interaction between copper wire with microwave radiation is weak to create a strong coupling and the temperature tend to be distributed homogeneously. Horn antennas are not effective devices for heating PCBs eventually. The idea of setting PCBs position can be successful only in a process with another effective heating device.

#### 4.1.2 USING RECTANGULAR WAVEGUIDES AS HEATING CAVITIES

Rectangular waveguides used as heating cavities are studied in an attempt to find devices which would satisfy two conditions: oriented electric field distribution (or in other words, known electric field distribution) and effective heating.

Waveguide is an electric conductor consisting metal tubing, usually circular or rectangular in cross section, used for the conduction or directional transmission of microwave [13].

The waveguide acts as a high-pass filter in that most of the energy above a certain frequency (cutoff frequency) will pass through the waveguide, whereas most of the energy that is below the cutoff frequency are attenuated by the waveguides [60]. The frequencies, at which waveguides are often used, are microwave frequencies. In scope of this investigation, rectangular waveguides are taken into account (figure 4.11).



Figure 4.11: A rectangular waveguide [61]

#### 4.1.2.1 THE BASIC EQUATION

A waveguide has a width  $a$  in  $x$ -direction and a height  $b$  in  $y$ -direction ( $a > b$ ) and carries power in  $z$ -direction

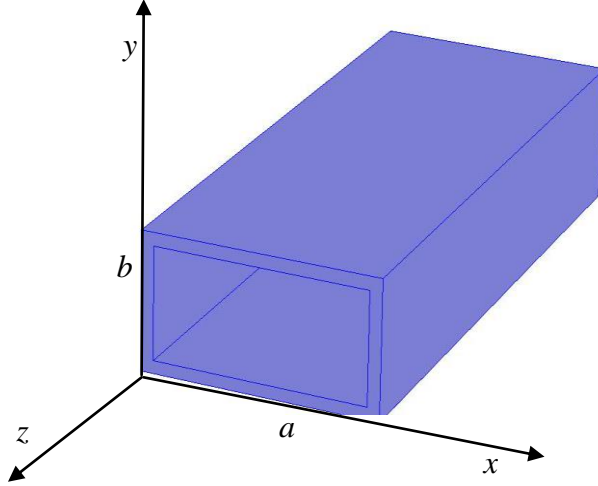


Figure 4.12: Cross section of a waveguide with the width  $a$  and the height  $b$

The electromagnetic energy cannot propagate the waveguide if both  $z$ -component of magnetic field  $H_z$  and  $z$ -component of electric field  $E_z$  are zero. Hence the allowed field configuration is only transverse magnetic ( $TM$ ), in which  $H_z = 0$  or only transverse electric ( $TE$ ), in which  $E_z = 0$  [13].

In this investigation,  $TE$  mode is in the focus with the assumption of  $E_z = 0$ . Then working through Maxwell equations, following [13, 60] the  $E$  field and  $H$  field can be determined by the equations:

$$E_x = A_{mn} \frac{n\pi}{b\epsilon} \cos\left(\frac{m\pi x}{a}\right) \sin\left(\frac{n\pi y}{b}\right) e^{-jk_z z} \quad (4.3)$$

$$E_y = A_{mn} \frac{n\pi}{a\epsilon} \sin\left(\frac{m\pi x}{a}\right) \cos\left(\frac{n\pi y}{b}\right) e^{-jk_z z} \quad (4.4)$$

$$E_z = 0 \quad (4.5)$$

$$H_x = A_{mn} \frac{m\pi k_z}{a\omega\mu\epsilon} \sin\left(\frac{m\pi x}{a}\right) \cos\left(\frac{n\pi y}{b}\right) e^{-jk_z z} \quad (4.6)$$

$$H_y = A_{mn} \frac{n\pi k_z}{b\omega\mu\epsilon} \cos\left(\frac{m\pi x}{a}\right) \sin\left(\frac{n\pi y}{b}\right) e^{-jk_z z} \quad (4.7)$$

$$H_z = -jA_{mn} \frac{k^2 - k_z^2}{\omega\mu\epsilon} \cos\left(\frac{m\pi x}{a}\right) \cos\left(\frac{n\pi y}{b}\right) e^{-jk_z z} \quad (4.8)$$

In the equations above, the constants are noticed as  $A_{mn}$  where  $m$  and  $n$  are the mode numbers, which implies that the amplitude for each mode can be independent of others. Nevertheless, the field components for all single modes must be related.

#### 4.1.2.2 CUTOFF FREQUENCY

The waveguide has a cutoff frequency  $f_c$ , at which all lower frequencies are attenuated by the waveguide and above it all higher frequencies propagate within the waveguide. The cutoff frequency defines a high-pass filter characteristic of the waveguide: above this frequency, the waveguide passes power and below this, the waveguide blocks or attenuates the power [60].

The cutoff frequency depends on the shape and the size of the cross section of the waveguide. The larger waveguide is, the lower frequency for that waveguide is.

Following [13] and based on equations from (4.3) to (4.8), the cutoff frequency for  $TE_{mn}$  mode can be solved as:

$$f_c^{mn} = \frac{c}{2} \sqrt{\left(\frac{m}{a}\right)^2 + \left(\frac{n}{b}\right)^2} \quad (4.9)$$

Both modes  $m$  and  $n$  cannot be zero. If they are, then the entire field components from (4.3) to (4.8) will be zero. When  $m=1$  and  $n=0$  then the formula for the cutoff frequency of a cross section waveguide ( $TE_{10}$ ) is given by:

$$(4.10)$$

$$f_c = \frac{c}{2a}$$

The waveguide will not transport energy at frequencies which are below the cutoff frequency. The only mode that is a propagating mode will be  $TE_{10}$  mode when the waveguide operates at a frequency above cutoff frequency. All other modes will be decaying. Hence the  $TE_{10}$  mode, which is the only mode that has the lowest cutoff frequency, is referred to as the dominant mode.

#### 4.1.2.3 THE MODEL OF RECTANGULAR WAVEGUIDE

In the scope of this study, the investigation of the microwave treatment for PCBs is desired to implement at the frequency of 2.45 GHz. Therefore the waveguide WR340 is selected.

WR	$f_L - f_U$	Insight width	Insight height
WR340	2.20-3.30 (GHz)	86.36 mm	43.18 mm

Table 4.1: Frequency band and dimension of rectangular waveguide WR340 [62]

where  $f_L$  and  $f_U$  are the lower and upper frequencies of frequency band of WR340, insight width and insight height are the interior dimension of the rectangular waveguide.

The idea here is using a waveguide body as a heating cavity. At the sides of the waveguide, there are two slits which can accept the electronic assemblies enter and escape the cavity on a running conveyor acting as an underload (figure 4.13) [59].

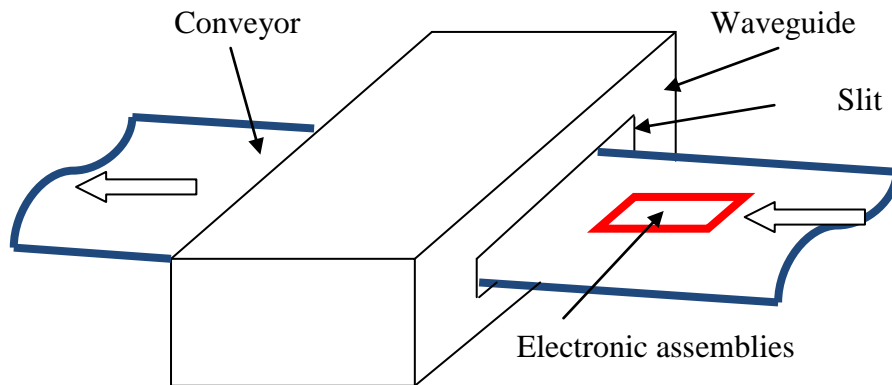


Figure 4.13: The sketch of the system using the waveguide as the heating cavity

The simulation results of the electromagnetic field distribution prove that it is regular as described in figure 4.14 below.

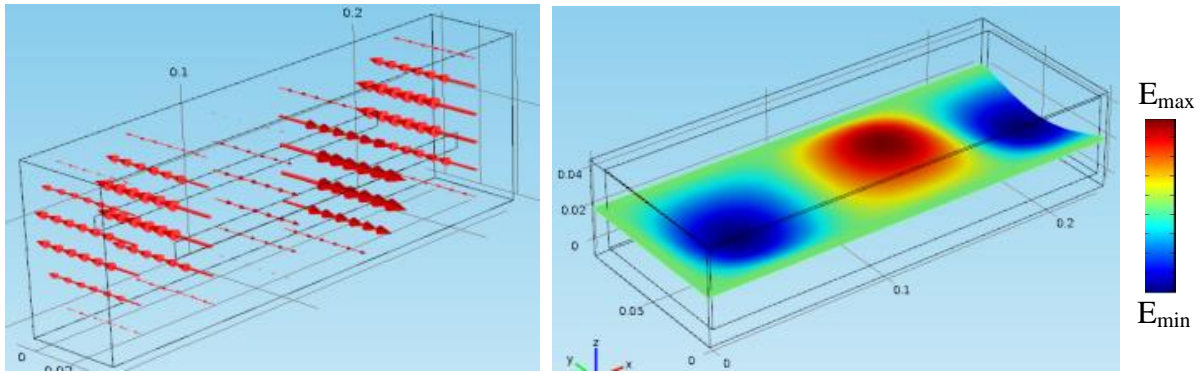


Figure 4.14: The polarization of electromagnetic waves (red arrows; left) and the slice view of the electric field distribution in a rectangular waveguide

The problem here is the height of the slits must not be only sufficient for the conveyor and electronic assemblies running through but also small enough for avoiding the energy loss.

To determine the loss energy via the slits, models including surrounding air are built with variable slit-heights (figure 4.15). And figure 4.16 shows how the electric field escapes through the slits to the surrounding air.

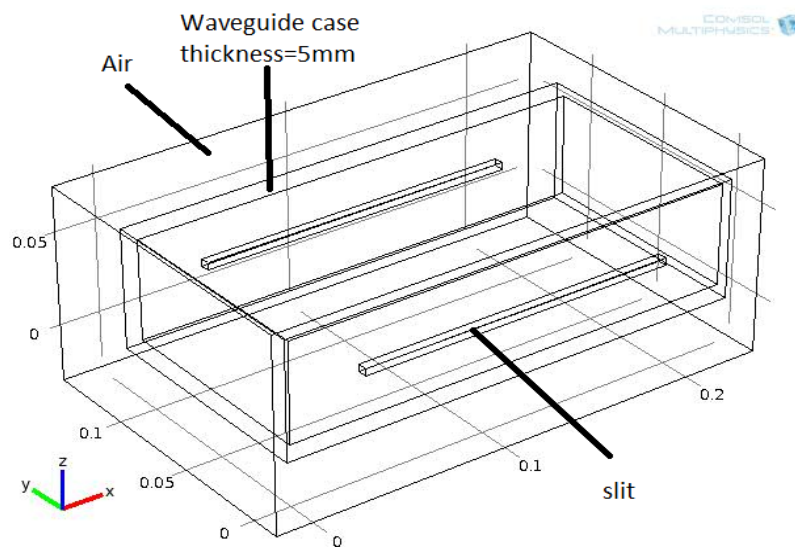


Figure 4.15: The model of the rectangular waveguide ( $86.36 \times 43.18 \times 230 \text{ mm}^3$ ), which the slits locate at the small sides with surrounding air

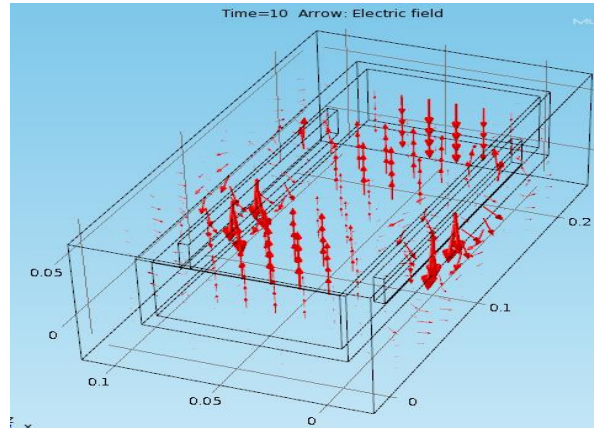


Figure 4.16: The electric field losses from the inside of waveguide to the surrounding air

The minimal slit-height should be 8 mm to allow at least a PCB and the conveyor running through. Thus the maximal slit-height needs to be determined. The loss energy can be found by calculating the electric field strengths at a same point in the areas of strongest energy, where the electronic assemblies will be laid in the microwave treatment. These calculations will be realized for waveguides with no slit, with slit-height= 8mm, 12mm, 16mm and 20mm with the input power of 200 W.

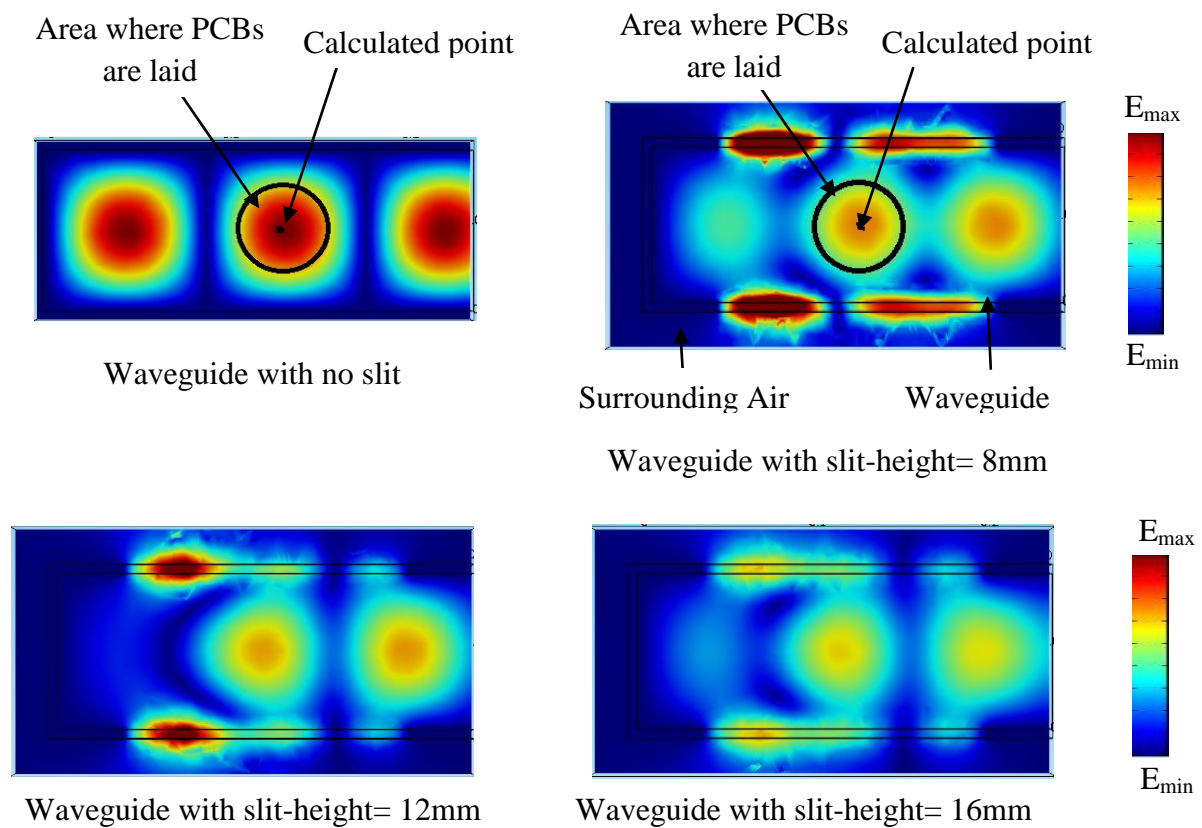


Figure 4.17: Display slices of electric field strengths cut the rectangular waveguides through the half of their heights



Figure 4.17 above illustrates the electric fields in the waveguides and the loss electric fields in the air for the case slit-height= 0, 8, 12, 16 mm. All for four pictures show the display slices of  $E$  field strengths, described by a color scale from blue (minimum) to red (maximum). The slice planes cut the waveguides at the half of the waveguide heights, therefore at the half of the slit-height as well. It is can be recognized by eyes that the  $E$  field strength decreases while the slit-height increases. The values of the  $E$  field strength for the calculated point will give more detail about the loss energy in following table and diagram.

Slit-height (mm)	$E$ field strength (V/m)	$\Delta E = E_0 - E_i$ (V/m); $i = 0 \dots 4$
0	$E_0 = 21222.58$	0
8	$E_1 = 15616.31$	5606.27
12	$E_2 = 13944.25$	7278.33
16	$E_3 = 12892.23$	8330.35
20	$E_4 = 11136.71$	10085.87

Table 4.2: The  $E$  field strengths of the calculated points (figure 4.17) and their loss energy for variable slit-heights

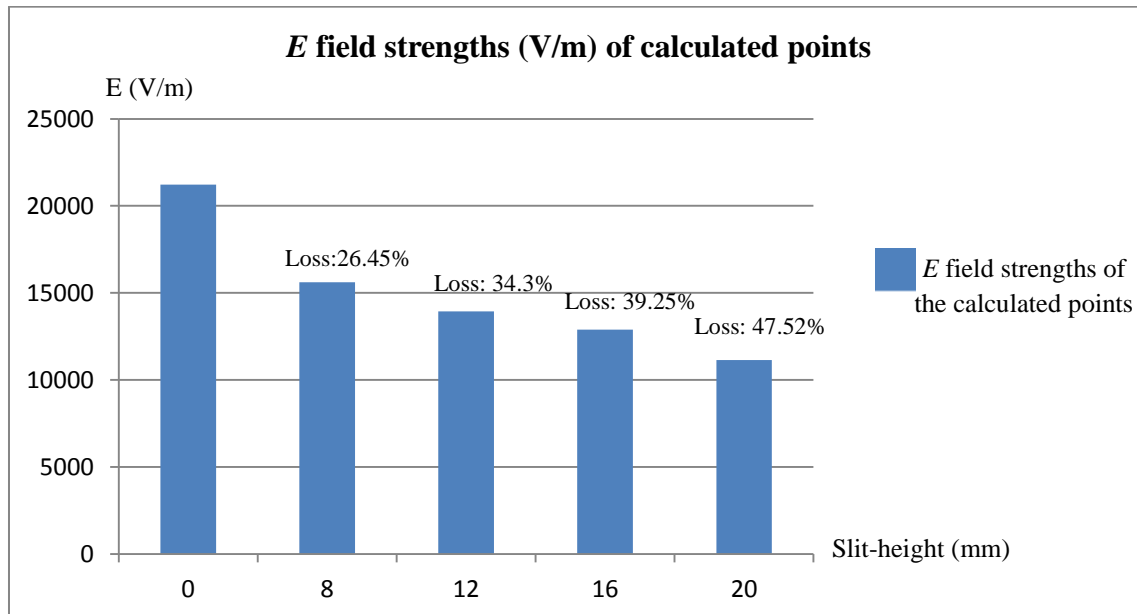


Figure 4.18: The chart shows electric field strengths of the calculated points of the case of no slit on the waveguide and slit-height= 0, 8, 12, 16, and 20 mm

From table 4.2 and figure 4.18, it seems that the loss energy is a big value even with the smallest slit-height (8mm) and therefore it is necessary to make an adjustment to reduce the loss energy through the slits. The change is just removing the slits to the big sides of the waveguide (figure 4.19) instead of the small sides (figure 4.15). The simulation results will represent the effectiveness of the adjustment (figure 4.20).

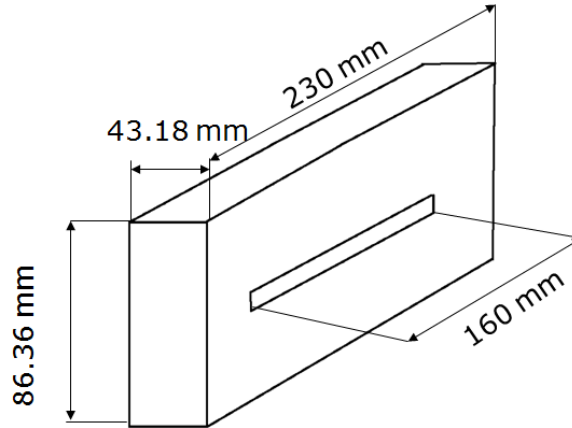


Figure 4.19: The slits are removed to the big sides of the rectangular waveguide [59]

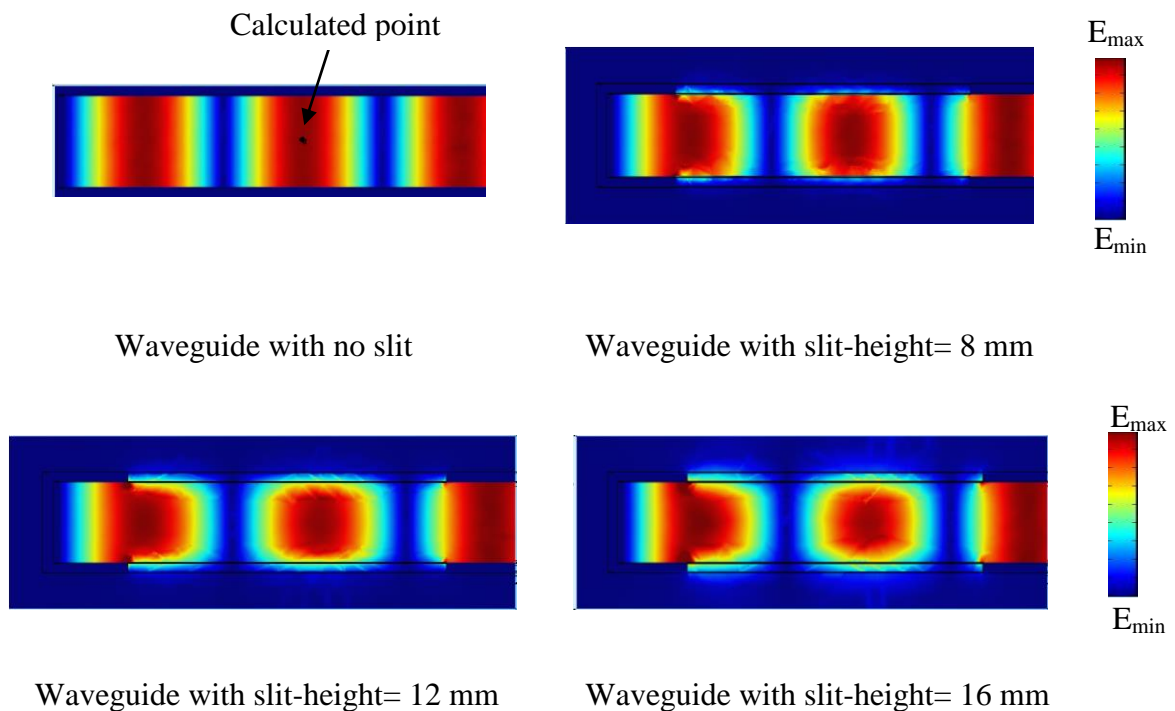


Figure 4.20: Display slices of electric field strength cut the rectangular waveguides through their half height in the case of slits in the big side

It is easy to realize by eyes that the change of the slits positions can reduce the loss energy (figure 4.17 and figure 4.20 have the same color scale to compare). The more detail will be given by table 4.3 and figure 4.21.

Slit-height (mm)	$E$ field strength (V/m)	$\Delta E = E_0 - E_i$ (V/m); $i = 0 \dots 6$
0	$E_0 = 21222.58$	0
8	$E_1 = 21050.51$	172.07
12	$E_2 = 20785.75$	436.83
16	$E_3 = 20507.35$	715.23
20	$E_4 = 20156.73$	1065.85
24	$E_5 = 19880.06$	1342.52
30	$E_6 = 19423.89$	1798.69

Table 4.3: The  $E$  field strengths of calculated points and their loss energy for variable slit-heights when slits are located in the big sides of the waveguide

The calculations are carried out till the slit-height is 30 mm. This height is more than sufficient for the system including conveyor, PCBs and their components. The loss energy in this case is far less than in the case of waveguides with slits in the small sides. The detail of the comparison can be seen in following chart.

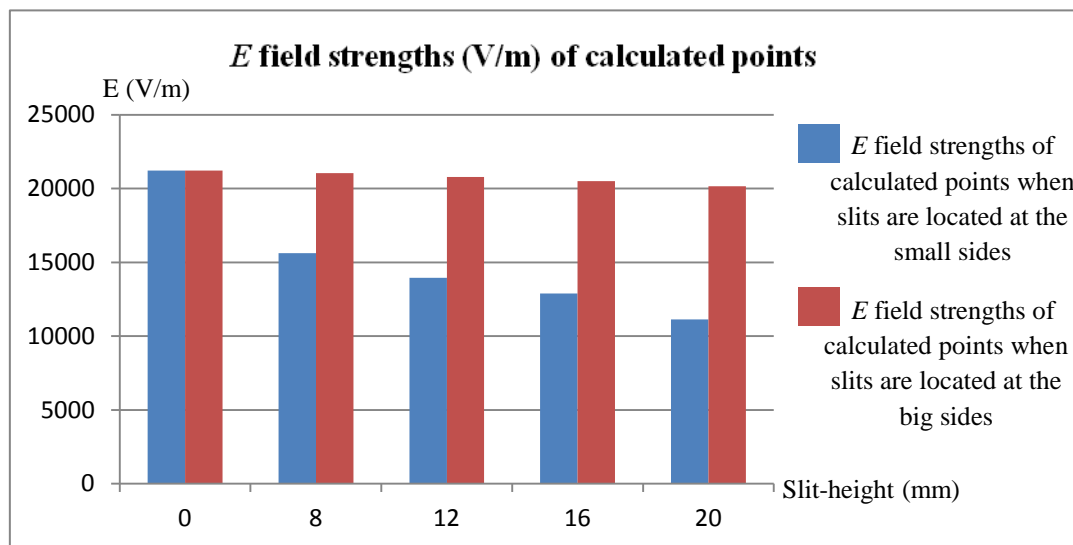


Figure 4.21: The comparison of  $E$  field at calculated point in cases waveguide with slits at small sides (blue) and waveguide with slits at big sides (red) for slit-height= 0, 8, 12,16, 20 mm

In the end of the day, based on the comparison, the final decision is that the waveguide with slits are set at the big sides of the rectangular waveguide.

#### 4.1.2.4 ADVANCED FORMS OF RECTANGULAR WAVEGUIDES AS HEATING CAVITIES

The curing process needs some time to let the coating on the electronic assemblies be heated up to the necessary temperature. Therefore instead of running continuously, the conveyor will run then stop for a while in the heating process.

This part brings an idea to reduce the stoppage time or even make the system run continuously but still heat the electronic assemblies and coating up to the necessary temperature. The idea is that using some advanced forms of waveguides based on rectangular waveguides for example: U form or multi-U form (figure 4.22 and 4.23).

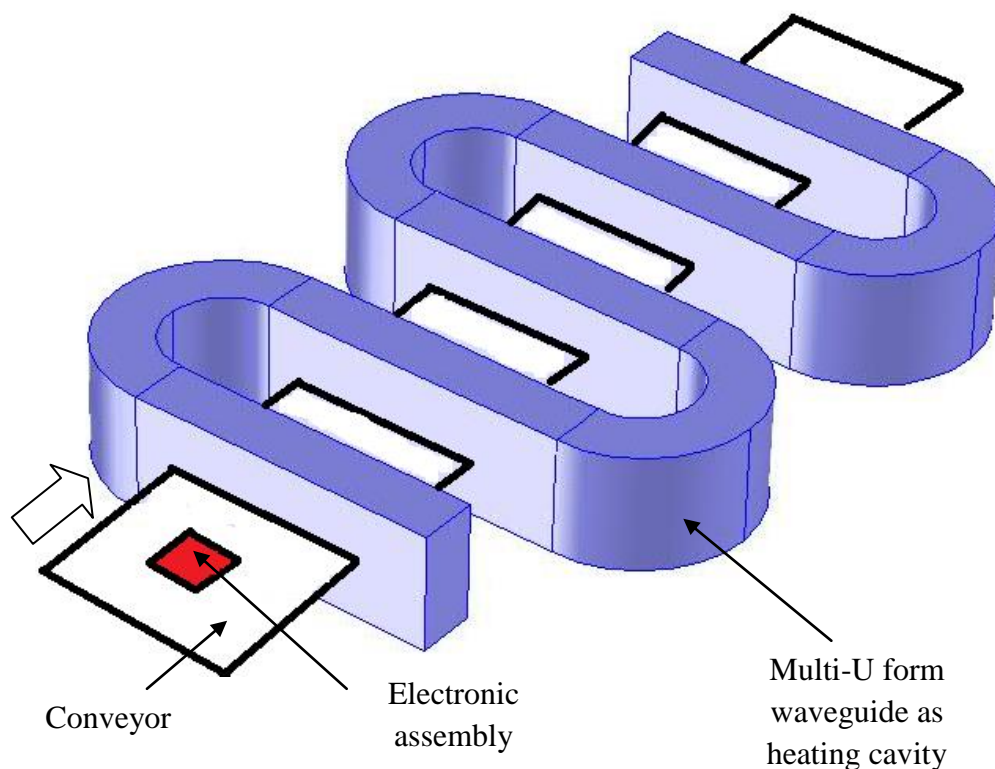


Figure 4.22: The sketch of system using a multi-U form waveguide as a heating cavity

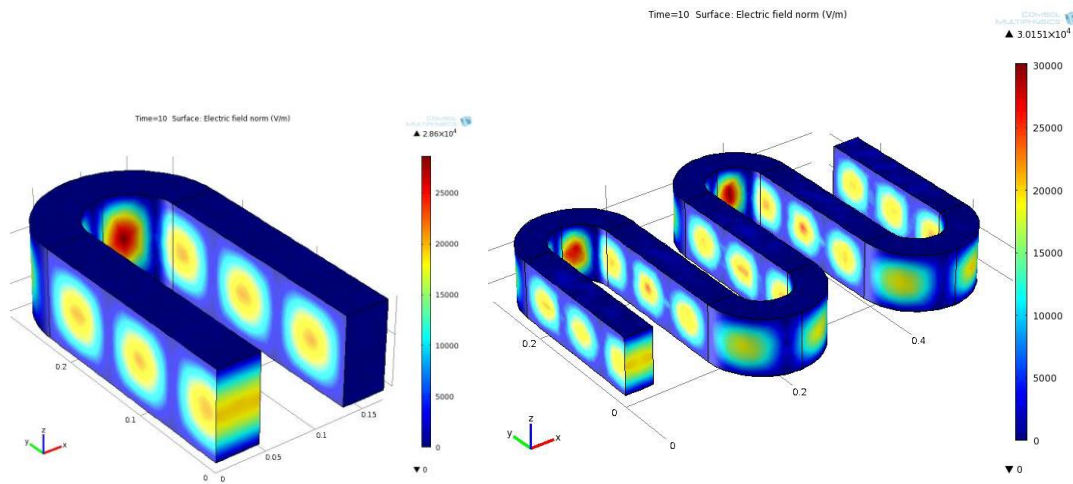


Figure 4.23: Electric fields in a U form waveguide and a multi-U form waveguide

The conveyor carries electronic assemblies and runs through two rectangular cavities (U form as in figure 4.23 (left)) or more than two cavities (multi-U form as in figure 4.23 (right)) instead of one cavity as in the case of using the rectangular waveguide. Since all cavities can heat the PCBs up, then the stoppage time can be reduce or even clear (when using multi-U form) by controlling the speed of the conveyor. Normally, for rectangular waveguides as heating cavities, only one port is used and the other is close, because an open waveguide with two ports will waste much more energy than an enclosed waveguide. With the enclosed waveguide, the microwave is reflected and therefore brings more harm to the electronic assemblies. With the multi-U form waveguide, the open waveguide as heating cavity is possible, because of the multiple use of the same wave and the microwave energy can be save for the heating process. Hence it also leads to the avoidance of reflection.

The following figure shows a view of heating a PCB by the U form waveguide. The arrow represents the electric field inside the cavity. The electric field due to the appearance of the copper wires increases the strength rapidly (expressed by the size of the arrow around the PCB) even in the outside of the U form cavity (in the surrounding air).

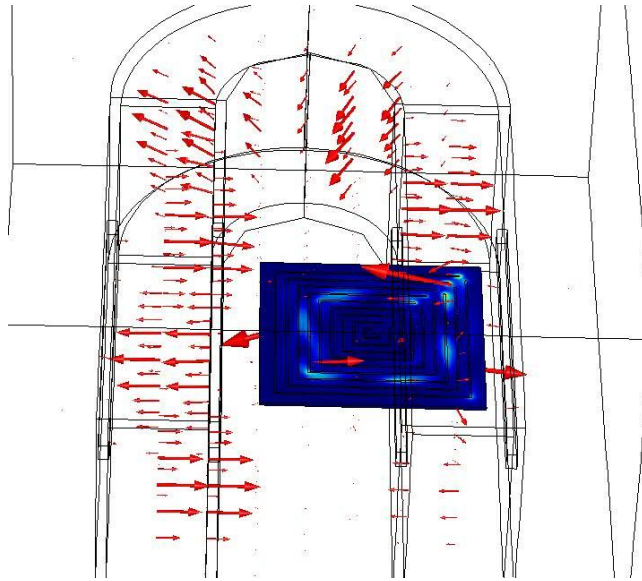


Figure 4.24: Simulation result illustrates the interaction of the PCB structure with microwave radiation of a U-form waveguide. The  $E$  field spreads out to the air following the copper wires

#### 4.1.2.5 THE INFLUENCE OF THE POLARIZATION

As mentioned above the reason that rectangular waveguides are investigated, is about the known region of electric field distribution. That also means that the temperature distribution can be intervened by utilizing the direction of the polarization.

#### PCB STRUCTURES CROSS THE POLARIZATION

For the investigation, a PCB model with an even copper wire is designed. First of all, the PCB is laid crossed the polarization which means the copper wire is crossed the polarization. The dimension of the PCB sample is  $(40 \times 30 \times 1.5 \text{ mm}^3)$ . The time of heating process is 10 seconds. The simulation result is shown in figure 4.25.

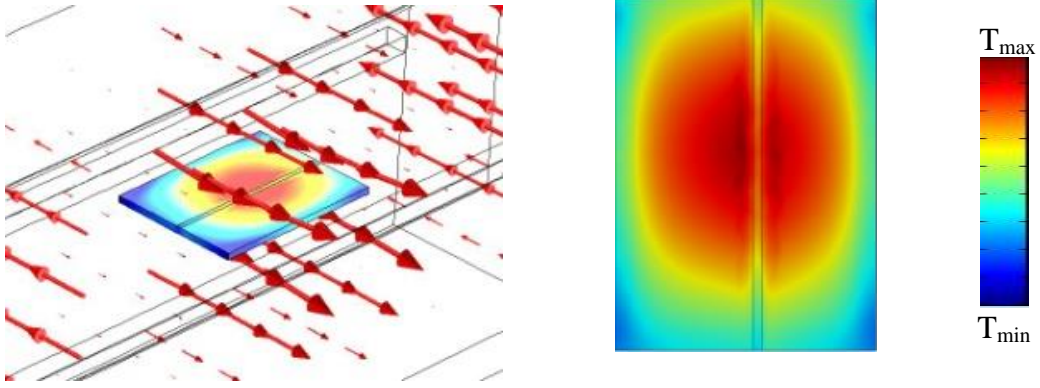


Figure 4.25: The polarization (red arrows) crosses the copper wire on PCB (left picture) and a close view describes the dominant dielectric heating in this case (right)

As displayed in figure 4.25, when the copper wire crosses the polarization, the coupling is weak. In this case the incident electric field makes an angle  $90^\circ$  with the wire. Therefore the antenna effect cannot dominate the dielectric heating of the substrate. The PCB is heated from the center to the edges. From the initial temperature (room temperature)  $20^\circ\text{C}$ , after 10s heating, the highest temperature area distributes in the center ( $T_{\text{max}} = 23.5^\circ\text{C}$ ). The temperature decreases from the center to the borders of the PCB ( $T_{\text{min}} = 21.5^\circ\text{C}$ ). There is no hotspot at all, only homogeneous temperature distribution with the difference of temperature  $2^\circ\text{C}$ , which can support well the curing process.

Since the coupling of the single copper wired PCB and the microwave radiation is weak, then the next step is that increasing the number of the copper wire from 1 to 2, 4 and 6 as the following figure.

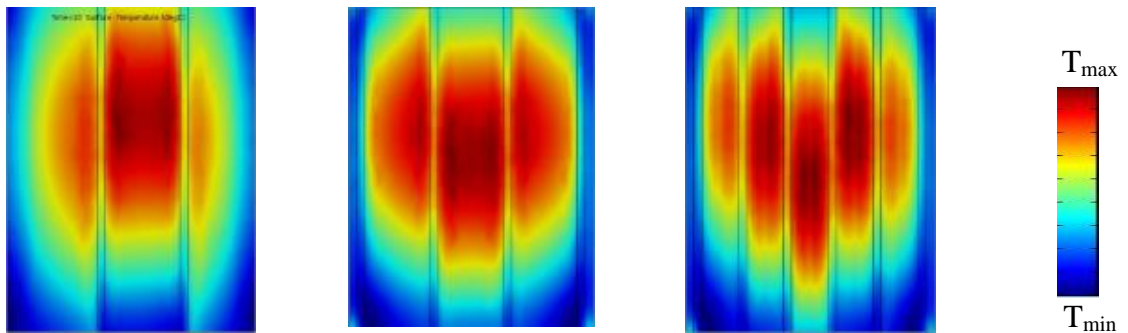


Figure 4.26: Simulations of PCBs with 2 copper wires (left), 4 copper wires (middle) and 6 copper wires which crossed the polarization show the homogeneous heat distribution



The results show separated areas of temperature. Each area is made by the edges of the PCBs and copper wires, because the electric field within each wire itself is very small. Hence the temperature spreads discontinuously. However, the width of the copper wire is small (1mm), therefore the discontinuation influences less on the heating. When all these areas are set together, they give a basic homogeneous temperature distribution. Finally it may confirm that in this position, the antenna effect is low and the dielectric heating can be achieved. Following figure exposes the simulation result of microwave process for the coating cure of a PCB with six wires crossed the polarisation. The picture in the left hand side illustrates the temperature distribution on the top of the PCB (underneath the coating layer). The picture in the right hand side expresses the temperature distribution on the surface of the coating layer.

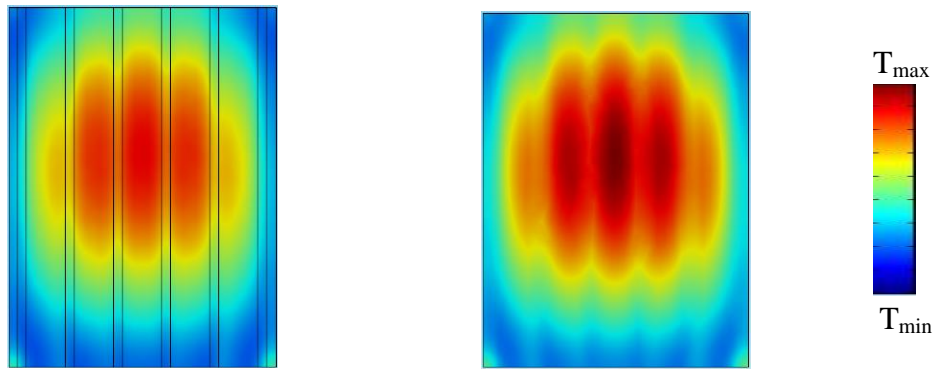


Figure 4.27: The temperature distribution on PCB (left) with highest temperature 79°C and the temperature distribution on the coating with 1mm thickness and  $\epsilon = 5.5-j$  (right), which is coated on the PCB. The highest temperature of the coating is about 88°C; simulation in 10 s

## PCB STRUCTURES WHICH ARE NOT CROSSED THE POLARISATION

The next step is that setting the single wired PCB along with the polarization. That means the direction of copper wires will have the same direction with the polarization. In this case, the coupling of microwave radiation and the copper wire is strong enough. Thus after 10s of heating, with power 200 W, the result shows that the interaction of the microwave radiation and the copper wire leads the heat distribution separating in 2 hotspots (periodical heating) and increases the maximal temperature to  $T_{\max} = 147^\circ\text{C}$  (figure 4.28). This can make the PCB defect locally in around the hotspots.



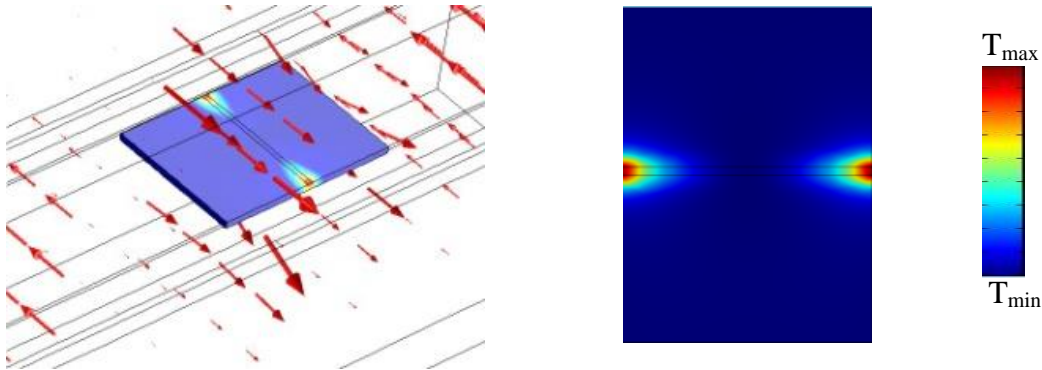


Figure 4.28: The copper wire on PCB is along with the polarization (left picture) and the close view shows the periodical heating in this case (right)

The result above cannot support the curing process of the coating as seen in the following figure 4.29. The simulation is carried out with a covered coating (thickness 1mm) on the PCB. The power is reduced to 100 W due to the high temperature in hotspots of the previous simulation (figure 4.28). Since the desired highest temperature after heating PCBs and coatings is 140°C, which is the maximum operating temperature of FR-4 [63] then the result (temperature) will be described by the colour scale from blue to red describing temperature from 20°C (initial temperature) to 140°C. The temperature on PCB and coating, which is higher than 140°C, will be represented by the brown-red colour.

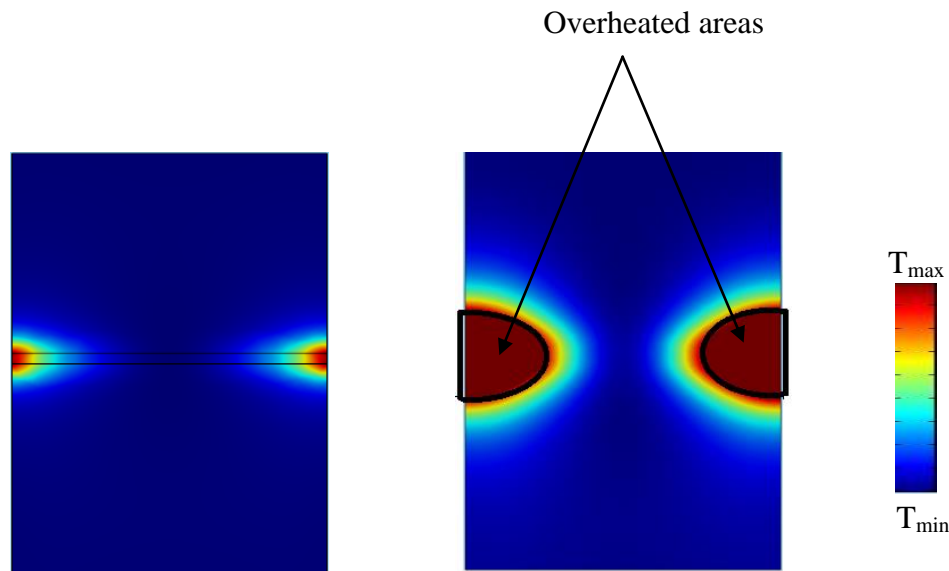


Figure 4.29: The temperature distribution on PCB (left) and coating (right); all four half eclipses are the overheated areas where temperature are over 140°C

From figure 4.29, the PCB will be defective locally at 2 hotspots and the coating cannot be cured. The coating is heated based on the electromagnetic wave which penetrates to the substrate material. The electromagnetic field in this case is deformed due to the coupling of the copper wire and microwave radiation.

In these two special positions (crossed and along the polarization), the polarization shows the rule on the coupling of microwave radiation and metallic structures. To understand more from the effect of polarization on the antenna effect, some extra simulations are carried out as well. In these tests, multi copper lines are built including two lines crossed the polarization connected by another line. The connecting line is rotatable to see how the polarization influences on the temperature distribution with variable directions of the copper lines (figure 4.30).

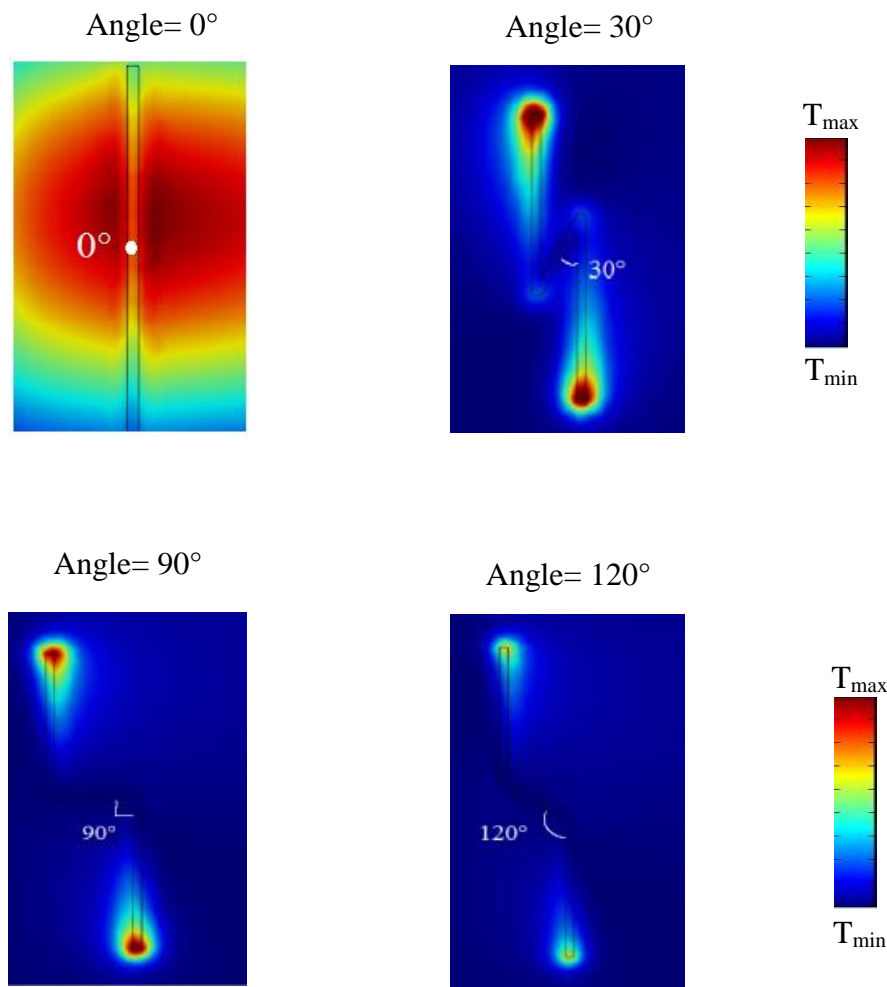


Figure 4.30: The temperature distribution on multi-copper-lines PCBs, which the angle of the connecting line with the other ones changes from 0 to 360°

The highest temperature of the cases angle=0° is  $T_{\max}=23.5^{\circ}\text{C}$ ; case angle= 30° is  $T_{\max}=130^{\circ}\text{C}$ ; case angle= 90° is  $T_{\max}=110^{\circ}\text{C}$  and case angle= 120° is  $T_{\max}=80^{\circ}\text{C}$ . All lowest temperatures are the room temperature  $20^{\circ}\text{C}$ . From figure 4.29 above, there are two points to notice. Firstly, when the angle of the connecting wire and two other ones is zero then the structure becomes a straight copper line crossing the polarization. In this case the coupling is weak and the dielectric heating is dominant with the temperature around  $20^{\circ}\text{C}$  (see detail in figure 4.25). Secondly, the hotspots tend to transfer to the open and end of a wire. As exposed in figure 4.28, the hotspots are on two sides of a single wire along the polarization. Nevertheless in the same direction (along the polarization), the connecting wire in the multi wired structure (in case angle= 90°) has no hotspot. The hotspots jumped to the sides of the other wires.

The main concept summarized here is that if any part of the conductive structure makes with incident electric field an angle  $\neq 90^{\circ}$  then there will be an antenna effect. Another point is the hotspots will start from the open side of a structure and it doesn't depend on how the structure is and the case all wires cross the polarization is an exception.

#### 4.1.2.6 FAILURE OF UNIFORM HEATING OF REAL PCBs

It is really difficult to manage the heat source in the microwave process for real PCBs due to complex conductive structures. Figure 4.31 below shows the simulation result of the real PCB (the sample showed in figure 3.9) in the microwave heating with the rectangular waveguide as a heating cavity.

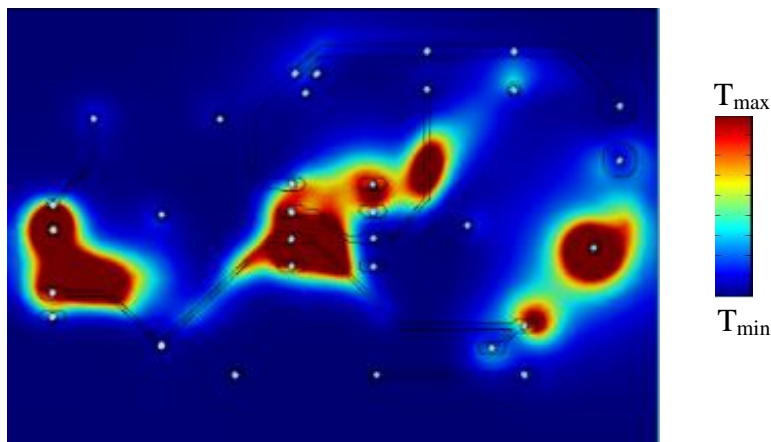


Figure 4.31: Temperature distribution on the simulated PCB where the dark red areas express the overheated areas (over  $140^{\circ}\text{C}$ )

As seen in figure 4.31, the real PCB cannot be uniformly heated. The main hotspots are on the main long copper wire and the hottest area is around the center where eight holes are located. Therefore to understand more about the effect on this PCB, some other tests will be realized.

In the following test, the main copper wire is removed in the center (figure 4.32) and the result displays that the coupling between microwave radiation and modified PCB is weaker than the coupling between microwave radiation and the original one.

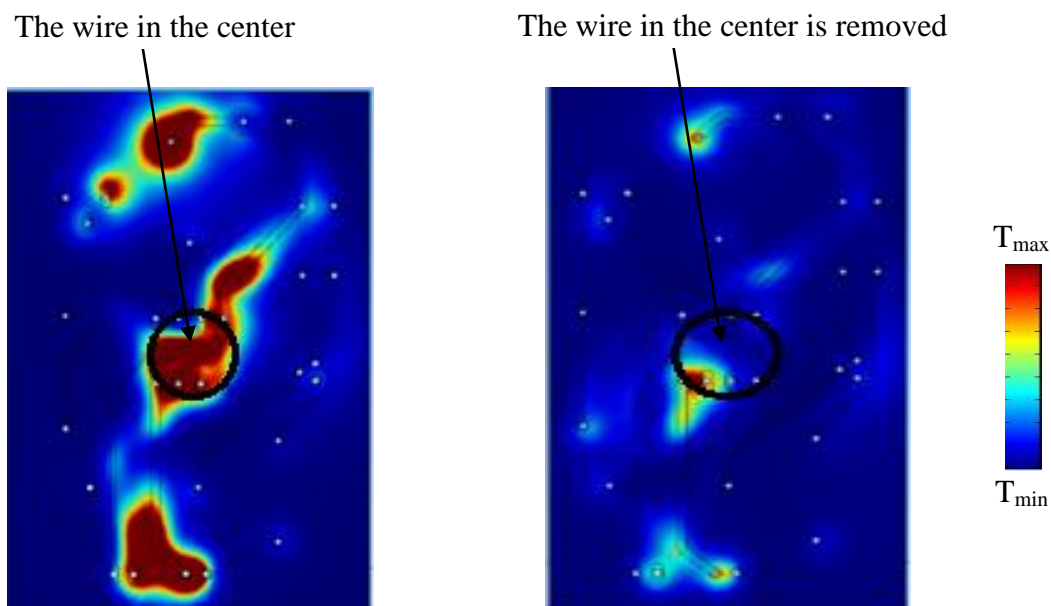


Figure 4.32: The coupling of microwave radiation and copper wires on the original real PCB (left) and the coupling on the PCB, on which the wire in the center is removed (right)

The next figure proves the impact of the polarization. The test is carried out with a half of original PCB lying in 2 directions. The result implies different temperature distribution.

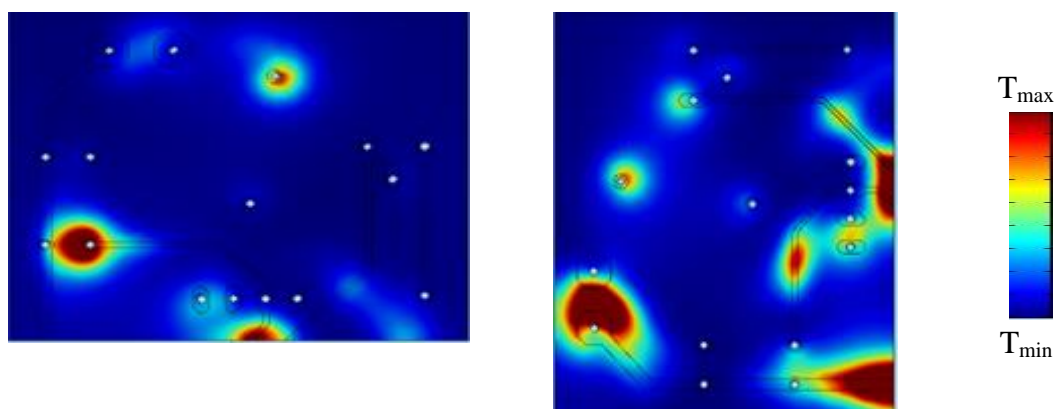


Figure 4.33: The impact of polarization on the real PCB tests with half PCB

## 4.2 SHIELDING/PROTECTING SENSITIVE STRUCTURES OF ELECTRONIC ASSEMBLIES

The uniform heating of electronic assemblies by using rectangular waveguide is limited. Another approach is using a shield to interfere the electromagnetic field which affects the PCBs. In this study, the microwave absorption of dielectric layers such as ceramics is utilized in the mean of “shield” to protect the PCBs structures. Other utilization, the microwave reflection ability of metallic faces is investigated as well.

### 4.2.1 CERAMIC SHIELDS

Ceramic shields are often used in electronic industry [64]. The relative permittivities of ceramics are about 8 to 10 [64]. Therefore if they are used to shield PCBs in a close distance (in simulation here is about 1mm). They can change the temperature distribution on PCBs as well as the temperature range as see in figure 4.34.

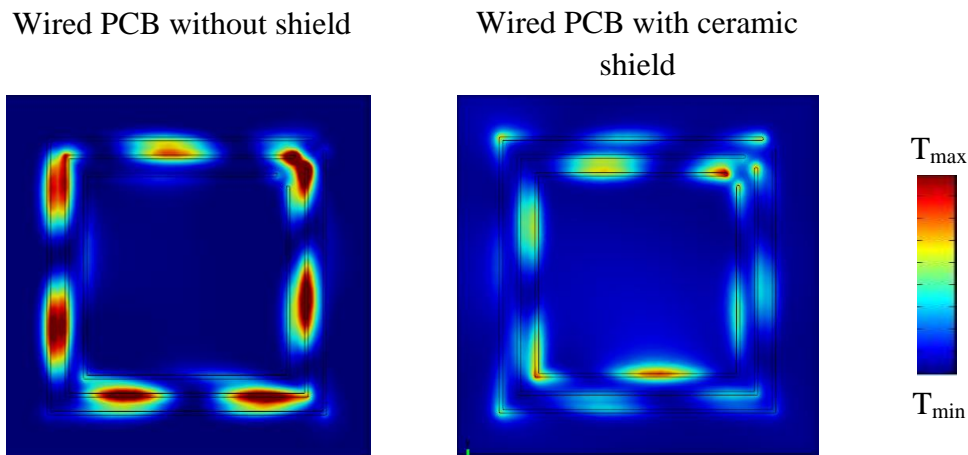


Figure 4.34: The temperature distribution of PCB without shield (left) and with ceramic shield (right) after microwave heating (simulation results)

The illustration presents the effect of the shield on the interaction of the PCB with the microwave radiation. For the comparison, the color scale from blue to red which expresses the temperature range for both cases (with shield and without shield) , is assigned to the temperature range of the shielded PCB (the range is from  $T_{\min}= 25^{\circ}\text{C}$  to  $T_{\max}= 39^{\circ}\text{C}$ ). Thus the hotspots of the unshielded PCB exhibits in dark red color which means temperature is over  $39^{\circ}\text{C}$ . Actually the temperature range of the unshielded PCB is from  $T_{\min}= 25^{\circ}$  to  $T_{\max}= 55^{\circ}\text{C}$ . In this case, the ceramic shield is not only change the temperature distribution but also

reduce the highest temperature of the hotspots. However the change of interaction does not suffice for supporting the curing process.

## 4.2.2 CONDUCTIVE SHIELDS

The ceramic shields due to high relative permittivities can reduce the wavelength of microwave which penetrates to them. This reduced wave affects the PCBs and decreases the temperature of the hotspots as well as the distance between hotspots. Unlike that, conductive shields will reflect the microwave and therefore can reduce or prevent harms from the coupling of PCBs and the microwave radiation.

### 4.2.2.1 FULLY CONDUCTIVE SHIELDS

The fully conductive shield means the conductive layer will cover the whole PCB. If the metallic structures are only in one side then the conductive shield will be in the other side as seen in figure 4.35. If the metallic structures located in both sides of PCB then the shield can cover the above the PCB.

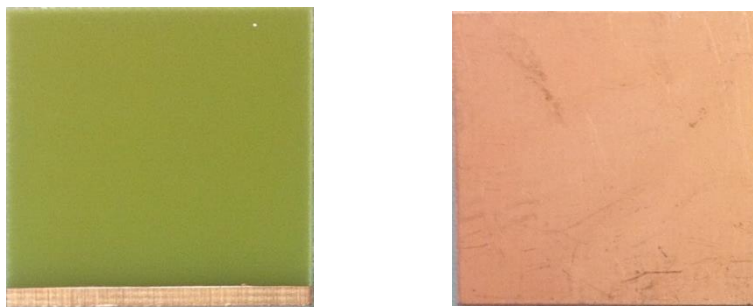


Figure 4.35: PCB sample with single wire on the top (left) and full copper shield at the bottom (right)

The test is carried out in microwave oven with the power of 200 W in 30 seconds. The dimension of single wired PCB is  $(30 \times 30 \times 1.5 \text{ mm}^3)$ . The following figure expresses the simulation results as well as the experimental results in the cases of the PCB with shield and without shield.

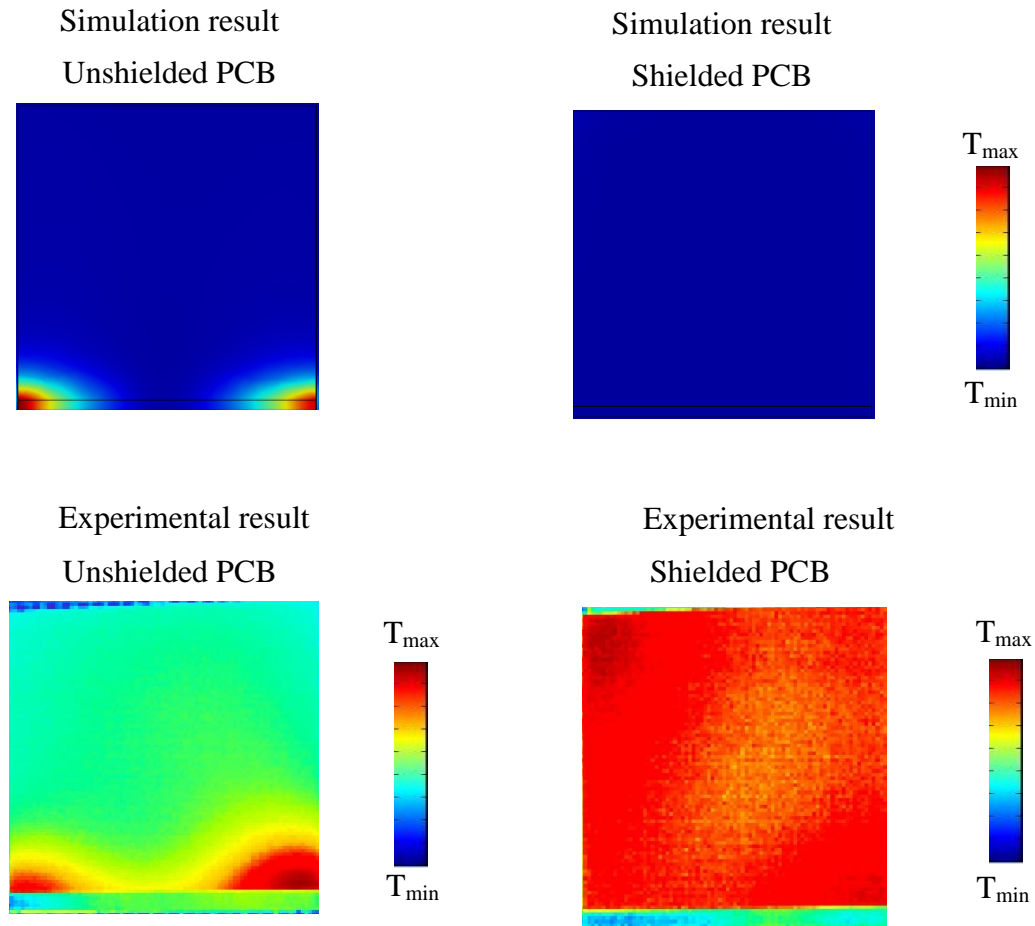


Figure 4.36: The simulation results and experimental results of the interaction between single wired PCBs in cases without shield (left) and with shield (right) with the microwave radiation

As shown in figure 4.36, the scale color from blue to red of the simulation results represents the temperature from  $T_{\min}$  (25°C) to  $T_{\max}$  (around 100°C). The simulation results of the PCB without shield and with shield are described in same color scale from blue to red. As seen in the figure, there are hotspots when the PCB is heated without shield but when PCB is shielded, the hotspots fail to appear and the maximal temperature decreases from around 100°C to around 30°C.

Two pictures of experimental results are captured separately after heating one by one. Thus the post processing of temperature distributions have different color scales. In the case of heating the PCB without shield, the color scale describes temperature from  $T_{\min}$  25°C (in blue) to  $T_{\max}$  around 80°C (in red). In the case of heating the shielded PCB, blue color represents the minimal temperature (25°C) and red color represents the maximal temperature (around 30°C). The thermo-graphic pictures of samples are taken after the samples are removed out of the microwave oven for a short time and therefore it can be the reason of the difference between the simulation results and the experimental results. But they all prove one



thing, that using full shields can protect PCBs from periodic heating. Shields can be used when heating PCB in different kind of cavities (microwave oven, waveguide...).

The next investigation is carried out for the real PCB. Actually the simulation results prove that the real PCBs with complicated metallic structures can be protected by shields as the following figure.

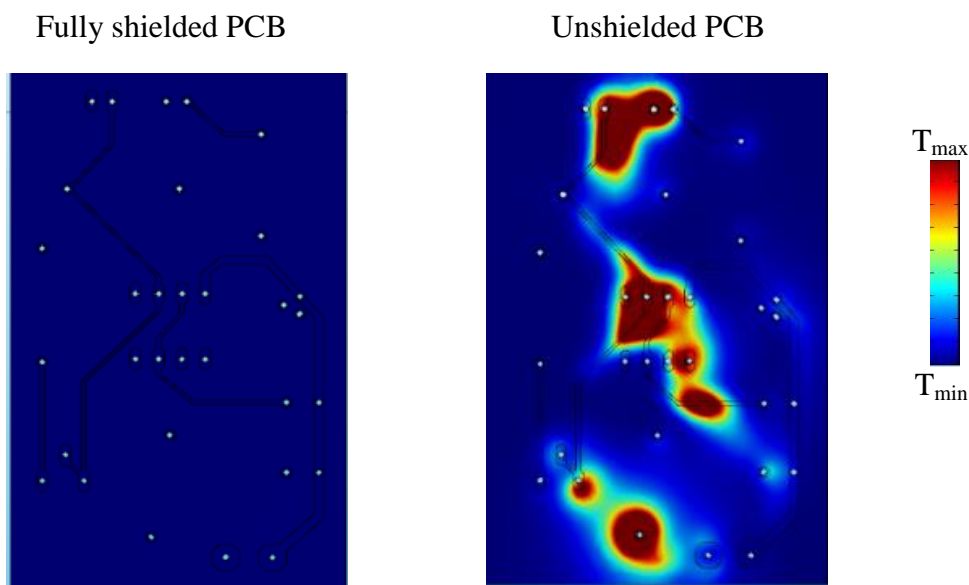


Figure 4.37: Simulation results exhibited the coupling of metallic structures of a real PCB and the microwave radiation when it is shielded (left) and unshielded (right)

As mentioned above, conductive shields will reflect the incident microwave and prevent harms to PCBs. However, the problem here is that do they also affect coating cures? To find the answer, another PCB heating test is realized including a coating (1 mm thickness) which covers the top of the PCB (figure 4.38).



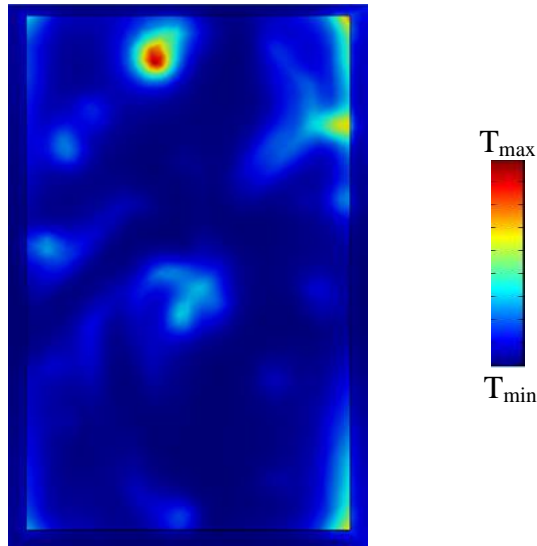


Figure 4.38: Temperature distribution on the coating which covers the shielded real PCB

From the illustration in figure 4.38, the coating is not heated uniformly. The maximal temperature is around 50°C but temperature distribution is inhomogeneous. In this case, the low electromagnetic field strength caused by the shield, still influence on the coating. So the temperature range is reduced but the coating is not cured.

#### 4.2.2.2 LOCALLY CONDUCTIVE SHIELDS

Since full shields can only protect PCB structures but fail in supporting the curing process, other use of shields can be utilized. Once when the hotspots which contain high temperature are known, then local shields can be applied to reduce the temperature of the hotspots. These local shields can be performed to manage the temperature following the desire of the user. Figure 4.39 shows the model including three copper coins locating 2 mm above the PCB. These three coins will act as three local shields covering three big known hotspots (as seen in figure 4.37). Figure 4.39 illustrates the simulations results of the heated PCB after locally shielding in comparison with the heated PCB without shield.

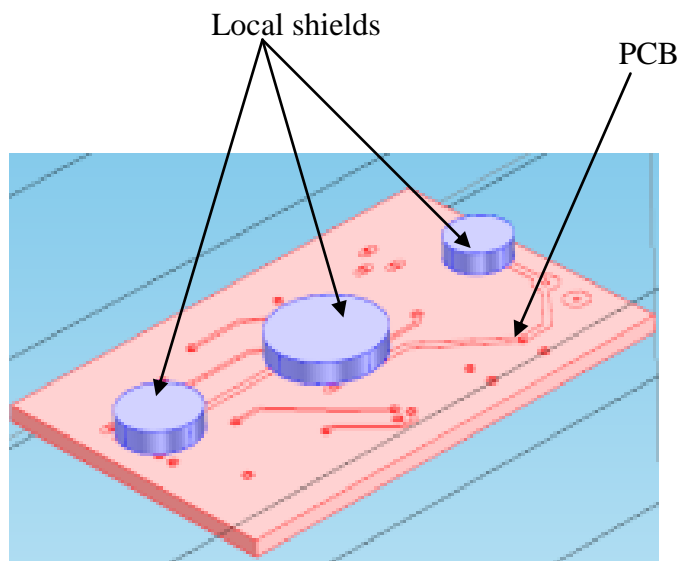


Figure 4.39: The model of real PCB with local shields

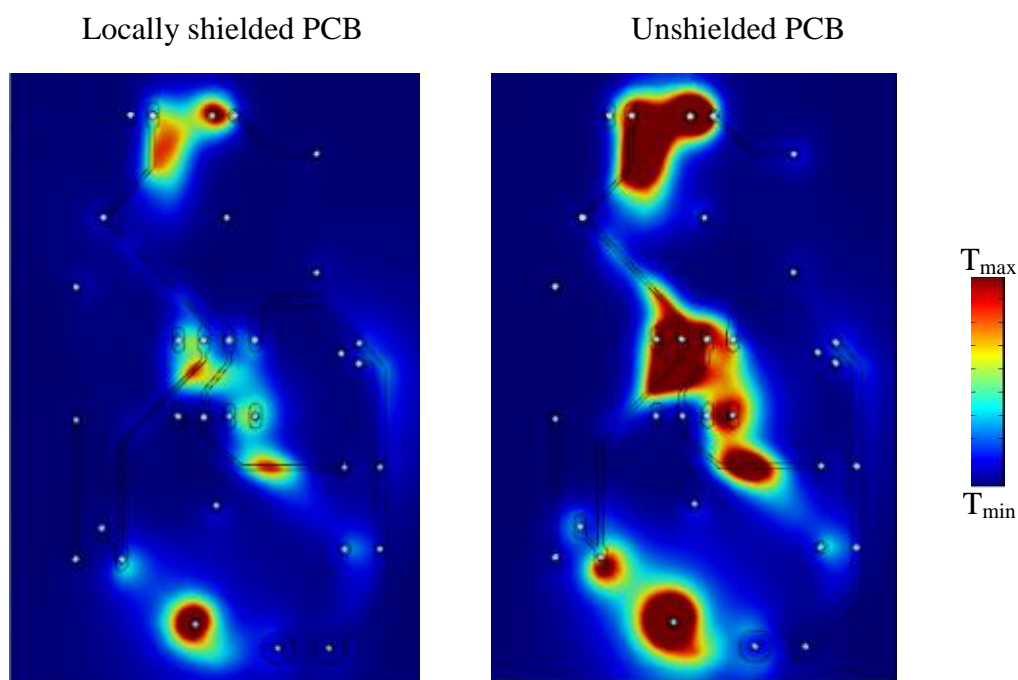


Figure 4.40: Simulation result of heated PCB with local shields (left) and heated PCB without shield (right)

It is clear to observe the significant reduction of temperature on the shielded PCB in comparison with the one on the unshielded PCB in figure 4.40. As mention above, local shields can be applied after the hotspot has been learned. The temperature in each hotspot is not the same. Therefore to get the desired temperature in each hotspot, shielding can be adjusted. Because shielding depends on the distance of the shield to the hotspot needed to be

shielded, thus the adjustment can be done by changing the distance of the shield for each hotspot. The following table expressed the influence of the distance from the shield to the shielded point on the electric field strength of the shielded point.

<b>Distance (mm) from shielded point to shield</b>	<b><i>E</i> field strength of shielded point (V/m)</b>
1	373.86
1.5	582.63
2	958.42
2.5	1169.77

Table 4.4: Relation between the distance from a shielded point in PCB to the shield and its *E* field intensity

From the table, the further distance is, the stronger electric field is. Hence the temperature of hotspots will be lower when shields get closer to them.

### 4.3 IMPROVING MICROWAVE PROCESSES OF COATING CURES

The investigated optimizations above could not support the curing process of the coatings thoroughly. The study implied that those optimizations although could influence on the interaction between PCB structures with the microwave radiation but fail to support coating cures for PCBs with FR-4 as substrates. Therefore the optimization based on material properties is taken into account. The meaning of “based on materials” here is changes of coating materials as well as substrate materials (the heated objects) to get homogeneous temperature distributions of coatings.

#### 4.3.1 BASED ON COATING MATERIALS

The electromagnetic field directly influences on the temperature distribution within a dielectric material in microwave process. Thus for the theoretical prediction it is essential to know the dielectric property. The permittivity of a material is the most important for the microwave heating.

The permittivity which is supported is  $\varepsilon_r = 5-j$ . Here the real part  $\varepsilon' = 5$  and the imaginary part  $\varepsilon'' = 1$ . By theory, changing  $\varepsilon'$  and  $\varepsilon''$  can make the change of temperature distribution in the coatings. Changing  $\varepsilon'$  mean choosing another material with another permittivity, meanwhile changing  $\varepsilon''$  is carried out by using additives, absorbed by the coatings, for example water molecules [65].

##### 4.3.1.1 EFFECT OF REAL PARTS OF PERMITTIVITIES

From the previous study in the influence of the substrate's permittivity, if the real part of the permittivity increases, then the wavelength of the standing wave decreases. So in other words, hotspots get closer to each others. When the distances between them go to zero then the homogeneous temperature distribution can be performed. Therefore in this investigation, permittivities of coatings need to be risen to observe the change of temperature distributions on them. The simulation is carried out for PCBs with dimension ( $40 \times 30 \times 1.5 \text{ mm}^3$ ), the input power 200 W and 1 mm thickness of coatings, and in 30 seconds by microwave oven.

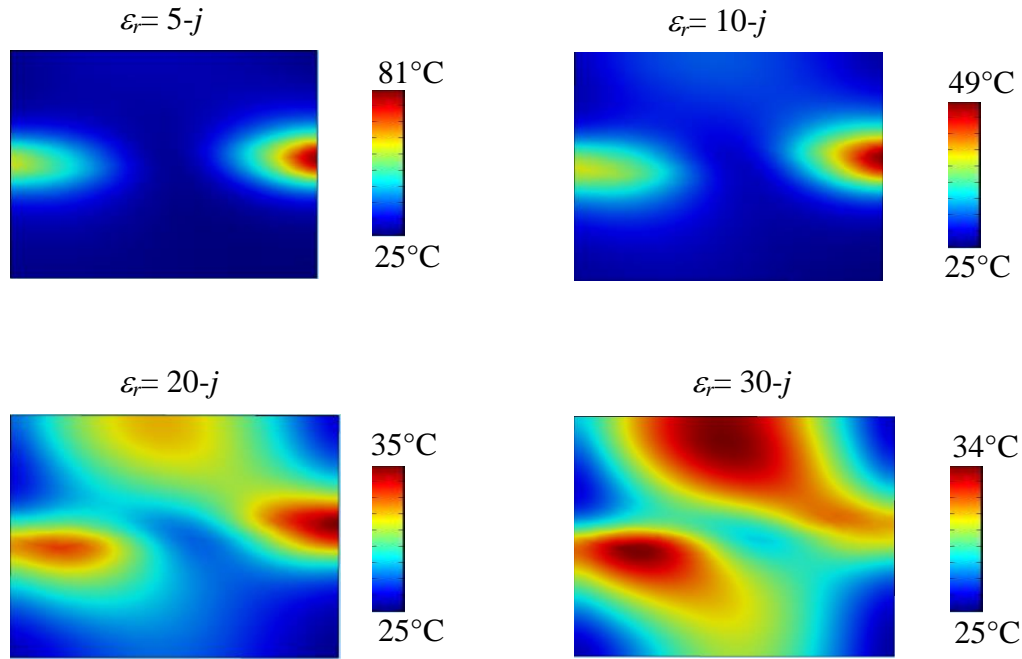


Figure 4.41: The effect of real parts of coatings' permittivities on the temperature distribution on the coatings

As seen in figure 4.41, the bigger the value of the real part is, the more homogeneous the temperature distribution is. The most important in this case is that the difference between the maximal temperature and the minimal temperature is smaller. That means the combination of the increased real part of the coating's permittivity and local shields might help for slowing down the temperature rising up in hotspots. This way by far is just a confirmation of the idea from theory because it is really difficult to find out a material which can satisfy all, the property as a coating and have a high real part of permittivity at the same time.

#### 4.3.1.2 EFFECT OF IMAGINARY PARTS OF PERMITTIVITIES

Unlike changing the real part of the permittivity which is a package of theory, increasing the imaginary part in reality can be applied by using additives, e.g. water molecules. The water molecules can be absorbed by coatings to maximum 50% of their volume [65]. The problem here is that there is no existing study about values of permittivities respecting to the additives. Therefore in the simulation, the imaginary part increased means more additives are added. The simulation is realized in 30 seconds and input power of 200 W.

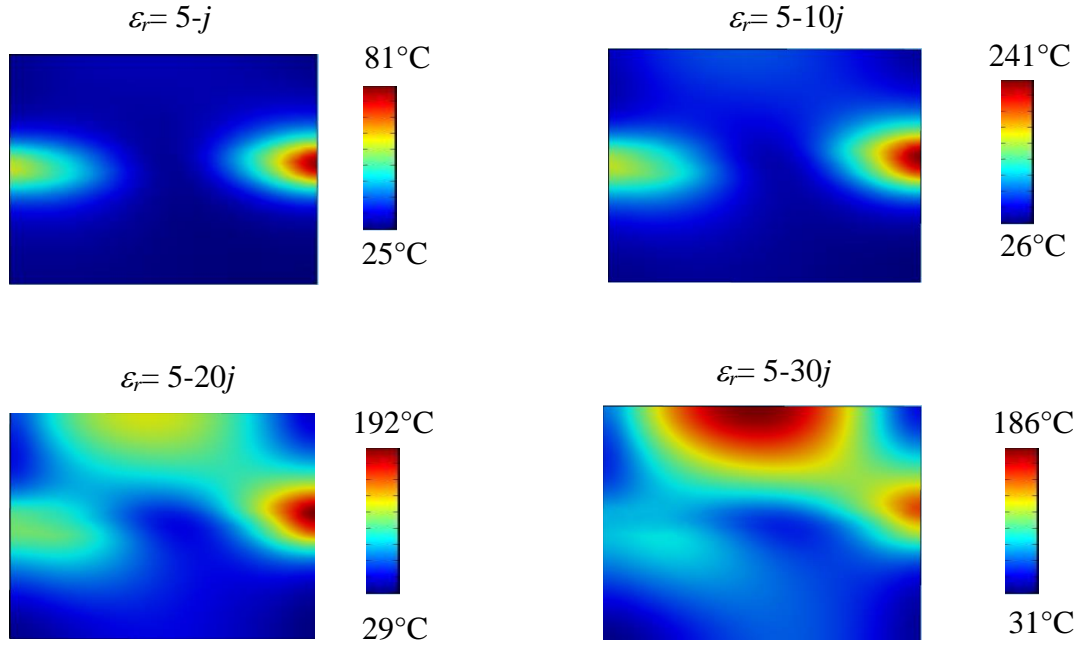


Figure 4.42: The effect of imaginary parts of coatings' permittivities on the temperature distributions on coatings

The simulation results are positive. The increase of the imaginary part makes the temperature distribution go homogeneously. However, the differences between maximal temperatures and minimal temperatures on the coatings after heating are too much. For example, when the imaginary part is 30, the temperature difference is 155 K. And as shown in figure 4.42 in this case, there are big areas with higher temperatures and only some small areas with low temperatures. So in curing processes, this would mean that most areas on coatings are able to be cured and only some small areas could not be cured. This significantly different temperature in this case may be caused by the different abilities in microwave energy absorption between coating materials and additives. Additionally the low thermal conductivity of coatings also can create a poor heat transfer and contribute to the temperature difference.

#### 4.3.2 BASED ON SUBSTRATE MATERIALS

The study has considered in the treatment of the outer factors of the PCBs like the electric field and changing permittivities of coatings but they all cannot lead to the support for coating cures thoroughly. This section will take attentions in the PCBs themselves to get to the goal. Revising all previous investigations, the problem of the non-uniform heating is usually the great difference between the maximal temperature and the minimal temperature on the heated objects (PCBs and coatings). Actually curing processes can be dependent on the temperature distributions on PCBs. If these distributions are homogeneous, then they can support the

curing processes. To get to the uniform heating, the challenge of great temperature difference needs to be surpassed. The problem takes place due to the antenna effect as mention in the whole study. But as taking a look in another aspect, it could be caused by the low speed of heat transfer within PCB substrates (FR-4) themselves either. Thus the investigation will be taken care about the speed of the heat transfer within the substrates, which directly involve to the thermal conductivity of substrate materials. In the reality, materials which have high conductivities such as ceramics are also used as PCB substrates.

#### 4.3.2.1 THERMAL CONDUCTIVITY

Thermal conductivity  $\kappa$  is the property of a material's ability to conduct heat, which appears in Fourier's law for heat conduction [66]. Thermal conductivity is measure in watt per Kelvin-meter ( $\text{W}\cdot\text{K}^{-1}\cdot\text{m}^{-1}$  or  $\text{W}/(\text{K}\cdot\text{m})$ ) or in imperial units (IP) ( $\text{Btu}\cdot\text{hr}^{-1}\cdot\text{ft}^{-1}\cdot\text{F}^{-1}$  or  $\text{Btu}/(\text{hr}\cdot\text{ft}\cdot\text{F})$  where Btu is the British thermal unit equal to about 1055 joules, and Btu/hr involve the power, ft is feet and F is Faraday).

#### MEASUREMENT OF THERMAL CONDUCTIVITIES

There are a number of ways to measure thermal conductivities. Depending on the thermal properties and medium temperatures, one of these ways can be suitable for a limited range of materials. There is a distinction between steady-states and transient techniques.

When temperatures of materials do not change with time, steady-state techniques are useful. This makes the signal analysis straightforward (steady states imply constant signals). The disadvantage is that a well-engineered experimental setup is usually needed [66].

The transient techniques perform a measurement during the process of heating up. Their advantage is quicker measurements. Transient methods are usually carried out by needle probes.

## BASIC EQUATIONS

Following [66] the conductivity is given by:

$$\kappa = \frac{\Delta Q}{\Delta t} \frac{1}{A} \frac{x}{\Delta T} \quad (4.11)$$

Where  $\frac{\Delta Q}{\Delta T}$  is the rate of heat flow,  $\kappa$  is the thermal conductivity,  $A$  is the total cross sectional area of the conducting surface,  $\Delta T$  is the temperature difference, and  $x$  is the thickness of conducting surface separating the two temperatures. The dimension of the thermal conductivity =  $M^1 L^1 T^{-3} K^{-1}$

$\Delta T/x$  is the temperature gradient

It is defined as the quantity of heat,  $\Delta Q$ , transmitted during time  $\Delta t$  through a thickness  $x$ , in a direction normal to a surface of area  $A$ , per unit area of  $A$ , due to a temperature difference  $\Delta T$ , under steady state conditions and when the heat transfer is dependent only on the temperature gradient.

Alternatively, it can be thought of as a flux of heat (energy per unit area per unit time) divided by a temperature gradient (temperature difference per unit length)

$$\kappa = \frac{\Delta Q}{A \Delta t} \frac{x}{\Delta T} \quad (4.12)$$

### 4.3.2.2 THE EFFECT OF THERMAL CONDUCTIVITIES ON TEMPERATURE DISTRIBUTIONS

The key to get the uniform heating is the increase of the speed of heat transfers, which means increasing thermal conductivities. The thermal conductivity of the original substrate FR-4 is 0.3 (W/(K·m)). In this investigation, the simulations of single wired PCBs with variable thermal conductivities are realized. The tested samples have dimension (40×30×1.5 mm<sup>3</sup>) and are heated in 10 seconds with the power of 200 W. The most interested value now is the difference of temperature between the maximal and the minimal temperature distributed on the PCBs. The following figure shows the simulation results done by the rectangular



waveguide. All simulation results have same minimal temperature and maximal temperature = minimal temperature +  $\Delta T$ .

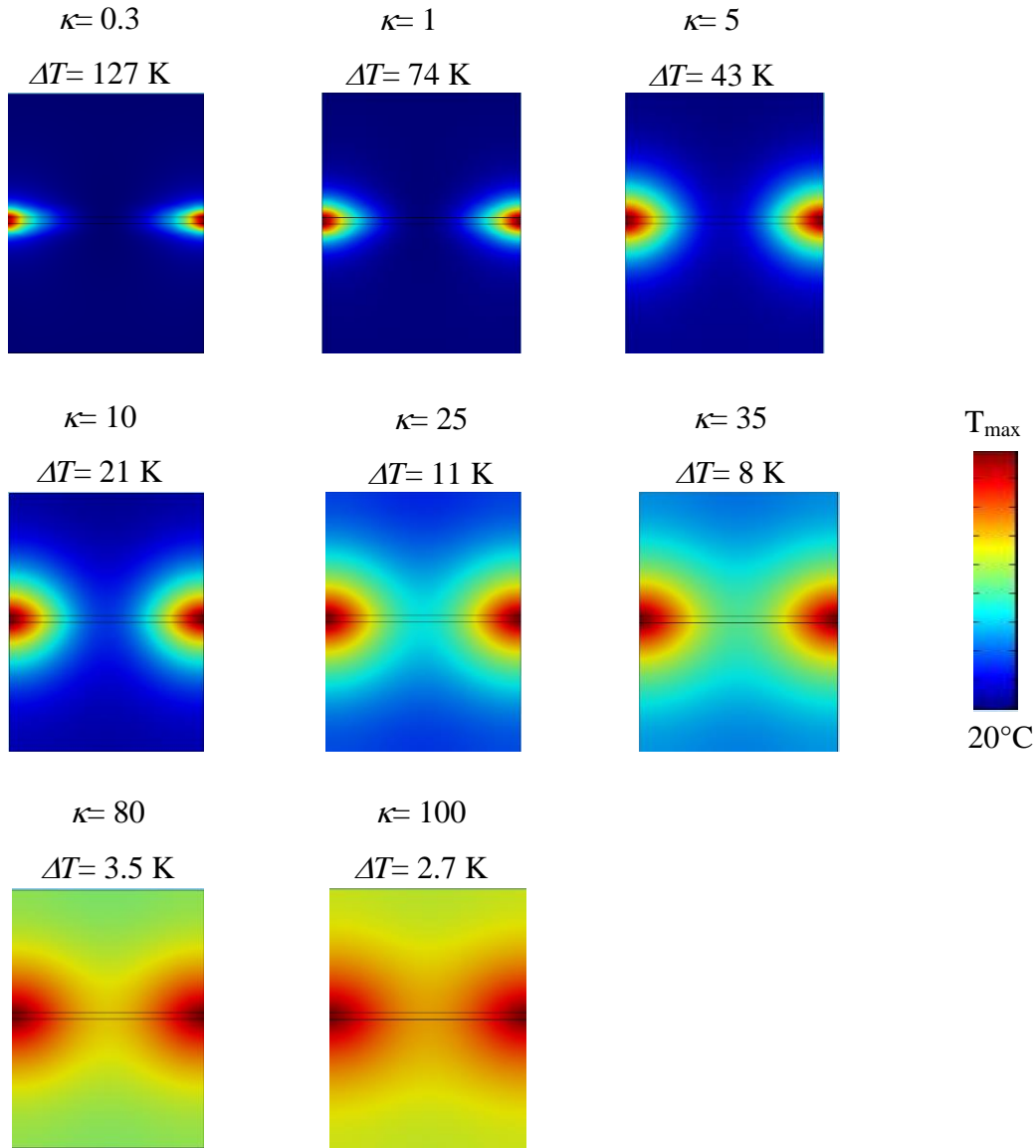


Figure 4.43: Temperature distributions on the PCBs depending on the thermal conductivity

The tests are carried out in the rectangular waveguide because when the single wired PCBs are laid along the polarization, the interaction of the microwave radiation and copper wires will be strong. In this case, the results can clearly expose the effect of changing thermal conductivity of the substrates.

The simulation results prove that the uniform heating can be reached by the enhancement of  $\kappa$ . When  $\kappa$  is in the interval form 80 to 200, which means the thermal conductivity of the ceramic with AlN (Aluminum Nitrite) as the main composition [67], then  $\Delta T$  will be very

small and the uniform heating will definitely occur. When  $\kappa$  is in the interval from 18 to 40, which means the thermal conductivity of ceramic with  $\text{Al}_2\text{O}_3$  (Aluminum Oxide) as the main composition [67], then  $\Delta T$  will be around 6 K to 15 K and the uniform heating will be possible. The following chart displays the relation between thermal conductivity and  $\Delta T$ .

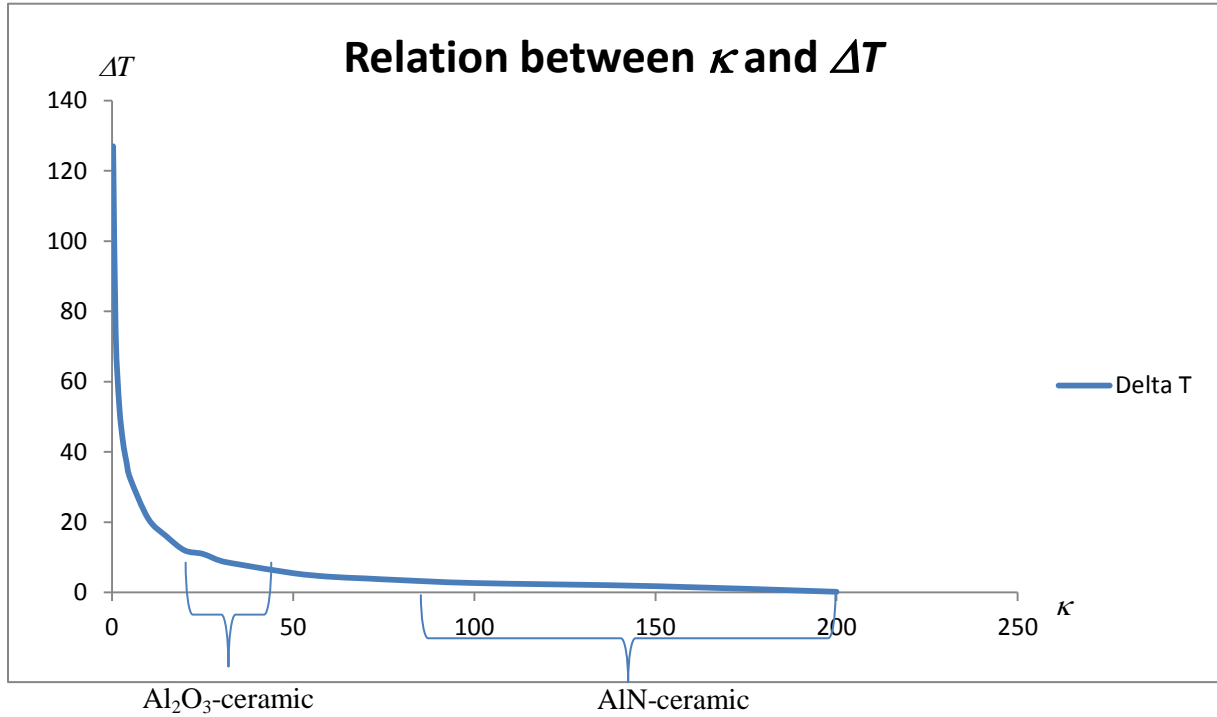


Figure 4.44: Relation between  $\kappa$  and  $\Delta T$  in the series tests of single wired samples

The chart is built from the series of simulations of the single wired PCBs. They illustrate good results in term of homogeneous temperature distributions of the single wired PCBs.

The next step will be taken into account is the simulation of real PCBs (figure 4.45). Unlike the tests of the single wired PCBs, the tests of the real PCBs will be carried out in microwave oven. Because the real PCBs with the complicated structures, and there will be many wires along the polarization if the waveguide is used as the heating cavity. That can make the coupling of the microwave radiation and copper wires be stronger, the temperature in the hotspots rising rapidly. And in fact, the interactions between real PCBs with the microwave radiation in the heating processes by microwave oven are sufficient to observe the impact of thermal conductivities.

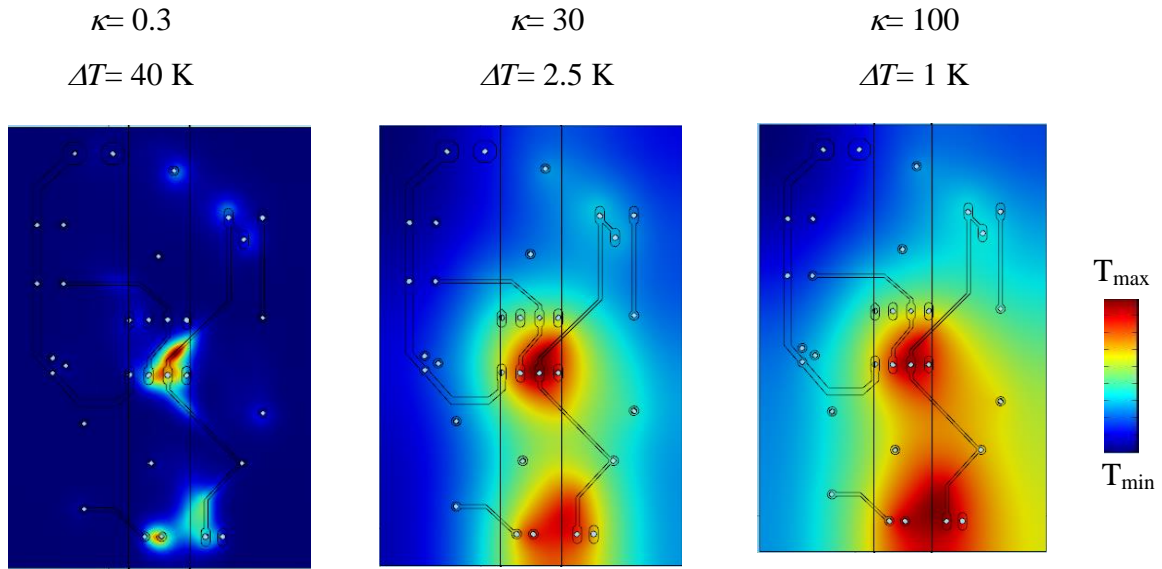


Figure 4.45: The temperature distribution of real PCB with FR-4 substrate (left),  $\text{Al}_2\text{O}_3$ -ceramic substrate (middle) and AlN-ceramic substrate (right) after microwave heating

Those results above describe a potential uniform heating of PCBs with ceramics as substrates. These results promise good coating cures. The simulations of the real PCBs with  $\text{Al}_2\text{O}_3$ -ceramic and AlN-ceramic as substrates prove that fact (figure 4.46).

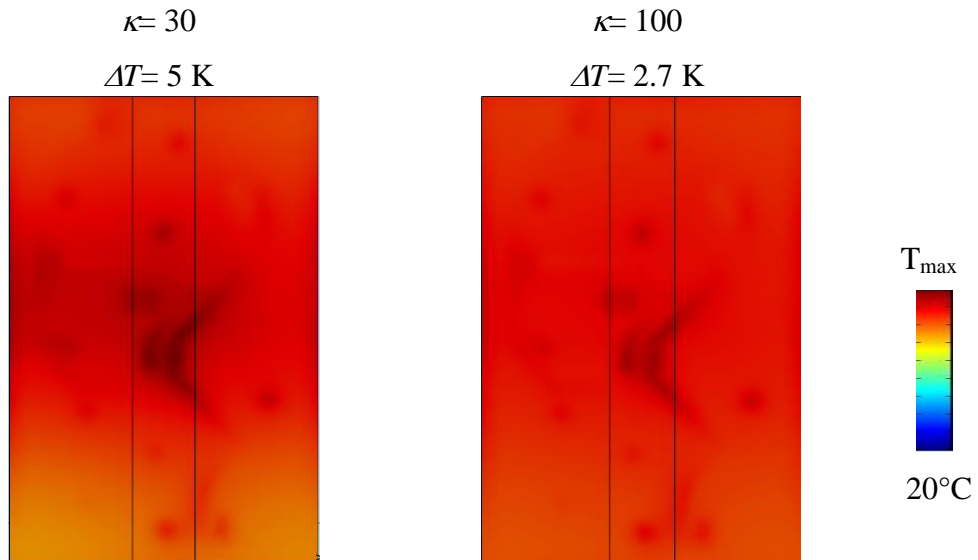


Figure 4.46: The simulation results of the real PCBs with coatings covered on for the  $\text{Al}_2\text{O}_3$ -ceramic and AlN-ceramic as substrates

As shown in figure 4.46, the coating covered on the PCB with AlN-ceramic as substrate expresses a better ability in uniform heating in comparison with the one covered on the PCB with  $\text{Al}_2\text{O}_3$ -ceramic as substrate. The coating material has a low thermal conductivity (below

1), therefore it affects the whole heating process and results in a bigger  $\Delta T$  when compares to the  $\Delta T$  in the case of heating the PCBs without coatings shown in figure 4.45.

To investigate more about this, another PCB sample is made. This time the microwave process for the sample will be carried out in both simulation and experiments for the PCB with the AlN-ceramic substrate.

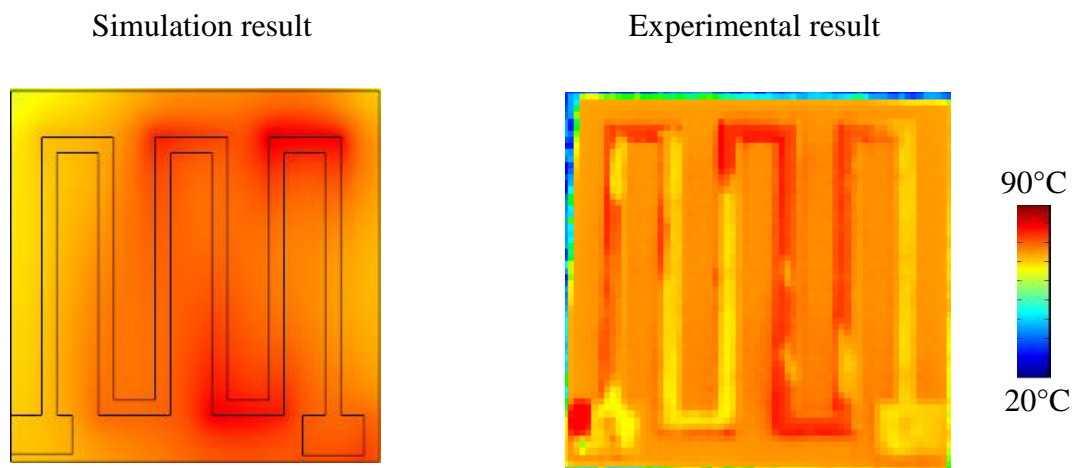


Figure 4.47: The simulation result (left) and experimental result (right) of the tested sample

The tests give the relatively alike view of the temperature distribution on both simulated PCB and experimental PCB. The highest temperature of both is about 88°C.

#### 4.4 SUMMARY

This section discusses about how to solve the periodical heating which can disturb the curing process. The investigation focuses on the methods to optimize the microwave treatment of PCB structures in order to support coating cures. The summaries can be taken now are:

- The system using horn antenna is not possible to heat electronic assemblies due to the less energy gained by the heated objects. But it reveals the impact of the electromagnetic field polarization.

The use of rectangular waveguides as heating cavities can show more effect of the electromagnetic field polarization, because the distribution of the field is oriented and known. When the whole PCB structures and the incident electric field are orthogonal, then PCBs will be heated homogeneously. Thus curing processes of coatings are supported. Otherwise, PCB structures will become very sensitive. In this situation, the coupling of the microwave radiation and metallic structures are very strong and therefore the temperature of hotspots rises up rapidly. The failure in the microwave

heating at frequency 2.45 GHz of real PCBs with FR-4 as substrates by using the rectangular waveguide as the heating cavity involves to the failure of the mechanisms utilizing the positions and the known electromagnetic field distribution in this kind of substrate.

- Ceramics and conductive shields can be used for managing the field which penetrates to the PCBs. In this case, shields can protect PCBs by reducing the electromagnetic field around them but cannot clear hotspots. A full conductive shield can make PCBs be totally protected but lacking energy to heat up coatings. However, using local shields can prevent rapid raises of temperatures of the known hotspots. This management can be utilized in combination with other methods to protect PCBs in microwave process.
- The most important parameter that can influence much on the microwave heating process is the permittivity of a material. The coating's permittivity by theory can change the temperature distribution on the PCBs. Increasing the real part of the coating's permittivity to a high value makes the temperature distribution on the coating itself become homogeneous but this is only the study which might support the material developers for investigating such materials with high real part of permittivities as coatings. Increasing the imaginary part can be realized by using additives and this method makes the temperature distribution undergo homogeneously but the low speed of heat transfer of the coating's material lead to some small areas which have very lower temperatures than the rest of the coating. In this case, locally shielding may help to reduce the speed of rising temperatures of the hotspots.

Although all investigations mentioned above cannot lead to the expected solution but can help for figuring out the way to reach the goal. That is the solution based on substrate materials of PCBs and the focus point is the increase of the heat transfer's speed. This involves directly to thermal conductivities of substrate materials. The use of materials with high thermal conductivities such as ceramics can lead substrates to high speeds of heat transfers, therefore reduce the  $\Delta T$  and support the curing process. The disadvantage of this method is the difficulty in metallization of PCB structures and the high cost.

## CHAPTER 5

### CONCLUSION

The basic of the work represented in this dissertation was the investigation of the interaction between PCB structures with the microwave radiation in term of temperature distributions for supporting coating cures. The desired solution certainly was the uniform heating of coatings. For this purpose, simulation has been chosen as a tool to analyze, predict and optimize the problem in term of the safety engineering. The matching of simulation results and experimental results has proven that the simulation could be reliable and capable to use in the future work.

In the scope of this study, many simulations have been carried out for PCB models with differently metallic structures. The investigations of how PCB structures react with the microwave radiation were intentionally realized from the basic substrates to the special structures and the structures of real PCBs. Based on that work, the process window, which allowed a safe coating cure without damages of participating PCBs, was determined.

The microwave heating of basic PCB substrates expressed the pure dielectric heating of substrate materials without any interference of PCB structures. The dominant dielectric heating was also the reason for more effectiveness of microwave processes for the cures of polymers (coating materials), when compared with a convection or infrared heating. This has been shown in many publications from various researches. As conductive structures were metalized on PCBs, they could disturb the pure dielectric heating of the substrates. Thereby with the appearance of metallic structures, the temperature distributions on PCBs were inhomogeneous, separated in many hotspots and could not support coating cures. From the simulation results as well as the experimental results, the input power of microwave treatments needed to be about 200 W for a standard PCB size or even lower for sensitive PCB structures if being required, so that the maximal electric field could not harm PCBs. The maximal time of the process normally was 30 seconds. The results of microwave treatments for the PCBs with straight wires, quadratically framed wires and FR-4 as substrates have exposed that the distances between hotspots were constants and the maximum amounted to about 40 mm. This interaction could be interpreted as a formation of standing waves along the

wires. This caused a locally constant current and heating processes based on Joule heating like an antenna effect. Whereas the maximal distance between hotspots  $d = \lambda_c/2$ , where  $\lambda_c$  was called the conductive wavelength, which was a reduced result of the propagating wave on PCBs.

After the reason for the periodical heating of PCB structures was revealed, the influences of parameters on microwave treatments for PCBs have been investigated. Thereby the temperature distributions and maximal temperature of PCB substrates were depend on the positions where PCBs were laid. This could be the notice for experiment manipulators to manage the microwave processes to reach the desired effectiveness (willing a rushing heating when put the PCBs to the higher energy area or kept it safe by putting the PCBs in a lower energy area if sensitive PCB structures). The study has also shown that there have been copper wires lengths, with which the induced electric fields on PCBs were resonant with the incident electric field. This resonance made temperatures of PCBs exceed the maximums allowed (120°C to 150°C). In different locations and with distinct directions of wires, the sensitive wire's lengths were not similar and so were the highest temperature of PCBs. Therefore in this case, for each wire's length the simulations could be utilized to forecast whether a position and direction of a wire, which were in plan to locate PCBs, would bring more harm to them than the other places. The forecast could help the experiment manipulators to avoid the resonance of induced electric fields and incident electric fields. The avoidance could be simply done when using microwave oven by moving the PCBs to another position or directions of wires (because in a new position the sensitive wire's length would be different).

Other parameters such as relative permittivities of substrate materials and microwave frequencies have also displayed their effects on the temperature distributions. The greater relative permittivities of substrate materials were, the smaller distances between hotspots would be. Thereby the conductive wavelength  $\lambda_c$  was considered as a function of the relative permittivities of participating materials in the microwave heating (equation (3.14)). Hence the maximal distances between hotspots would be dependent on the weighting factors of participating materials, here were the substrate materials and the air surrounding PCBs ( $w_{PCB} \approx 37\%$  and  $w_{AIR} \approx 63\%$ ). If coatings had been covered the PCBs, they would rather had taken the place of the air and had 63% of weighting factor of the influence on the conductive wavelength. Thus increasing the weighting factor of coatings and reducing the weighting factor of substrate materials could lead to homogeneous temperature distributions on PCBs. This would be the suggestion of the ways to support coating cures. Beside relative

permittivities of substrate materials, microwave frequencies have shown their impact as well. Enhancing the microwave frequencies could make hotspots be closer. If the hotspots were close enough in the relation to a PCB size, there would have been uniform heating of the PCBs consequently. So the idea of using high microwave frequencies in microwave process for electronic assemblies would be a direction in the future.

For the microwave treatments of real PCBs, it was very difficult to have a safe coating cure due to complications of PCB structures. Metallic walls of a microwave oven reflected the entire incident microwave wave propagating to them. Therefore the electric field distribution in microwave oven was irregular. From the knowledge obtained above, the positions of PCBs and the directions of wires affected microwave treatments for the PCBs. That meant designs of heating cavities, which had regular and known field distributions could be used for an easier management of the microwave process for PCBs. For that reason, a microwave horn and a rectangular waveguide have been chosen as alternative designs of heating cavities. The microwave horn without metallic walls has fail in heating PCBs due to the lack of effectiveness. The microwave treatments for PCBs by using the rectangular waveguide showed that the interaction between PCB structures with the microwave radiation was dependent on angles made by the incident electric field and the directions of wires. Thereby only when the incident electric field was orthogonal with the whole structures (meant the entire wires) then the induced electric field of PCBs would be zero and the PCBs could be heated uniformly (like PCB substrates). This uniform heating was able to support coating cures. Because in reality, the PCB structures are complicated and have different wire directions, thus using rectangular waveguide would not be successful in uniform heating of real PCBs.

Since the designs were not able to support coating cures of real PCBs, the investigation of using accessory packages have been realized. Thereby dielectric layers such as ceramics, which had the ability of microwave absorption or conductive faces, which could reflect the incident microwave, were utilized as shields to protect PCBs. The ceramic shields could reduce the temperature of heated PCBs and also change temperature distributions. The fully conductive shields would totally protect the heated PCBs but lack energy due to the total reflection. Therefore, PCBs shielded fully could not support coating cures. Once when the hotspots have been learned, local shields could be operated to manage the temperature of hotspots. The shields themselves could not support the curing process but in a combination with other methods would be able to manage the heating process.



The study of improving the microwave process for coating cures was carried out based on the analysis above (increase the weighting factor of the coatings and reduce the weighting factor of the PCBs). From that relative permittivities of coatings were increased in two terms: the real part and the imaginary part. Increasing these two terms made the dielectric heating of the coating dominate the periodically heating of PCBs. That would lead to a potential microwave treatment for PCBs which could support coating cures. The increase of the imaginary part could be done by using additives or fillers. Meanwhile the enhancement of the real part was a theory suggestion. The reduction of the weighting factor of PCBs has been realized by using substrate materials with high thermal conductivities such as ceramics. Both  $\text{Al}_2\text{O}_3$ -ceramic and AlN-ceramic exposed their advantages in the homogeneous microwave heating of PCBs. In comparison, the AlN-ceramic with higher thermal conductivity showed more effect on the uniform heating of PCBs than the  $\text{Al}_2\text{O}_3$ -ceramic. Using this kind of substrate materials would really support safe coating cures by the means of microwave irradiation. The disadvantages of this were the difficulty of metallization and a high cost.

## CHAPTER 6

### OUTLOOK

As a work of analyses, prediction and optimization, the simulation can be carried on to use in the future work. In the scope of this dissertation, the investigation of microwave processes is restricted in the microwave frequency of 2.45 GHz. Therefore the simulation of microwave processes for PCBs and coating cures are limited. The microwave frequency is definitely affects temperature distributions of electronic assemblies. As described in chapter 3, the more microwave frequency increases the less distance of hotspots is, with the assumption of all material properties at frequency 2.45 GHz. Hence it is not a bad idea to investigate the effect of the microwave radiation on the microwave heating of PCBs concerning variable frequencies for supporting microwave-cures of coatings. For each frequency level the material properties should be chosen at its level. A microwave oven with adjustable frequencies can be the laboratory equipment.

The samples of electronic assemblies in this work are the PCBs with metallic structures only. Therefore the development in the next step can be the investigation of electronic assemblies with components combined in. In this case, the rush of mesh density is not only challenge from the thin thickness of the metallic structures but also comes from the pins and solder joints of the components. The suggestion for the advanced simulations here is the simplification of the geometric such as: neglect tiny dimensions of the solder joints, set the dimensions of the pins equal to the holes. That can help the simulations run smoothly and save the CPU time and memory storages. Because of the simplifications, results need to be austere qualified by experimental results.

Conflicting results have been exhibited from various researches in microwave-cures of polymeric materials. Although most of the investigations confirmed that the microwave process of the polymer cure can accelerate the polymerization but there have been some contrary results. Thus it is required more research works to have an agreement. About the influence of material properties, the coating materials thereby can potentially use additives to get the uniform heating of the microwave-curing process. This is interesting for material

developers to investigate which filler and how much filler needed to achieve the desired solution.

# APPENDIX A

## LIST OF ABBREVIATIONS

$f$	[GHz]	Frequency
$f_c^{mn}$	[GHz]	Cutoff frequency where m, n are mode numbers
$f_l$	[GHz]	Approximate frequency limit of transmission line
$E$	[V/m]	Electric field
$E_x$	[V/m]	Electric field in x-direction
$E_y$	[V/m]	Electric field in y-direction
$E_z$	[V/m]	Electric field in z-direction
$H$	[A/m]	Magnetic field
$H_x$	[A/m]	Magnetic field in x-direction
$H_y$	[A/m]	Magnetic field in y-direction
$H_z$	[A/m]	Magnetic field in z-direction
$D$	[C/m <sup>2</sup> ]	Electric displacement field
$B$	[Wb/m <sup>2</sup> ]	Magnetic flux density
$J$	[A/m <sup>2</sup> ]	Current density
$\rho$	[C/m <sup>3</sup> ]	Electric charge
$\nabla \cdot$	[1/m]	Divergence operator
$\nabla \times$	[1/m]	Curl operator
$\epsilon$	[F/m]	Permittivity
$\epsilon_0$	[F/m]	Permittivity of free space
$\epsilon_r$	[F/m]	Relative permittivity
$\epsilon'$	[F/m]	Real part of the relative permittivity
$\epsilon''$	[F/m]	Imaginary part of the relative permittivity
$\epsilon_{PCB}'$	[F/m]	Real part of the relative permittivity of the PCB substrate

$\epsilon_{AIR}'$	[F/m]	Real part of the relative permittivity of the air
$w_{PCB}$	[%]	Weighting factor of the PCB substrate
$w_{AIR}$	[%]	Weighting factor of the air
$\sigma$	[ $\Omega \cdot m$ ]	Electric conductivity
$\omega$	[rad/s]	Angular frequency
$\mu$	[N·A <sup>-2</sup> ]	Permeability
$\mu_r$	[N·A <sup>-2</sup> ]	Relative permeability
$\mu_0$	[N·A <sup>-2</sup> ]	Permeability of free space
$\alpha$	[-----]	Attenuation constant
$\delta$	[-----]	Phase shift
$\beta$	[-----]	Phase constant
$\gamma$	[-----]	Propagation constant
$\vartheta_p$	[m/s]	Phase velocity
$\Gamma$	[-----]	Reflection coefficient
$\Pi$	[-----]	Transmission coefficient
$\eta$	[ $\Omega$ ]	Instinct impedance
$\eta_0$	[ $\Omega$ ]	Instinct impedance of free space
$\Omega$	[m <sup>3</sup> ]	Volume domain
$S_1$	[m <sup>2</sup> ]	Boundary 1 (area)
$S_2$	[m <sup>2</sup> ]	Boundary 2 (area)
$\hat{n}$	[-----]	Normal vector
$k$	[cm <sup>-1</sup> ]	Wavenumber
$T$	[°C] or [K]	Temperature
$\Delta T$	[°C] or [K]	Temperature difference
$P$	[J]	Power loss
$P_d$	[W/m <sup>-3</sup> ]	Power dissipation
$N_j$	[-----]	Edge element

$\Delta Q/\Delta T$	[-----]	Rate of heat flow
$c$	[m/s]	Velocity of light
$\lambda$	[mm]	Wavelength in free space
$\lambda_c$	[mm]	Conductive wavelength
$\kappa$	[W/(m·K)]	Thermal conductivity
$\theta_H$	[°]	Flare angle of H-plane horn
$\theta_E$	[°]	Flare angle of E-plane horn
$R_H$	[mm]	Length of the horn of H-plane horn
$R_E$	[mm]	Length of the horn of E-plane horn
$S$	[W·m <sup>-2</sup> ]	Poyting vector
$F$	[-----]	A continuous differentiable vector field
$A_{mn}$	[-----]	Amplitude for each mode (m and n are mode numbers)
PCB		Printed Circuit Board
WR		Rectangular Waveguide
WR340		Rectangular Waveguide type 340
FR-4		Fiberglass-epoxy laminate
FEM		Finite Element Method
FDM		Finite Difference Method
BEM		Boundary Element Method
CFD		Computational Fluid Dynamic
Al <sub>2</sub> O <sub>3</sub>		Aluminum Oxide
AlN		Aluminum Nitrite
UV light		Ultraviolet light
AR		Acrylic Resin
ER		Epoxy Resin
SR		Silicone Resin
UR		Urelythane Resin

XY	Paraxylylene
$E$ field	Electric field
$H$ field	Magnetic field
$TM$	Transverse Magnetic
$TE$	Transverse Electric
$TE_{mn}$	Transverse Electric of modes $m, n$
VSWR	Voltage Standing Wave Ratio
BMBF/PTKA	Bundesministerium für Bildung und Forschung/Projectträger Karlsruhe
AiF/IGF	Arbeitsgemeinschaft Industrielle Forschung/ Industrielle Gemeinschaftsforschung
BMBF/PTJ	Bundesministerium für Bildung und Forschung/Projectträger Jülich

## APPENDIX B

### HOW TO MAKE A SUCCESSFUL SIMULATION OF THE MICROWAVE PROCESS FOR ELECTRONIC ASSEMBLIES

As mentioned in chapter 2, the simulation of microwave processes for electronic assemblies is particular. It is distinct from microwave processes for other objects (for example food). Here the facing problem is not only the dielectric heating of materials but also the heat distribution affected by the conductive structure due to the antenna effect. Normally one has to decide simplify the whole geometry due to the big difference between geometric objects in this case. Thereby in this part, the techniques to solve the problem of the simplification which is sufficient for reliable results and save the CPU memory will be presented. This part is based on the experiences of the writer when deal with the simulation of the microwave process for electronic assemblies. Conditions such as boundary conditions, equations or other settings are not in the focus, because they are similar as the other microwave processes and users can consult in the COMSOL Multiphysics Help. Notice that this part represents the work on COMSOL Multiphysics version 4.x. For version 3.x, the process is different.

The microwave oven, waveguide, rod antenna, underlay can be drawn by the design tool of the software itself. In this case the conductive structures can be designed by the COMSOL or by an external program if they are complicated (figure 1A).

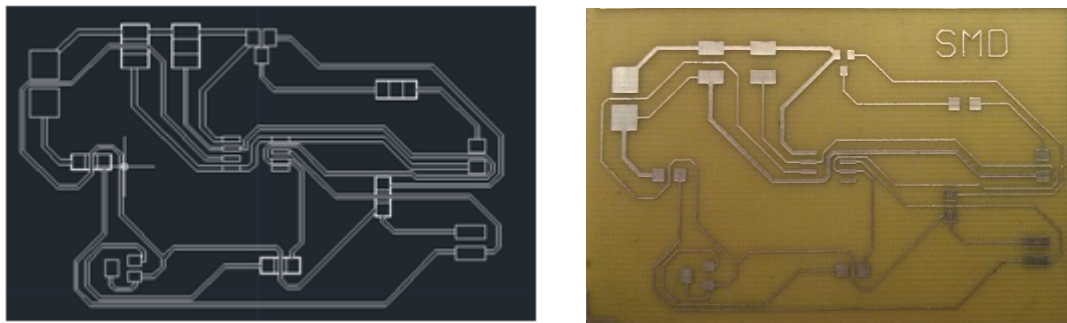


Figure B.1: Metallic structure designed by external program (left) and the real sample (right)

The problem here is the difficulty in control the scale of importing geometries. Therefore it is better to draw only the metallic structures in 2D by external program, not all 3D structures, and PCB substrates can be easily created by the simulation program itself. This can reduce the difference, because the scale is needed to be control in the frame of the PCBs substrates (the dimension is accurate).



The next important tip here is that individual sections based on material should be created. For example the domains assigned to the air, have to group in a section, the underlay, PCBs substrates and metallic structures should be set in separated sections. Section of the copper wires can be embedded to the top plane of the 3D PCB substrate (figure 2A) afterwards, and assigned as a perfect conductor. Figure 3A will show the simulation result of this sample.

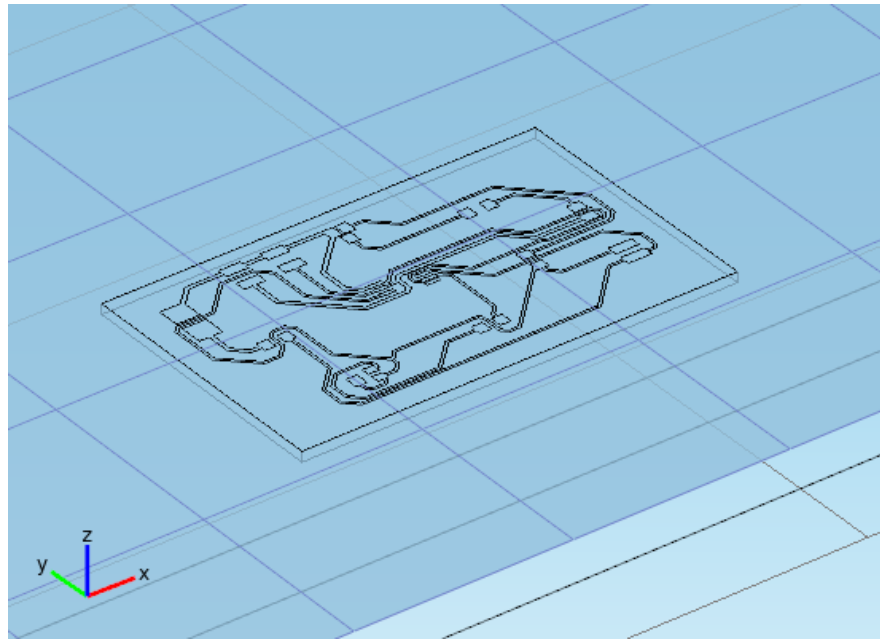


Figure B.2: The 2D metallic structure designed by external program can be embedded on the PCB substrate

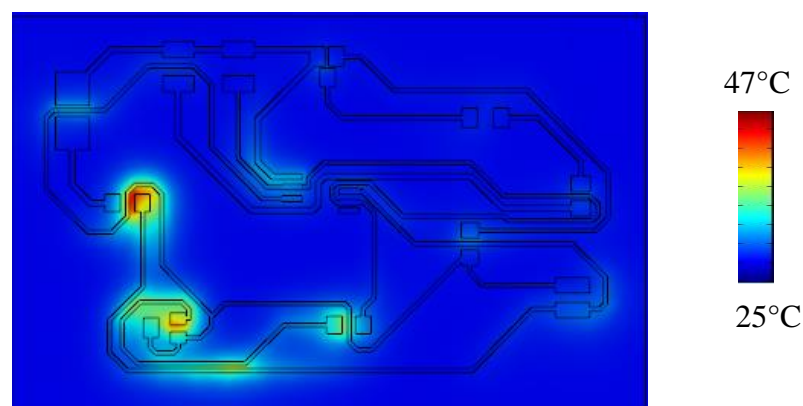


Figure B.3: The simulation result of the sample above after 30 seconds microwave process with the power of 200 W

The real PCB samples with metallic structures in both sides and the holes connected them, are more complicated (for example figure 3.9). The match of conductive structures in both sides requires more accuracy. Hence it is better to use the design tool of the simulation program. It

may be more difficult to draw but ensure the accuracy. In this case working planes in the geometry design tool is utilized. The top and bottom planes of the PCB substrate are chosen as the working planes, where the conductive structures are created. After the work with geometry is done, metallic structures including the inner faces of the holes need to be assigned as perfect conductor (figure 4A). The simulation result of the microwave treatment of this sample can be revised in figure 3.11.

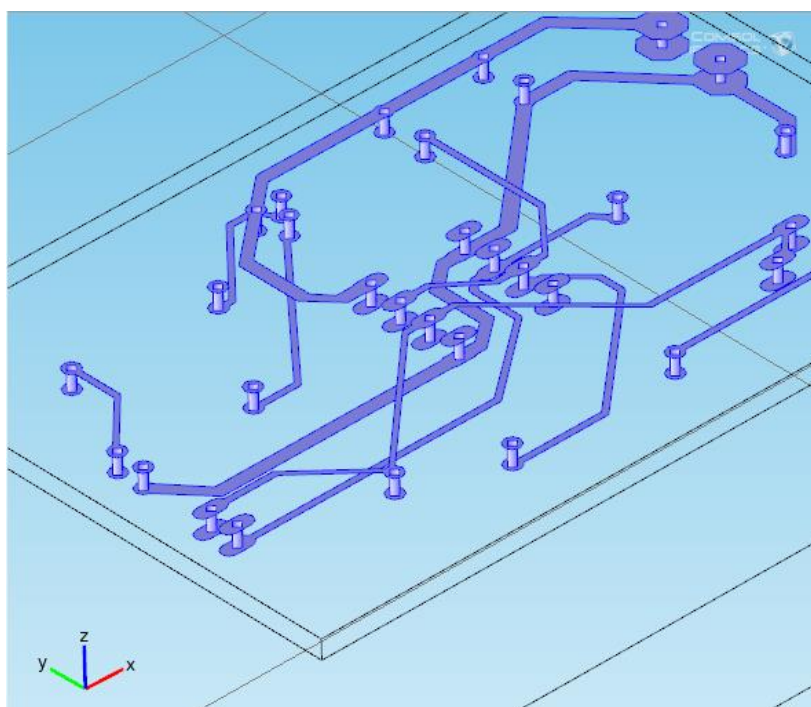


Figure B.4: The metallic structures on the top and at the bottom of PCB substrate including holes connecting them

In advanced, to simulate the electronic assemblies including components, conductive structures still can be kept designing in 2D and components can be drawn in 3D. The dimensions of the pins can be set as equal as the dimensions of the holes to reduce the CPU memories in the computation.

# APPENDIX C

## DIVERGENCE THEOREM

Suppose solid region  $V$  is a subset of  $\mathbb{R}^3$  (3D space),  $S$  is the boundary surface of  $V$  with a positive orientation. The flux of a differentiable vector field  $\bar{F}: \mathbb{R}^3 \Rightarrow \mathbb{R}^3$  across surface  $S$  in the direction of the surface outward unit normal vector  $\hat{n}$  satisfies the equation [68, 69]:

$$\iiint_V (\nabla \cdot \bar{F}) dV = \iint_S (\bar{F} \cdot \hat{n}) dS \quad (\text{C.0.1})$$

Remark [70]:

The volume integral of a divergence of a field  $F$  in a volume  $V$  in the space equals to the outward flux (normal flow) of  $F$  across the boundary  $S$  of  $V$ .

The expansion part of the field  $F$  in  $V$  minus the contraction part of the field  $F$  in  $V$  equals the net normal flow of  $F$  across  $S$  out of the region  $V$ .

# APPENDIX D

## GALERKIN METHOD

Galerkin methods, invented by the Russian mathematician Boris Grigoryevich Galerkin are a class of methods for converting a continuous operator problem (e.g. differential equation) to a discrete problem.

The convergence of Galerkin approximation of a general problem in this section is defined and analyzed by a bilinear form in a Hilbert space. Let  $V$  be a Hilbert space and let  $a(\cdot, \cdot)$  be the continuous bilinear respectively defined in  $V$ . As an abstract problem in weak formulation, Galerkin method is introduced as [48, 49]:

$$\text{- Find } u \in V \text{ such that for all } v \in V: a(u, v) = f(v) \quad (\text{D.0.1})$$

where  $f$  is a bounded function in  $V$ .

**Galerkin equation**, known as Galerkin Dimension Reduction is given as [48, 49]:

$$\text{- Choose a subspace } V_n \subset V \text{ of dimension } n \text{ and solve the projected problem:}$$

$$\text{Find } u_n \in V_n \text{ such that for all } v_n \in V_n: a(u_n, v_n) = f(v_n) \quad (\text{D.0.2})$$

The equation has remained the unchanged and only the spaces have changed [50]. By reducing the problem to a finite-dimensional vector subspace  $u_n$  is allowed to compute as a finite linear combination vectors in  $V_n$ .

The key property of the Galerkin method is that the error is orthogonal to the selected subspace and known as **Galerkin orthogonality** [93]. Since  $V_n \subset V$ ,  $v_n$  can be used as a test vector in the original equation. Subtracting these two, the Galerkin orthogonality relation for the error can be obtained:

$$\epsilon_n = u - u_n \quad (\text{D.0.3})$$

This is the error between  $u$  and  $u_n$ . Therefore:

$$a(\epsilon_n, v_n) = a(u, v_n) - a(u_n, v_n) = f(v_n) - f(v_n) = 0 \quad (\text{D.0.4})$$

The matrix form of Galerkin method is often used to compute the solution by a computer program and is built as [48]:

- Let  $e_1, e_2, \dots, e_n$  be the basic for  $V_n$ . It is sufficient to use these to test the Galerkin equation: find  $u_n \in V_n$  such that  $a(u_n, e_i) = f(e_i)$  for  $i = 1, \dots, n$ . (D.0.5)
- $u_n$  is expanded respecting to this basic:

$$u_n = \sum_{j=1}^n u_j e_j \quad (\text{D.0.6})$$

- Insert (D.0.6) to (D.0.5) then:

$$a\left(\sum_{j=1}^n u_j e_j, e_i\right) = \sum_{j=1}^n u_j a(e_j, e_i) = f(e_i) \quad i = 1, \dots, n \quad (\text{D.0.7})$$

- Compare equation (D.0.7) with the linear system of equation in the form  $Ax = b$  then:

$$A_{ij} = a(e_j, e_i); \quad b_i = f(e_i)$$

# REFERENCES

- [1] CLUSTER CONSULTING GROUP: Global Electronic Market Data. *Resource information*: <http://www.custerconsulting.com/resources/> (retrieved 13.05.2013).
- [2] McCLUSKEY, F. P.; PODLESAK, T.; GRZYBOWSKY, R.: *High Temperature Electronics*, 1<sup>st</sup> edition. CRC Press, 1996.
- [3] KAZMIERKOWSKI, M. P.; KRISHNAN, R.; BLAABJERG, F.: *Control in Power Electronics: Selected Problems*. Academic Press, 2002.
- [4] MEREDITH, R.J.: *Engineers Hand Book of industrial Microwave heating*. Short Run Press Ltd., Exeter, 1998.
- [5] NOWOTTNICK, M.: Forschungsthemen (Projeckte). *Resource Information*: <http://www.igs.uni-rostock.de/forschung/zuverlaessigkeit-und-sicherheit-elektronischer-systeme/forschungsprojekte/> (Retrieved 20.02.2014).
- [6] DYMAX: Rework and Removal of UV light-Curable Conformal Coatings. In: *Technical Bulletin*. *Resource Information*: <http://www.dymax.com/de/pdf/literature/> (Retrieved 20.04.2013).
- [7] THOSTENSON, E. T.; CHOU, T.-W.: Microwave processing: fundamentals and applications. In: *Composites: Part A 30*. P. 1055-1071, 1999.
- [8] REDDI, K. R.; MOON, Y. B.: Simulation of new product development and engineering changes. In: *Industrial Management & Data Systems*, Vol. 112, No. 4. P: 520-540, 2012.
- [9] BANKS, C. M.; CARSON, J.; NELSON, B.; NICOL, D.: *Discrete-Event Simulation*. Prentice Hall, 2001.
- [10] ALLEN, M. P.; TILDESLEY, D. J.: *Computer Simulation of Liquids*. Oxford University Press, New York, 1987.

- [11] OSEPCHUK, J. M.: A History of Microwave Heating Applications. In: *IEEE Transaction on Microwave Theory and Techniques*, Vol. MTT-32, No.9, September 1984.
- [12] MOLECULAR EXPRESSIONS<sup>TM</sup>: Basic electromagnetic wave properties. *Resource Information*: <http://micro.magnet.fsu.edu/primer/java/wavebasics/> (Retrieved 20.12.2013).
- [13] ORFANIDIS, S. J.: Electromagnetic waves and Antennas (2008). *Resource Information*: <http://www.ece.rutgers.edu/~orfanidi/ewa/> (Retrieved 02.01.2014).
- [14] POZAR, D. M.: *Microwave Engineering*, 4<sup>th</sup> Edition. Wiley, 2005.
- [15] SUTTON, W. H.; BROOKS, M. H.; CHABINSKY, I. J., EDITORS: Microwave processing of materials. In: *Materials Research Society Proceedings*, Vol. 24, Pittsburgh: Materials Research Society, 1988.
- [16] UMAR, Z.: Design and numerical simulation of a microwave based heating process for flowing liquids. Institut für Gerätesysteme und Schaltungstechnik, Falkultät für Informatik und Electrotechnik, Universität Rostock. Diplom Arbeit, 2012.
- [17] GUPTA, M.; E. W. W. L.; WONG, W. L.: *Microwaves and Metals*. Wiley (Aisa) Pte Ltd, 2007.
- [18] SIORES, Dr. E.; DO REGO, D.: Microwave Application in Material Joining. In: *Journal of Material Processing Technology* 48. P. 619-625, 1995.
- [19] MICROWAVETEC: Interaction of Microwave Irradiation with Materials. In: *The theoretical basic of microwave technologies*. [http://www.microwavetec.com/theor\\_basics.php](http://www.microwavetec.com/theor_basics.php) (Retrieved 15.10.2013).
- [20] GABRIEL, C.; GABRIEL, S.; GRAAZ, E. H.; HALSTEAD, B. S. J.; MIGOS, D. M. P.: Dielectric parameters relevant to microwave dielectric heating. In: *Chemical Society Review*, volume 27, 1998.
- [21] METAXAS, A. C; R.J.M.: *Industrial Microwave Heating*. Vol. IEE Power Engineering Series 4. London: Peter Peregrinus Ltd, 1983.

- [22] SALSMAN, J.: Measurement of Dielectric Properties in the Frequency Range of 300 MHz to 3 GHz as a Function of Temperature Density<sup>1</sup>. In: *Defense Technical Information Cente*, 1992.
- [23] METAXAS, A. C.: *Foundation of Electroheat: A Unified Approach*. Wiley, 1996.
- [24] OPEN DIRECTORY PROJECT: Printed Circuit Board Assemblies. *Resource Information*:  
[http://www.dmoz.org/Business/Electronics\\_and\\_Electrical/Contract\\_Manufacturing/Printed\\_Circuit\\_Boards/Assembly/](http://www.dmoz.org/Business/Electronics_and_Electrical/Contract_Manufacturing/Printed_Circuit_Boards/Assembly/) (Retrieved 11.12.2013).
- [25] HESS, E. R; PE: *The Pros of Conformal Coatings*. GarrettCom, Inc, November 2006.
- [26] EMPFASIS: Five Types of Conformal Coatings. *Resource Information*:  
<http://www.empf.org/empfasis/2009/may09/conformal.html> (Retrieved 20.12.2013).
- [27] SCH TECHNOLOGIES: Conformal Coatings Curing and Drying. In: *Technical Bulletin April 09*. <http://www.conformalcoating.co.uk/documents/> (Retrieved 10.12.2013).
- [28] NEXUS CONFORMAL COATING CONSULTANCY: How to successful Cure Conformal Coating on a Printed Circuit Board (PCB). *Resource Information*:  
<http://www.conformalcoatingconsultancy.com/cms/Curing-vs-drying> (Retrieved 24.12.2013).
- [29] MARTINELLI, M.; ROLLA, P. A.; TOMBARI, E.: A method for dynamic dielectric measurements at microwave frequencies: applications to polymerization process study. In: *IEE Transaction on Instrumentation and Measurement*. P: 417-421, 1985.
- [30] KRANBUEL, D.; DELOS, S.; YI, E.; MAYER, J.; JARVIE, T.; WINFREE, W.; HOU, T.: Dynamic dielectric analysis: nondestructive materials evaluation and cure cycle monitoring. In: *Polymer engineering and Science*. P: 338-345, 1986.
- [31] HARAN, E. N.; GRINGGAS, H.; KATZ, D.: Dielectric properties of epoxy resin during polymerization. In: *Journal of Applied Polymer Science*. P: 3505-3518, 1965.
- [32] KAPPE, C. O.: High speed combinatorial synthesis utilizing microwave irradiation. In: *Current Opinion in Chemical Biology*. P: 314-320, 2002.



- [33] WILLIAM, N. H.: Curing of epoxy resin impregnated pipe at 2450 MHz. In: *Journal of Microwave Power*. P: 123-127, 1967.
- [34] MARAND, E.; BAKER, H. R.; GRAYBEAL, J. D.: Comparison of reaction mechanism of epoxy resins undergoing thermal and microwave cure from in-situ measurements of microwave dielectric properties and infrared spectroscopy. In: *Macromolecules* 25. P: 2243-2252, 1992.
- [35] WEI, J.; HAWLEY, M. C; DELONG, J. D.: Comparison of microwave and thermal cure of epoxy resins. In: *Polymer Engineering and Science*. P: 1132-1140, 1993.
- [36] JORDAN, C.; GALY, J.; PASCAULT, J-P.: Comparison of microwave and thermal cure of an epoxy/amine matrix. In: *Polymer Engineering and Science*. P: 233-239, 1995.
- [37] MIJOVIC, J.; CORSO, W. V.; NICOLAIS, N.; D'AMBROSIO, G.: In-situ real time study of crosslinking kinetics in thermal and microwave fields. In: *Polymer for Advanced Technologies*. P: 231-243, 1998.
- [38] MIJOVIC, J.; WIJAYA, J.: Comparative calorimetric study of epoxy cures by microwave vs. thermal energy. In: *Macromolecules*. P: 3671-3674, 1990.
- [39] SINGER, S. M.; LOW, J.; DELONG, J. D.; HAWLEY, M. C.: Effects of processing on tensile properties of an epoxy/amine matrix: continuous electromagnetic and/or thermal curing. In: *Sample Quarterly*. P: 14-18, 1989.
- [40] BAI, S. L.; DJAFARI, V.; ANDREANI, M.; FRANCOIS, D.: A comparative study of the mechanical behavior of epoxy resin cured by microwaves with one cured thermally. In: *European Polymer Journal*. P: 875-884, 1995.
- [41] KNOTHE, K.: *Finite Elemente*. Springer Velag, Berlin, 1991.
- [42] DIXIT, U. S.: Finite Element Method: An introduction. *Resource Information*: [http://www.iitg.ernet.in/scifac/qip/public\\_html/cd\\_cell/cdc\\_06\\_07.htm](http://www.iitg.ernet.in/scifac/qip/public_html/cd_cell/cdc_06_07.htm) (Retrieved 05.01. 2014).
- [43] CAUSON, D. M.; MINGHAM, C. G.: *Introductory Finite Difference Method for PDEs*. Ventus Pulishing ApS, 2010.

- [44] COOK, R., MALKUS, D., PLESHA, M., WITT, R.: *Concept and Application of Finite Analysis*, 4<sup>th</sup> Edition. Wiley (Asia) Pte Ltd, Singapore, 2002.
- [45] COMSOL MULTIPHYSICS: Microwave Heating Module. *Resource Information:* COMSOL Help.
- [46] TAPSANIT, P.: The simulation of waveguide and microwave heating by numerical method. Physics department, Khonkaen University: Lecture presentation, 2011.
- [47] HARELL II, E. M.; HEROD, J. V.: Linear Method of Applied Mathematics. *Resource Information:* <http://www.mathphysics.com/pde/vectorid.html> (Retrieved 15.01.2014).
- [48] DURAN, R. G.: Galerkin Approximation and Finite Element Methods. *Resource Information:* [http://mate.dm.uba.ar/~rduran/class\\_notes/fem.pdf](http://mate.dm.uba.ar/~rduran/class_notes/fem.pdf) (Retrieved 15.03.2014).
- [49] SCHOLARPEDIA: Galerkin Methods. *Resource Information:* [http://www.scholarpedia.org/article/Galerkin\\_methods](http://www.scholarpedia.org/article/Galerkin_methods) (Retrieved 15.03.2014).
- [50] ZHAN, Y.; MA, N.: Galerkin Method. *Resource Information:* [http://www.sd.ruhr-uni-bochum.de/downloads/Galerkin\\_method.pdf](http://www.sd.ruhr-uni-bochum.de/downloads/Galerkin_method.pdf) (Retrieved 15.03.2014).
- [51] DUBCOVA, L.; SOLIN, P.; CERVENY, J.; KUS, P.: Space and Time Adaptive Two-Mesh *hp*-FEM for Transient Microwave Heating Problems. *Resource Information:* <http://spilka.math.unr.edu/hermes/> (Retrieved 30.12.2013).
- [52] HOANG, H.; USMANI, A.: *Finite Element Analysis for Heat Transfer: Theory and Software*. Springer Velag, London, 1994.
- [53] COMSOL MULTIPHYSICS: Material library. *Resource Information:* COMSOL Help.
- [54] YAN, H.; YAN, L.; ZHAO, X.; ZHOU, H.; HOANG, K.: Analysis of electromagnetic field coupling to a microtrip line connected with nonlinear components. In: *Progress In Electromagnetics Research B*, Vol. 51. P: 291-306, 2013.
- [55] WANG, L.; SU, D.; WANG, Y.: Coupling of External Electromagnetic Field to Printed Circuit Board. In: *Antennas, Propagation and EM Theory*. ISAPE 2008, 8<sup>th</sup> International Symposium on, 2008.

- [56] LEONE, M.; SINGER, H. L.: On the Coupling of an External Electromagnetic Field to a Printed Circuit Board Trace. In: *IEEE Transaction on Electromagnetic Compatibility*, Vol. 41, No. 4, November 1999.
- [57] ANTENNA-THEORY.COM: Permittivity. *Resource Information:* <http://www.antenna-theory.com/definitions/permittivity.php> (Retrieved 21.09.2012).
- [58] ANTENNA-THEORY.COM: Introduction of horn antennas. *Resource Information:* <http://www.antenna-theory.com/antennas/aperture/horn.php> (Retrieved 20.09.2012).
- [59] NANOWANE PROJECT: Project Meeting Discussion, 2012.
- [60] ANTENNA-THEORY.COM: Introduction to waveguide. *Resource Information:* <http://www.antenna-theory.com/tutorial/waveguides/waveguide.php> (Retrieved 02.09.2012).
- [61] AMITEC ELECTRONICS: Photo Gallery. *Resource Information:* <http://www.amitecltd.com/photo-gallery1.html> (Retrieved 05.08.2012).
- [62] FLANN MICROWAVE: Waveguide and Flange Data. *Resource Information:* <http://www.flann.com/> (Retrieved 14.05.2011).
- [63] PLASTICS INTERNATIONAL: FR-4 Glass/Epoxy Phenolic. *Resource Information:* <http://www.plasticsintl.com/datasheets> (Retrieved 12.03.2011).
- [64] MAZIERSKA, J.; JACOB, M. V.; HARRING, A.; KRUPKA, J.; BARNWELL, P.; SIMS, T.: Measurements of loss tangent and relative permittivity of LTCC ceramics at varying temperatures and frequencies. In: *Journal of the European Ceramic Society*, Vol. 23, Issue 14. P: 2611-2615, 2003.
- [65] BREMERKAMP, F.: Intergration eines Soptionsspeicher in das Wärmermanagement von elektronischen Baugruppen, Institut für Gerätesysteme und Schaltungstechnik, Falkultät für Informatik und Electrotechnik, Universität Rostock, Doktorarbeit, 2013.
- [66] SAYLOR.ORG: Thermal Conductivity. *Resource Information:* <http://www.saylor.org/site/wp-content/uploads/2011/04/> (Retrieved 15.07.2013).

- [67] ELECTRONIC COOLING: The thermal conductivity of ceramics. *Resource Information:* <http://www.electronics-cooling.com/1999/09/the-thermal-conductivity-of-ceramics/> (Retrieved 23.06.2011).
- [68] WOLFRAM MATHWORLD: Divergence Theorem. *Resource Information:* <http://mathworld.wolfram.com/DivergenceTheorem.html> (Retrieved 02.03.2014).
- [69] PAUL'S ONLINE MATH NOTES: Divergence Theorem. *Resource Information:* <http://tutorial.math.lamar.edu/Classes/CalcIII/DivergenceTheorem.aspx> (Retrieved 02.03.2014).
- [70] DIVERGENCE THEOREM. (SECT. 16.8): Divergence Theorem in space. *Resource Information:* <http://math.msu.edu/~gnagy/teaching/11-fall/mth234/L39-234-tu.pdf> (Retrieved 02.03.2014).
- [71] SOKOLOWSKI, J. A.; BANKS, C. M.: *Principles of Modeling and Simulation: A Multidisciplinary Approach*. Wiley, March 2009.
- [72] ZHANG, K.; LI, D.: *Electromagnetic Theory for Microwaves and Optoelectronics*. 2<sup>nd</sup> Edition, Springer Verlag, 2008.
- [73] LEWIS, D. A.; SUMMERS, J. D.; WARD, T. C.; McGRATH, J. E.: Accelerated Imidization Reactions using Microwave radiation. In: *Journal of Polymer Science*, Part A. P: 1647-1653, 1992.
- [74] MIJOVIC, D.; KENNEY, J. M.; MAFFEZZOLI, A.; BELLUCI, F.; NICOLAIS, L.: The principles of dielectric measurement for in-situ monitoring of composite processing. In: *Composite Science and Technology*. P: 277-290, 1993.
- [75] BUI, T. D.: Computer simulation of heat protection coatings for PCBs, Institut für Gerätesysteme und Schaltungstechnik, Fakultät für Informatik und Electrotechnik, Universität Rostock, Diplom Arbeit, 2008.
- [76] POLYCARPOU, A. C.: *Introduction to the Finite Element Method in Electromagnetics*. Morgan & Claypool Publishers' series, USA, 2006.
- [77] SÜLI, E.: Lecture notes on finite Element Method for Partial Differential Equations. Mathematical Institute, University of Oxford, 2012.

- [78] HUMPHRIES, S.; ALBUQUERQUE, Jr.: *Finite Element Method for Electromagnetics*. CRC Press, USA, 2010.
- [79] SANTOS, T. et al.: 3D Electromagnetic Field Simulation in Microwave Ovens: a Tool to Control Thermal Runaway, In: *COMSOL Conference*, Paris, 2010.
- [80] BUI, T. D.; BREMERKAMP, F.; NOWOTTNICK, M.: Coupling of wired PCB with microwave radiation – 3D simulation and experimental valuation. In: *COMSOL Conference Proceeding*, Stuttgart, Germany, 2011.
- [81] SHIEEL, W., WITTKE, K., NOWOTTNICK M.: *Niedrigtemperaturmontage hoch integrierter elektronischer Baugruppen durch selektive Mikrowellen erwärmung MICROFLOW*. Dr. Marcus S. Detert, Templin, 2008.
- [82] BREMERKAMP, F.; NOWOTTNICK, M.; SEEHASE, D.; BUI, T. D.: Behavior of Printed Circuit Board due to Microwave Supported Curing Process of Coating Materials. In: *Journal of Microwave Power and Electromagnetic Energy* 46, Nr.2. P: 68-75, June 2012.
- [83] NOWOTTNICK, M.; BREMERKAMP, F.; BUI, T. D.: Mikrowellenhärtung von Beschichtungen und Vergussungsmassen für elektronische Baugruppen. In: *Jahrbuch Mikroverbindungstechnik* 2012/2013. 1. Auflage. DVS Media, S: 124-135, 2012.
- [84] BUI, T. D.; BREMERKAMP, F.; NOWOTTNICK, M., SEHASE, D.: Protection of Printed Circuit Board structures in Microwave Process. In: *EuroSimE Conference Proceeding*, Wroclaw, Poland, 2013.
- [85] BREMERKAMP, F.; NOWOTTNICK, M.; BUI, T. D.: Microwave curing of PCB Coatings. In: *Proceeding of 13<sup>th</sup> International Conference on Microwave and High Frequency Heating* (AMPERE 2011), Toulouse, France, September 2011.
- [86] NOWOTTNICK, M.; BREMERKAMP, F.; BUI, T. D.: Mikrowellenhärtung von Beschichtungen und Vergussungsmassen für elektronische Baugruppen. In: *Elektronische Baugruppen und Leiterplatten – EBL 2012 (GMM-FB 71)*, Stuttgart, 2012.
- [87] LÖW, R. C.: Stress Evaluation and Reliability of Electrically Conductive Adhesive Interconnections, Technischen Fakultät, Universität Freiburg, Doktorarbeit, 2009.

- [88] ZIMMERMAN, W. B. J.: COMSOL Multiphysics and the basics of numerical analysis. *Resource Information:* [http://www.asianscientist.com/books/wp-content/uploads/2013/05/6141\\_chap01.pdf](http://www.asianscientist.com/books/wp-content/uploads/2013/05/6141_chap01.pdf) (Retrieved 17.01.2014).
- [89] ALL SEALS INC: Temperature range by polymer. *Resource Information:* <http://www.allsealsinc.com/> (Retrieved 02.03.2013).
- [90] YOKOGAWA, S.; KAKUHARA, Y.; TSHUCHIYA, H.: Joule Heating Effects on Electromigration in Cu/Low- $\kappa$  Interconnects. In: *Reliability Physics Symposium*, IEEE International. P: 837-843, 2009.
- [91] FOLZ, D. C.: Variable frequency microwave curing of polyurethane, Virginia Polytechnic Institute, State University, Master thesis, Virginia, 2011.
- [92] ADAMIETZ, R.; TILFORD, T.; FERENETS, M.; PAVULURI, S.; DESMULLIEZ, M. P.Y.; BAILEY, C.: A Microwave Curing System for Microelectronic assemblies. In: *4<sup>th</sup> Electronic System-Integration Technology Conference*, ESTC 2012, Amsterdam, 2012.
- [93] SUBSTECH: Thermal properties of ceramics. *Resource Information:* [http://www.substech.com/dokuwiki/doku.php?id=thermal\\_properties\\_of\\_ceramics](http://www.substech.com/dokuwiki/doku.php?id=thermal_properties_of_ceramics) (Retrieved 25.06.2011)

# ERKLÄRUNG

Ich erkläre, dass ich ein Verfahren zur Erlangung des Doktorgrades bisher an keiner wissenschaftlichen Einrichtung beantragt habe. Die vorgelegte Dissertation wurde weder im Ausland noch im Inland in gleicher oder ähnlicher Form einer anderen Prüfungsbehörde vorgelegt. Ich erkläre, dass ich die eingereichte Dissertation selbstständig und ohne fremde Hilfe verfasst, alle andere als die von mir angegebenen Quellen und Hilfsmittel nicht benutzt und die den benutzten Werken wörtlich oder inhaltlich entnommenen Stellen als solche kenntlich gemacht habe.

Rostock im März 2014

Trinh Dung Bui